1-1-2011

Improved methods for distribution of superelevation

Udai Hassein
Ryerson University

IMPROVED METHODS FOR DISTRIBUTION OF SUPERELEVATION

By:

Udai Hassein

B.Sc. Al- Mustansiriya University, 1994

Baghdad, Iraq

A thesis presented to

Ryerson University

in partial fulfillment of the

requirements for the degree of

Master of Applied Science

in the program of Civil Engineering

Toronto, Canada, 2011

Author's Declaration

I hereby declare that I am the sole author of this thesis or dissertation.

I authorize Ryerson University to lend this thesis or dissertation to other institutions or individuals for the purpose of scholarly research.

_____

Udai Hassein

I further authorize Ryerson University to reproduce this thesis or dissertation by photocopying or by other means, in total or in part, at the request of other institutions or individuals for the purpose of scholarly research.

_____

Udai Hassein

Borrower's Page

No.	Borrower's Name	Address	Phone No.	Date	Signature
1					
2					
3					
4					
5					
6					
7					
8					
9					
10					
11					
12					
13					
14					
15					
16					
17					
18					
19					
20					
21					
22					
23					
24					
25					
26					
27					
28					
29					

IMPROVED METHODS FOR DISTRIBUTION OF SUPERELEVATION

Udai Hassein
MASc., Department of Civil Engineering, Ryerson University, 2011

Abstract

The American Association of State Highway and Transportation Officials (AASHTO) provide 5 methods for distributing highway superelevation (e) and side friction (f). Method 1 (linear) is inferior to Method 5 (curvilinear). AASHTO Method 5 deals with speed variations, but its complex mathematical calculation affects design consistency. Safety margin is the difference between design and maximum limiting speed. This thesis describes distribution of superelevation (e) and side friction factor (f) based on the EAU and SAU methods using AASHTO and two different curves from the unsymmetrical curve; the equal parabolic arcs "EAU Curve" and a single arc unsymmetrical curve "SAU Curve". The thesis also describes e and f distributions based on the optimization model. The EAU and SAU methods and Parametric Cubic Optimization Model improve highway design consistency based on safety margins. Examples show the methods and optimization model are superior to AASHTO methods.

Acknowledgment

I would like to express my most heartfelt appreciation to my supervisor Dr. Said Easa, for his professionalism, wisdom, experience, suggestions, guidance, encouragement and patience throughout my thesis research program. Dr. Easa assisted me in my research tremendously. He presented me with my thesis idea and the chosen software. In addition, he presented me with several references that relate towards the software to assist me. Dr. Easa instructed me in the publications associated to my thesis. His unfailing optimism and continued support always allowed me to overcome the difficulties to complete this research. I am grateful to him for giving me the knowledge to understand the mathematical optimization modeling to be applied to my thesis.

I would also like to acknowledge the faculty and students in the Civil Engineering Department at the University of Ryerson. Special thanks to Dr. Kaarman Raahemifar for his perceptive suggestions for my research, and to Dr. Ali Mekky as well as Dr. Ahmed El-Rabbany, who served as the members of my thesis defense committee. I would also like to extend great appreciation towards Dr. Medhat Shehata, Dr. Ahmed Shaker, Dr. Li He and Dr. Murtaza Haider for providing guidance in my studies at Ryerson. I would like to say a special thanks to my friends and colleagues at Ryerson University, for supporting my research and offering helpful suggestions throughout my thesis. Finally, I want to say thanks to my family for their patience, especially to my wife for her forbearance during my work, without whose understanding and moral support, I would not have achieved to

concentrate on my work dedicatedly. I would also like to offer my gratification to my friends who sacrificed their time to help me complete my thesis successfully.

Table of Content

Author's Declaration ..... **iii**

Borrower's Page ..... **iv**

Abstract ..... **v**

Acknowledgment ..... **vi**

Table of Content ..... **viii**

List of Figures ..... **xii**

List of Tables ..... **xv**

List of Symbols ..... **xvii**

Chapter 1: Introduction **1**

1.1 Research Background 1

1.2 Research Objectives 3

1.3 Thesis Organization 4

Chapter 2: Literature Review **7**

2.1 Highway Geometric Design 7

2.1.1 Horizontal Alignments 8

2.1.1.1 Theoretical Considerations 10

2.1.1.2 Side Friction Factor 12

2.1.1.3 Vehicle Stability on Horizontal Curves 14

2.1.2 Vertical Alignments 22

2.1.2.1 Vertical Curve Equation 25

2.1.2.2 EAU Vertical Curve Equations....28
2.1.2.3 SAU Vertical Curve Equations....31
2.1.3 Cross Section along with Superelevation....36
2.2 Superelevation Distribution Methods....38
2.2.1 AASHTO Methods....40
2.2.3 Fundamental subject within Superelevation Design....50
2.2.4 Superelevation Distribution Approach by Other International Agencies....52
2.3 Highway Consistency....53
2.3.1 Choices for Design Speed....54
2.3.1.1 Traditional Design Speed Method....54
2.3.1.2 Speed-Environment Approach....55
2.3.2 Superelevation Distribution to Maximize Design Consistency of Highway....58
2.4 Summary....59
Chapter 3: Existing Methodology for Superelevation Design....61
3.1 Superelevation Design Considerations....61
3.1.1 Maximum Superelevation....61
3.1.2 Minimum Superelevation....63
3.1.3 Maximum Side Friction Factors....63
3.1.4 Minimum Radius....64
3.1.5 Choice of Design Superelevation and Side Friction....65
3.2 Superelevation Distribution based on AASHTO Method 5....66
3.3 Analytical Formulas....71

3.4 Evaluation of the AASHTO methods 74
3.4.1 Method 5 Evaluated by Nicholson.....76
3.4.2 Method 5 Evaluated by Easa.....77
3.5 Superelevation Design based on Safety Margin 79
3.5.1 Aggregate Analysis.....83
3.5.2 Disaggregate Analysis 87
Chapter 4: Development of New Methods and Model for Superelevation Distribution.....89
4.1 Introduction.....89
4.2 Improved Superelevation Distribution for a Single Curve 91
4.2.1 Distribution Using Fixed Curves (EAU Method).....91
4.2.2 Distribution Using Fixed Curves (SAU Method) 96
4.3 Improved Superelevation Distribution for a System of Curves.....98
4.3.1 Distribution Using System of Curves (EAU Method).....99
4.3.2 Distribution Using System of Curves (SAU Method) 100
4.3.3 Safety Margin Computation.....100
4.3.4 Distribution Using Parametric Cubic Model 103
4.4 Lingo Program (Optimization Software) 105
4.5 Summary 106
Chapter 5: Applications and Results.....108
5.1 Data Selection 108
5.2 Superelevation Distribution for Single Curve.....111
5.2.1 Numerical Example 1 (AASHTO Method 5 – Single Curve) 111

5.2.2 Numerical Example 2 (EAU Method – Single Curve) 113
5.2.3 Numerical Example 3 (SAU Method – Single Curve) 115
5.3 Superelevation Distribution for System of Curves 117
5.3.1 Numerical Example 4 (AASHTO Methods – System of Curves) 117
5.3.2 Numerical Example 5 (EAU Method – System of Curves) 120
5.3.3 Numerical Example 6 (SAU Method – System of Curves) 122
5.3.4 Numerical Example 7 (Parametric Cubic Model – System of Curves) 123
5.4 Sensitivity Analysis 125
5.4.1 Single Curve 125
5.4.2 System of Curves 130
5.5 Summary 132
Chapter 6: Conclusions and Recommendations 135
6.1 Conclusions 135
6.2 Future recommendations 138
References 139
Appendix A 145
Appendix B 147
Appendix C 148
Appendix D 152

List of Figures

Figure 1. 1 Thesis Organization.....6

Figure 2. 1 Geometry for Simple Horizontal Curves (Easa, 2002) 9

Figure 2. 2 Dynamics of Vehicle Motion on Superelevated Curve (NYSDOT Report 2003) 15

Figure 2. 3 Free body diagram of the forces at the center of gravity of the vehicle in motion on a superelevated curve.....16

Figure 2. 4 Different forces and moments experienced by a vehicle negotiating a circular curve (TAC, 1999) 20

Figure 2. 5 vertical curve combinations (AASHTO, 2004).....23

Figure 2. 6 Traditional unsymmetrical and equal-arc unsymmetrical (EAU) vertical curves (Easa, 2007) 31

Figure 2. 7 Geometry of the new single-arc unsymmetrical vertical curve (SAU); (Easa, 2007). 34

Figure 2. 8 Comparison of new and existing unsymmetrical vertical curves (Easa, 2007) .

Figure 2. 9 Methods of Distributing Superelevation and Side Friction (AASHTO,2004) 51

Figure 2. 10 Superelevation distribution methods recommended by several international agencies for high-speed facilities.....52

Figure 2. 11 Estimation of design speed (Rural,1993) 56

Figure 2. 12 Representative Operating Speed Distribution (Nicholson, 1998) 57

Figure 3. 1 Side Friction Factors based on Design (AASHTO, 2004) 68

Figure 3. 2 Method 5 Procedure for Development for Superelevation Distribution (AASHTO, 2004).....68

Figure 3. 3 Design Superelevation Rates for Maximum Superelevation Rate of 10 Percent (AASHTO, 2004).....70

Figure 4. 1 Development of Proposed Methods 90

Figure 4. 2 Development Procedures for Superelevation Distribution of EAU Method (***emax*** = 8%).....96

Figure 4. 3 Development Procedures for Superelevation Distribution of SAU Method (**emax** = 8%) 98

Figure 5. 1 Design Side Friction Factor and Superelevation Rate for Method 5 (***emax*** = 8%).....111

Figure 5. 2 Design Side Friction Factor and Superelevation Rate for EAU Method (***emax*** = 8%).....113

Figure 5. 3 Design Side Friction Factor and Superelevation Rate for SAU Method (***emax*** = 8%).....115

Figure 5. 4 Compare of Cubic Model, Quadratic Model, and AASHTO Methods (AASHTO 2001).....124

Figure 5. 5 The difference between AASHTO Method 5 and EAU Method (***emax*** = 8%)

Figure 5. 6 The difference between AASHTO Method 5 and SAU Method (***emax*** = 8%).

Figure 5. 7 The diffrence between Method 5 and EAU Method (***emax***=10%) 127

Figure 5. 8 The diffrence between Method 5 and SAU Method (***emax***=10%).....127

Figure 5. 9 Comparison of ***f*** between Method 5, EAU and SAU Methods 128

Figure 5. 10 Means and Standard Deviation of Safety Margins for all Methods and Optimization Models 131

Figure 5. 11 Coefficient of Variation of Safety Margins for all Methods and Optimization Models.....132

Figure A. 1 Method 5 Design Superelevation Rates for Maximum Superelevation Rate of 8 Percent.....145

Figure A. 2 EAU Method Design Superelevation Rates for Maximum Superelevation Rate of 8 Percent.....145

Figure A. 3 SAU Method Design Superelevation Rates for Maximum Superelevation Rate of 8 Percent.....146

Figure C. 1 Superelevatlon and Sideways Friction versus Curve Radius (Method 1) 148

Figure C. 2 Superelevatlon and Sideways Friction versus Curve Radius (Method 2) 149

Figure C. 3 Superelevatlon and Sideways Friction versus Curve Radius (Method 3) 149

Figure C. 4 Superelevatlon and Sideways Friction versus Curve Radius (Method 2 Modiffed) 150

Figure C. 5 Superelevatlon and Sideways Friction versus Curve Radius (Method 5) 150

Figure C. 6 EAU Method for Superelevation and Side Friction versus Curve Radius ...151

Figure C. 7 SAU Method for Superelevation and Side Friction versus Curve Radius....151

List of Tables

Table 2.1 Average Running Speeds (AASHTO ,2004).....47

Table 3. 1 Minimum Radius that use Limiting Values for both e and f (AASHTO, 2004)69

Table 3. 2 Minimum Radii for Design Superelevation Rates, Design Speeds, and $\boldsymbol{emax}$ = 10% (AASHTO, 2004).....70

Table 3. 3 Accuracy of Approximation of Equation (3.31) for Practical Parameter Values of AASHTO (Easa, 2003).....84

Table 3. 4 Linear Optimization Model (Discrete $\boldsymbol{ei}$); (Easa, 2003) 86

Table 4.1 Optimazation Model for Superelevation Distribution Using Parametric Cubic Curve.....105

Table 5.1 Parameters for Developing of Superelevation Distribution used for Examples 1, 2 and 3.....109

Table 5. 2 Input data for examples 4, 5, 6 and 7 [a].....110

Table 5. 3 Method 5 of Design Superelevation Rates for Different Radii ($\boldsymbol{emax}$ = 8%)112

Table 5. 4 EAU Method of Design Superelevation Rates for Different Radii ($\boldsymbol{emax}$ = 8%).....114

Table 5. 5 SAU Method of Design Superelevation Rates for Different Radii ($\boldsymbol{emax}$ = 8%).....116

Table 5. 6 Safety Margins for Diffrence Methods and Optimization Model.....119

Table 5. 7 Comparison of Means, Standard Deviation and Coefficient of Variation of Safety Margins for all Methods and Optimization Models 120

Table 5. 8 Distribution Method Comparisons for $\boldsymbol{e}$ and $\boldsymbol{f}$ within AASHTO, NCHRP439, Discrete, Quadratic, EAU, SAU, Cubic.....133

Table C. 1 Input Data for Example 8.....148

Table D. 1 EAU Method for Superelevation Distribution (Single Curve).....152

Table D. 2 SAU Method for Superelevation Distribution (Single Curve) 153

Table D. 3 EAU Method for Superelevation Distribution (System of Curves).....154

Table D. 4 SAU Method for Superelevation Distribution (System of Curves).....155

List of Symbols

The following symbols are used in this thesis:

A = algebraic difference in grade;

a, b, c, d = parameters of cubic function of f distribution;

CV = coefficient of variation of the safety margin;

e, f = superelevation and side friction factor, respectively;

e_i = design superelevation of Group i,

e_{min} = minimum superelevation;

e_{max} = maximum permissible design superelevation;

e_{2m} = superelevation utilizing Method 2 (modified);

f_{max} = side-friction coefficient;

f_i = design side friction of Group i;

$f\ max_i$ = maximum side friction of Group i;

g = acceleration of gravity;

g_1 = slope for leg 1;

g_2 = slope for leg 2;

i = index for curve group, where i=1,2,...,K;

j = index for set of curves, j=1,2,...,N;

h_{PI} = PI counterbalance from the 1/R axis;

h_{PVC} = elevation of PVC for SAU curve;

K = number of curve groups;

L_1 = length for the first arc;

L_2 = length for the second arc;

L = total length for the curve;

M = maximum safety margin;

m_i = safety margin of group i;

$Mean$ = mean of the safety margin;

N = total number of curves in highway segment;

q_i = curve frequency for Group i;

R = curve radius;

R_i = curve radius for Group i;

R_{min} = minimum curve radius;

R_{eo} = smallest potential radius relying by superelevation only;

R_{fo} = smallest potential radius relying by side friction only;

R_{me}= smallest potential radius utilizing minimum superelevation;

R_{PI} = radius of at the point of intersection, PI;

R_{EAU} = the ratio for the length of the shorter tangent for EAU curve;

r_1 = rate of change of grade for the first arc for EAU curve;

r_2 = rate of change of grade for the second arc for EAU curve;

r_{PVC} = rate of change of slope for SAU curve;

S_{min} = minimum allowable mean safety margin;

SD = standard deviation of the safety margin;

t = the third derivative of y for SAU curve;

V = vehicle design speed;

V_D = design speed;

V_i = design speed for Group i;

VL = limiting speed;

V_R= running speed, km/h;

$Variance$ = variance of the safety margin;

y_{BVC} = elevation at BVC point for EAU curve;

y_{EVC} = elevation at EVC point for EAU curve; and

Z = objective function.

Chapter 1: Introduction

1.1 Research Background

Three main elements are involved with highway geometric design: horizontal alignments, vertical alignments and cross section. Horizontal alignment has tangents such as straight paths with no curvature and has circular curves that are horizontal which connect tangents either with or without a transition spiral curve. Vertical alignments have flat tangents along with upgrade and downgrade tangents where parabolic curves connect. Other options of vertical alignments are unsymmetrical curves: EAU (Equal Arc Unsymmetrical vertical curve) curve and SAU (Single Arc Unsymmetrical vertical curve) curve. EAU curve contains two equal arcs and the curve has uneven horizontal projections for the tangents (Easa, 1994). The SAU curve has a single arc, which acquires the cubic function form, furthermore, the SAU curve lies above the flatter arc and under the sharper arc for the EAU vertical curve, therefore making it smoother (Easa, 2007).

The highway curve is a very complex feature, indeed one of utmost complexity within our highways. Over half of the fatalities connected to collisions on rural highways are located on curved sections. Therefore, corresponding transition sections and the curves represent the most critical areas for safety improvements. Geometric design consistency of the highway is one of the more important roles for improving highway safety. Design consistency provides harmonized driving within sections of the road. Several methods

have been developed in distributing highway superelevation (*e*) and side friction (*f*) by AASHTO.

The American Association of State Highway and Transportation Officials (AASHTO), prior to 2005, provided us with 5 methods for distributing highway superelevation (*e*) and side friction (*f*). AASHTO applies Method 2 and 5 for low speed and high speed, respectively, with distributing superelevation rates for speed variations, along with both urban and rural possibilities. Method 5 focuses on technical qualities for both Methods 1 and 4, as well as distributing intermediate superelevation rates among them focusing on complex unsymmetrical parabolic curves. This aims to increase superelevation rates along with the safety margin of compliant speed variation which is unspecified in Method 1; this also satisfies side friction factor within sharper curves from avoiding irregular driving that can be ingrained within Method 4.

The goal is to improve highway safety in the geometry design by considering a system of curves and ensuring that the design consistency of the successive geometric elements act in a coordinated way so that they produce coordinated driver performance consistent with driver expectations (Lunenfeld & Alexander, 1990; Krammes et al., 1995).

This thesis presents two main contributions. First, the thesis implements the EAU and SAU curves for distribution of superelevation, instead of the traditional unsymmetrical vertical curve used in AASHTO Method 5 to form the basis of the EAU and SAU Methods, respectively. Second, the thesis uses the general cubic curve designed for the f

distribution and a component of the aggregate analysis, which is provided by Easa (2003), to form the Parametric Cubic Optimization Model. The EAU and SAU methods and Parametric Cubic Optimization Model use design speed of horizontal curves to improve highway design consistency based on safety margins.

The proposed model finds the best superelevation distribution for a specified highway data by utilizing the complete superelevation design area (of which AASHTO curves are a subset). The developed optimization model determines the best distribution of superelevation, where such an optimization model has an objective function subject to constraints.

1.2 Research Objectives

In the first section, the objective is:

1) To show the improved methods for distribution of superelevation regarding highway design issues with the current superelevation distribution. This thesis will show two straightforward methods for determining superelevation rates of the highway curve design that takes into account the inconsistency within the design speed along with the friction factor; these methods can be utilized for both the evaluation of and design for current highway curves.
2) To provide the methodology of determining the proposed methods for the superelevation rate utilized within the highway curve design. A relationship between the existing methods and the proposed methods will be completed using Tables and charts.

3) To present examples and show the difference and benefit between the proposed methods and AASHTO Method 5.

In the second section, the objectives are:

1) To determine a methodology that evaluates the AASHTO methods of superelevation distribution on a highway geometric design regarding safety.
2) To evaluate the safety margin within the difference between the speed limit and the design speed from one curve to the next.
3) To present the safety margin concept by formulation for the improved methods along with numerical examples showing its application.
4) To develop a Parametric Cubic Optimization Model determining the best distribution of superelevation, where such an optimization model has an objective function subject to constraints that improve design consistency of highway based on the safety margin.
5) To conclude that for evaluation purposes, the proposed methods and models apply means, standard deviation and coefficient of variation of safety margins to determine the best superelevation distribution design capable of use as a measure which reflects both safety and consistency.

1.3 Thesis Organization

This thesis is organized into 6 chapters.

- Chapter 1 includes the outline and general purpose of this thesis.

- Chapter 2 presents a comprehensive literature review of highway geometric design. It also explains EAU and SAU vertical curve Equations, respectively. Furthermore, superelevation distribution methods utilized within highway consistency are discussed and present a useful backdrop for what follows.
- Chapter 3 provides the existing methodology for superelevation design considerations and the evaluation of the AASHTO methods. A description of safety margin is analyzed. The safety margin concept is subsequently introduced.
- Chapter 4 provides method developments of superelevation distribution, focusing on the proposed methods, the EAU Method, SAU Method and the Parametric Cubic Optimization Model.
- Chapter 5 is the application and analytical solutions for the AASHTO Methods, EAU Method, SAU Method and the Parametric Cubic Optimization Model. Examples are given for superelevation distribution and safety margin. Comparisons of distribution superelevation and side friction for all methods and models are presented.
- Chapter 6 provides a conclusion and future recommendations.

The overview of the thesis organization is shown in Figure 1.1

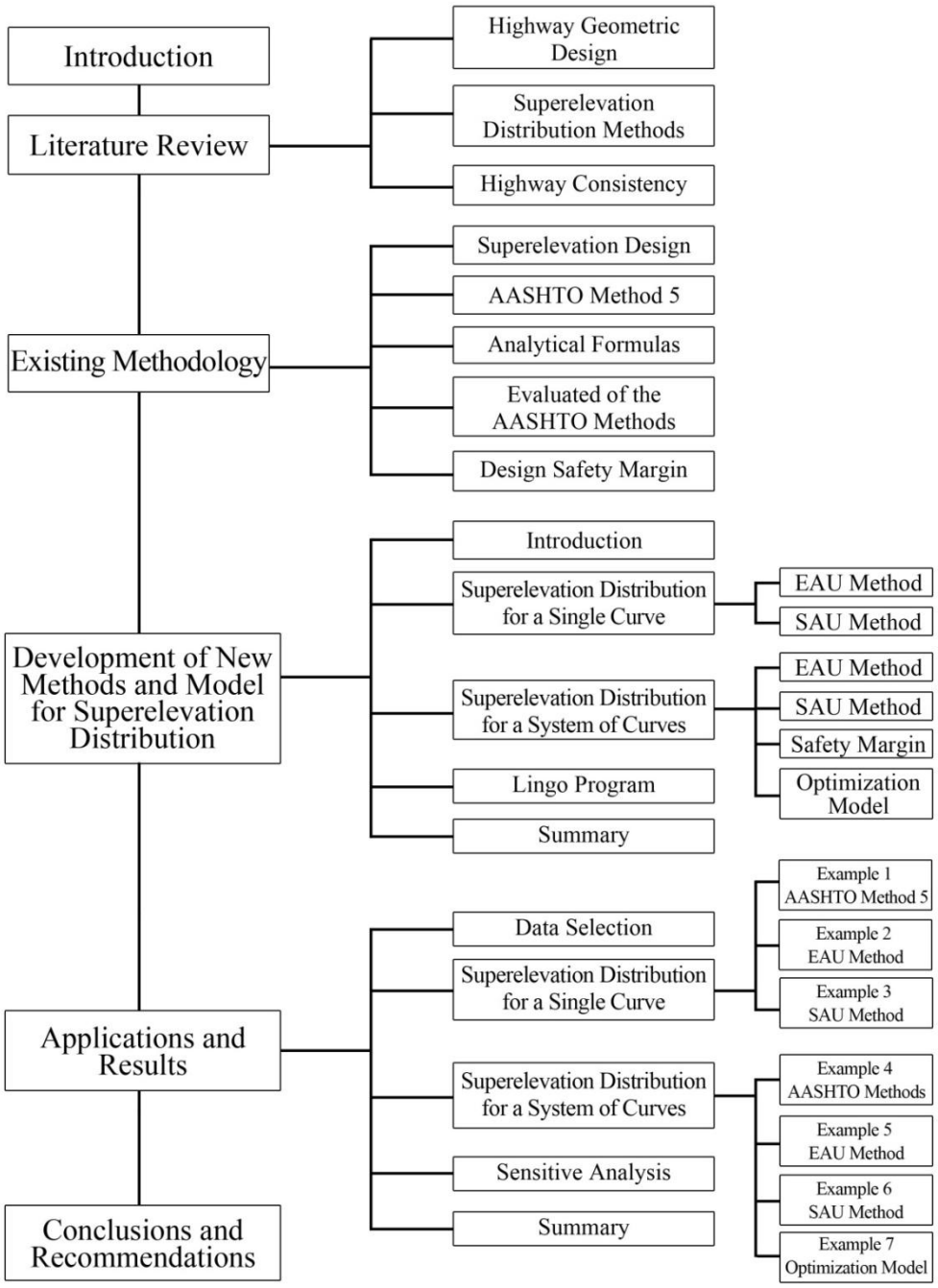

Figure 1. 1 Thesis Organization

Chapter 2: Literature Review

This chapter presents a comprehensive literature review of three main sections. The first section being highway geometric design that is based on three elements: horizontal and vertical alignments along with cross section. The second section is superelevation distribution methods, which is described by four sub-sections: AASHTO Methods, Fundamental subject, NCHRP 439 Assessment and the superelevation distribution approach by other international agencies. The third and final section is highway consistency, which is further explained by four sub-sections: highway geometric design consistency, choice of design speed and superelevation distribution to maximize design consistency of highway.

2.1 Highway Geometric Design

Highway geometric design involves three main elements: horizontal alignment, vertical alignment, and cross sections. Horizontal alignment focuses on straight tangents that connect together with circular horizontal curves; depending on whether they are accompanied by transitional spiral curves or not. Horizontal curves can be complex or simple curves. A complex curve is also known as a reverse curve, when it is composed of two consecutive simple curves within opposite directions, whereas it can be called a compound curve, when it is composed of two consecutive simple curves within a similar direction.

Vertical alignments focus on straight alignments, such as: flat, upgrade or downgrade alignments that are linked together with vertical curves. The vertical curves are typically parabolic curves, crest curves or sag curves. Additional alternatives of vertical alignments are comprised of unsymmetrical curves as well as reverse parabolic curves (Easa, 2002). Another alternative to vertical alignment is curvilinear alignment where aged rural highways contain a sequence of consecutive curves within short tangents. For highway design balance, the geometric elements should be designed to provide a continuous smooth and safe operation with speed that is to be practical within normal conditions of that roadway (AASHTO, 2004). Cross section specifies both the width along with the side slope for traveled ways.

2.1.1 Horizontal Alignments

Horizontal alignment is defined as "…the configuration of the roadway as seen in plan and generally consists of tangent sections, circular curves, and in some instances spiral transitions." (TAC, 2007) An important role in the roadway design process is a horizontal curve considering the relations between design speed, superelevation, side friction and curvature, which are important to the assembly of a design that is safe, efficient and consistent within driver expectations. Both horizontal and vertical alignment shortcomings can be dangerous. However, horizontal alignment is normally regarded as more serious, considering horizontal deficiencies establish discrepancies in design that reduce safety (TAC, 2007). Easa (2002) discussed a simple horizontal curve within radius *R* along with deflections angle *i* can be seen within Figure 2.1. The *T* and *L* elements can be calculated in terms of *R* and *i* as shown below:

$$T = R \tan (i/2) \quad (2.1)$$

$$L = \pi R (i/180) \quad (2.2)$$

where, T = tangent distance; E = external distance; M = middle ordinate; C = length of Chord; and L = curve length

Spiral transitions are applied occasionally to initiate the vehicle in a more gradual manner with the directional change. Vehicle stability contribution from spiral transitions has been discovered to be minimally relative (Harwood et al., 1994). NCHRP (2001) recommends AASHTO (2001) to provide further guidance to identify areas where spiral transitions curves result in safety benefits.

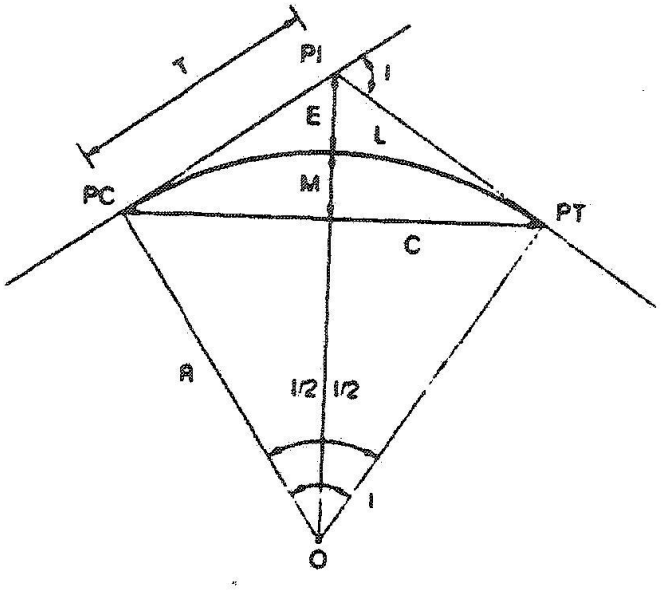

Figure 2. 1 Geometry for Simple Horizontal Curves (Easa, 2002)

It is quite common that drivers have a tendency to steer in a spiral path when they enter and exit a horizontal curve. NCHRP (2000) has discussed how the spiral transition curve

length has an effect on the operation of safety margin for the roadway. The main benefit of using a spiral transition curve was design consistency. Using spiral transition curves is not common practice within areas of North America. Both AASHTO (2004) and TAC (2007) recommend the use of transition curves within horizontal alignment design. But the guidelines, however, are not mandatory. Spiral transition curves, according to NCHRP (2000), were found to improve safety within sharp horizontal curves. They suggested that spirals should be used where the centripetal exceeded 1.3 m/s^2.

Limited contribution for vehicle stability stated that use for spiral transition curve prevents further investigation herein. A spiral transition curve provides a gradual degree of curvature into the horizontal curve. Furthermore, the spiral curves contribute in reducing the lateral change encountered by a vehicle as it follows a horizontal curve. However, the ensuing effect for diminished lateral change within stability has not been measured (Glauz et al., 1991). Tangents and circular curves are assumed by horizontal alignments as the main components involved. Horizontal Alignment Design requires many consideration factors, such as location for major utilities, climatic conditions, topography traffic volume, safety and consistency (TAC, 2007).

2.1.1.1 Theoretical Considerations

In horizontal alignment, concerning highway balance design, every geometric element must, based on practical economical design, be safe, have constant operation at speeds that are likely observed within normal conditions of a roadway containing a majority of drivers. Essentially, this is achieved by using speed as the main design control. The

roadway curve design needs to be based on a relationship between curvature and design speed as well as a relationship between side friction and superelevation (roadway banking). As a vehicle is moving within a circular path, the vehicle experiences a centripetal acceleration towards the curvature centre. This acceleration is continued by part of the vehicle's weight associated with the side friction between the pavement surface and vehicle's tires, by the roadway superelevation, or from a combination of both. Centripetal acceleration is at times associated with centrifugal force. Conversely, this force is imaginary where motorists believe it is pushing them in an outward direction while cornering when, actually, motorists are feeling the vehicle actually being accelerated within an inward direction. However, for purposes of conceptual expediency, the centrifugal force is utilized to show vehicle stability illustrated in Figure 2.2.

The relationships between curve radius, vehicle speed, side friction and superelevation are all very important to achieve a reliable design. According to AASHTO (2004), these relationships are connected to the laws of mechanics along with dynamics, however, it states "the actual values for use in design depend on practical limits and factors determines more or less empirically over the range of variables involved." The regulated horizontal relationships discussed earlier are dealt with in greater lengths within the following sections; however, brief details regarding vehicle handling, steering along with ride characteristics can prove to be useful in understanding the difficulty of achieving design factors and limits.

2.1.1.2 Side Friction Factor

Researchers have shown there is centripetal acceleration (a_r) that acts within a vehicle when it crosses a horizontal curve. This offsets the friction force among the pavement and tires along with a component for gravity, when the curve becomes superelevated. Lateral acceleration (a_f) acting in a vehicle within a curve can be called the side friction factor. Based on the Policy on Geometric Design of Highways and Streets from AASHTO, this factor is the side friction demand factor along with the gravitational constant *g*, therefore ($a_f = a_g$). When the curve becomes superelevated, frictional force is offset by gravity. Therefore, a third element for lateral acceleration as *e* enters within the equation. As shown within Figure 2.2, given that there are differences within speeds for different vehicles crossing a certain horizontal highway curve, an unstable force is placed on any vehicle within the curve. This offsets the friction among the pavement and tire and due to the thrusting of the tire side from the twists from the tire contact area along with the surface pavement.

The relation between the forces acting at the center of gravity of the vehicle in motion is dependent on the curve radius, the vehicle speed, and the superelevation. The lateral acceleration a_f that acts on the vehicle can be obtained from Equation 2.3:

$$a_f = a_r - a_e \tag{2.3}$$

where,

a_f = acceleration counter balanced by friction (g_f in m/s^2)

a_r= centripetal acceleration (v^2/gR)

a_e= acceleration counterbalanced by gravity due to superelevation ($g\ e/100$), m/s^2;

e = superelevation rate in percent;

f = side friction factor or side friction demand;

v = vehicle speed, m/s;

g = gravitational acceleration (9.81 m/s^2);

R = radius of curve in meter.

A simple curve equation utilized within the highway design curve along with superelevation as shown in Equation 2.4 (more details in following section).

$$R = \frac{V^2}{g\left(\frac{f+e}{1-ef}\right)} \tag{2.4}$$

Both AASHTO (2004) and TAC (2007) concur the quantity ($1-ef$) is about equal to 1.0; therefore, it is usually dropping within the equation, and having to produce a more moderate value for R. The simple formula is shown as

$$R = \frac{V^2}{g(e+f)} \tag{2.5}$$

where,

v = speed (Km/h)

g = force of gravity (9.81 m/s^2)

e = superelevation rate (percentage)

f = side friction factor (no unit)

The above equation can be solved for e by mathematical transposition so that:

$$e = \frac{V^2}{gR} - f \tag{2.6}$$

Side friction factor is used limitedly within Equation of point mass in order to avoid lateral skidding and to afford comfort control. However, this analysis based on 2D explains for vehicle dynamics resting on horizontal alignments.

2.1.1.3 Vehicle Stability on Horizontal Curves

There are many factors that go into vehicle cornering and behavior which makes the issue concerning stability fairly complicated. Highway safety is dependent upon normal conditions pertaining to weather, on how effective a vehicle can stay on the roadway and stay in their lane. As a vehicle passes through a curved alignment, the vehicle deals with centripetal acceleration acting towards the horizontal curve centre (AASHTO, 2004). Forces that counteract this type of acceleration involve the vehicle's weight, side friction and superelevation of the highway, developed at the pavement tire crossing point (Lamm et al. 1999).

The design guides for both AASHTO (2004) along with TAC (2007) help to simplify cornering dynamics with a focus on reducing the vehicle travelling within a 2D

horizontal alignment to a point mass during analysis. With this, vehicle movements are tracked by tangential and radial directions of motion. Figure 2.2 shows force of the radius that is applied to a vehicle as it travels at a consistent speed around a steady horizontal curve radius.

Vehicle motion dynamics within a curve have been recognized through much research. As a vehicle drives through a curve, centripetal acceleration powers the vehicle to the curve's centre. Two forces within a superelevated curve maintain the centripetal acceleration:

1) Frictional acceleration between both the pavement and tires,
2) Acceleration due to the vehicle component weight that is from the embankment is called superelevation (See Figure 2.2).

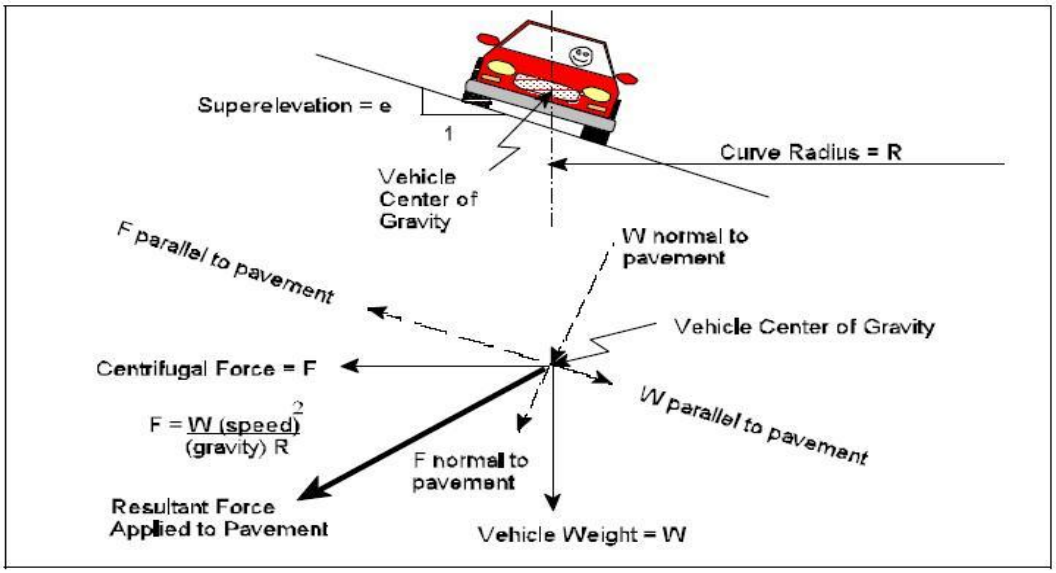

Figure 2. 2 Dynamics of Vehicle Motion on Superelevated Curve (NYSDOT Report 2003)

The force interaction that is found within the centre of gravity for the vehicle within motion that relates with the curve radius, both the *e* and speed is utilized within the design for horizontal curves on a highway. A lateral force that pushes the vehicle outward is the centrifugal force *F*. This is due to the lateral change within the vehicle's direction when it passes through the curve. The effect for the centrifugal force creates a lateral acceleration that forces the vehicle to the centre of the curve consequently changing the velocity vector for the vehicle. Superelevation makes the centrifugal force perpendicular with the slope for the superelevated curve; this is defined as *F* in Figure 2.2. This force combined with the component for the vehicle weight (*W* typical to the pavement) totals the normal result between the tires of the vehicle. The outstanding portion for the force *F* is resolved within the slope with the superelevation then shown as *F* that is parallel with the slope. The vehicle weight can also be determined by two components; weight that is normal with slope and weight that is parallel with the slope defined as *W* parallel and weight normal to the slope. Figure 2.3 below shows these forces within which the relation to the friction factor, superelevation, and the curve radius (*R*) can be derived.

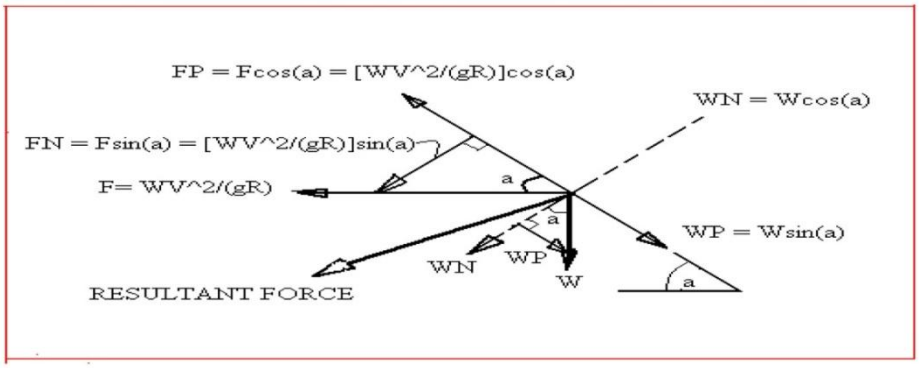

Figure 2. 3 Free body diagram of the forces at the center of gravity of the vehicle in motion on a superelevated curve.

Based on the mechanics laws and from Figure 2.3, it is shown:

$$WN = W\cos(a) \tag{2.7}$$

$$WP = W\sin(a) \tag{2.8}$$

$$FN = F\sin(a) = \frac{WV^2}{gR}\sin(a) \tag{2.9}$$

$$FP = F\cos(a) = \frac{WV^2}{gR}\cos(a) \tag{2.10}$$

Frictional force resting on the tires can be described as normal force multiplied by the friction factor:

$$(WN+FN)*f = W\cos(a) * f + \frac{WV^2}{gR}\sin(a) * f \tag{2.11}$$

From Figure 2.3,

$$e = \tan(a) = \frac{\sin(a)}{\cos(a)} \tag{2.12}$$

To avoid driving off the road and sliding involving vehicles that operate in designed speed, lateral forces need to be counterbalanced with the effect for the superelevation along with the frictional forces that are found on tires. Therefore, calculating forces within the slope, the following is determined:

$$W \cos(a) * f + \frac{WV^2}{gR} \sin(a) * f = \frac{WV^2}{gR} \cos(a) - W \sin(a) \quad (2.13)$$

This can be shown as:

$$\frac{W \sin(a)}{W \cos(a)} \left(\frac{V^2}{gR} f + 1\right) = \frac{V^2}{gR} - f \quad (2.14)$$

$$= \tan(a) \left(\frac{V^2}{gR} f + 1\right) = \frac{V^2}{gR} - f \quad (2.15)$$

Changing *tan (a)* within Equation 2.15 with *e* as shown in Equation 2.12, we get the following:

$$ef \frac{V^2}{gR} + e = \frac{V^2}{gR} - f \quad (2.16)$$

By calculating Equation 2.16 regarding *R*, the curve radius dependent on the superelevation, friction factor and the operating speed, we get the following for *R*:

$$R = \frac{V^2}{g\left(\frac{f+e}{1-ef}\right)} \quad (2.17)$$

The measure (1− *ef*) is about equal to 1.0; therefore, it is usually disregarded within the Equation, consequently creating a more conventional value for *R*. It is given as:

$$R = \frac{V^2}{g(e+f)} \quad (2.18)$$

where,

v = speed (Km/h)

g = force of gravity (9.81 m/s^2)

e = superelevation rate (percentage)

f = side friction factor (no unit)

The Equation above can be determined for e with mathematical transposition:

$$e = \frac{V^2}{gR} - f \quad (2.19)$$

$$\frac{V^2}{gR} = f + e \quad (2.20)$$

An exploitation of Equation 2.20 is described by both AASHTO (2004) and TAC (2007) geometric design guides. The basic relationship and point mass formula is considered in the guides into control vehicle operation resting on horizontal curves. Based on a 2D plan, the horizontal alignment is only considered without factoring any possible effect for vertical alignment. The main common exploitation for the formula of point mass is to isolate the R variable, to identify R_{min} for a specified vehicle speed, limiting the value for side friction factor and superelevation.

The next instability mode contemplated is vehicle rollover. Figure 2.4 shows the overturning moment that is produced as a vehicle travels through a horizontal curve. When the overturning moment is lesser than resisting moment, the vehicles would

rollover. According to Figure 2.4, avoiding body rollover along with other contributing factors like wind, can be acknowledged mathematically as (Lamm et al., 1999):

$$\left(\left(\frac{mV^2}{R}\right)cos\, a - Qsin\, a\right)h \leq \left(\left(\frac{mV^2}{R}\right)sin\, a - Qcos\, a\right)b \qquad (2.21)$$

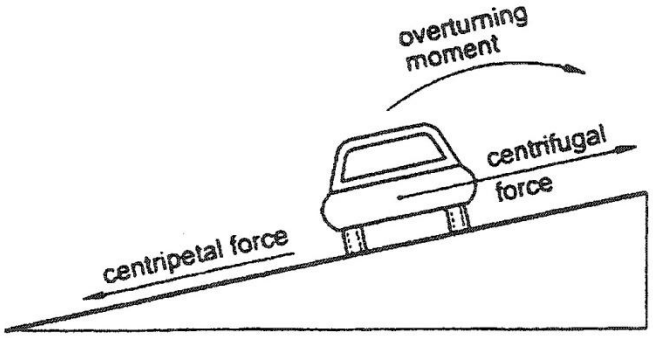

Figure 2. 4 Different forces and moments experienced by a vehicle negotiating a circular curve (TAC, 1999)

Noting that $F = mV^2/R$;

where, a = angle of roadway tilt, b = the horizontal distance between the outside of the vehicle's tire to the vehicle center of gravity, h = the vertical distance (perpendicular to the pavement surface) between pavement surface to vehicle center of gravity, W=Q = vehicle weight force.

Vehicle rollover is not accounted by North American design guidelines when heuristics for horizontal curves design are discussed. The simplified moment's summation within Equation 2.21 is not achieved for body roll. Under actual circumstances a transfer of vehicle weight into the tires resting on the exterior of the curve appears to move the

center of gravity of the vehicle in the direction of the exterior of the turn. The movement of the center of gravity of the vehicle decreases the moment arm of the gravitational force that proceeds to oppose rollover (Chang, 2001).

Chang (2001) explained vehicle stability resting on horizontal alignment compelling into description vehicle body roll along with discovering that the rollover might be more critical as compared with lateral skidding once contemplating modern vehicles. Furthermore, the threshold of rollover is actually less than what is presently considered correct within the AASHTO (2004) or TAC (2007) guidelines. In addition, Chang (2001) suggests that the consequence of the mechanism of vehicles on minimum radius of horizontal curves can be included in current design criteria to achieve greater consistency between vehicle design and highway.

Sliding or lateral skidding and vehicle rollover provide the two probable reasons for vehicle instability resting on horizontal alignments. There are several vehicle designs along with geometric simplifications prepared within current design guidelines with reference to these possible instabilities. Conceivably the most important issue is that the current design guidelines analysis are based on 2D alignment. Limiting values of design speed, side friction, central acceleration, and superelevation are all complemented together into an effort to present a satisfactory alignment.

Ultimately, a compact vehicle could slide well before it starts to roll over and on to the pavement, especially in wet conditions. Vehicles such as sport utility vehicles (SUV),

vans and trucks have higher centers of gravity than compact vehicles and could roll over before they start to skid and slide, especially within drier conditions along with lower speeds.

2.1.2 Vertical Alignments

Highway alignment is influenced by the topography for the surrounding land. Horizontal alignment is affected by topography; however, there are 3 categories that are separated below that explain in more detail based on terrain (AASHTO, 2004):

In level, sight distances of a highway tend to be long without major expense or construction difficulty. In rolling terrain, highway grade falls below and rises above the natural slopes consistency along with horizontal and vertical roadway alignment being restricted with occasional steep sections. In mountainous terrain, horizontal and vertical alignments require frequent longitudinal and transverse changes within ground elevation with regard to the street or road being abrupt, along with side hill excavation and benching.

Vertical alignment within a highway design is a 2D longitudinal profile cut through the centerline for a road vertically. Vertical alignment contains transition between tangents known as vertical curves and tangents or grades. A vertical curve is known as a parabolic function considering the rate for slope change tends to be constant (Mannering and Kilareski, 1998). Vertical curves are classified into two main categories: sag vertical curves and crest vertical curves. For both sag and crest curves, three entry and exit tangent situations can exist. Entry and exit tangents can both be positive, negative or have

opposite signs, where one is negative and the other is positive. Figure 2.5 shows sag and crest vertical curves of the various entry and exit combination grades.

The vertical curves shown in Figure 2.5 are symmetric, meaning the distance of the beginning for the vertical curve (BVC) going to the point for vertical intersection (PVI) is equal to half the overall amount of the curve length (*L*). Furthermore, the distance of the PVI to that of the end for the vertical curve (EVC) is half of the curve length. BVC and PVC are similar and that EVC can also be referred to as PVT (point of vertical tangent).

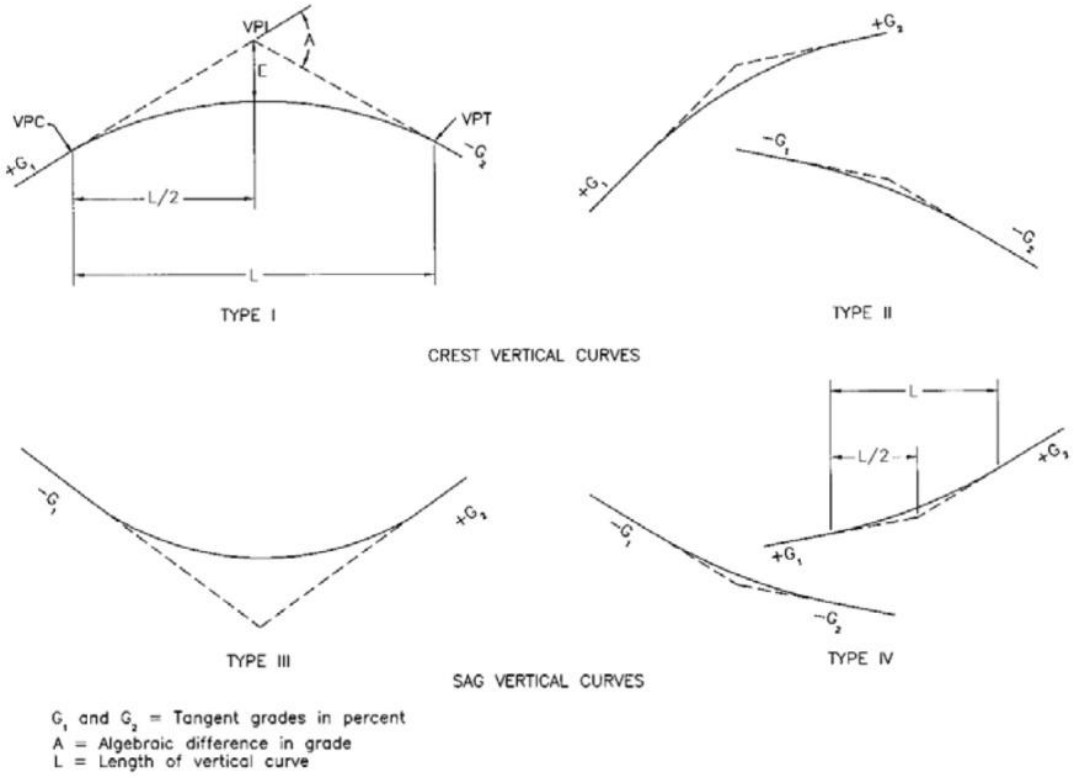

Figure 2. 5 vertical curve combinations (AASHTO, 2004)

VPI, PVI, or PI, means vertical point of intersection, point of vertical intersection, or point of intersection, respectively. All three acronyms can be used interchangeably and

refer to a major intersection for the entry (g_1) along with the exit (g_2) grades. To differentiate in grade between entry and exit tangents, the letter *A* is typically used.

Easa (1994) presented a new unsymmetrical vertical curve (EAU) of highways, which provides important advantageous features. In it, the curve has uneven horizontal projections for the tangents; however, its component of two equal parabolic arcs is efficiently connected within the common curvature point. Additionally, each arc contains a constant rate for change in grade. The rate of change of grades for the two arcs with regards to the EAU curve minimizes the difference and therefore presents an aesthetically pleasing and smooth ride. Furthermore, through this, not only the sight distance improves, but also the length requirement reduces, rider comfort increases, and the vertical clearance increases as compared to the traditional unsymmetrical vertical curve. These important features should make the EAU curve a significant element within vertical alignment design.

Easa (2007) developed a new single-arc unsymmetrical vertical curve (SAU), involving highways, which acquires the cubic function form. The rate of change within grade of a curve fluctuates gradually among the curves' beginning and end. The SAU curve lies above the flatter arc and under the sharper arc for the EAU vertical curve, therefore making it smoother. Furthermore, the SAU curve marginally improves the sight distance of the highway. The offsets for the EAU and SAU curves are equal by the curve mid-point, whereas the backward and forward offsets of SAU curve are not equal. Additionally, the SAU curve rate of change in grade at the mid-points is equal to the EAU curve average for the rate of change in grade for the two arcs.

2.1.2.1 Vertical Curve Equation

Vertical curves are mostly parabolas that are usually centered between tangents that they join within the PVI or VPI. Vertical curves are explained mathematically with the following relationship:

$$y = ax^2 + bx + c \tag{2.22}$$

where,

y = roadway elevation along the vertical curve

x = distance from PVC or BVC ; (m)

c = elevation at PVC or BVC since at $x = 0$, y = PVC elevation

Defining terms a, and b, the first result for Equation 2.22 is needed.

$$\frac{dy}{dx} = 2\,ax + b \tag{2.23}$$

Applying the periphery condition with PVC, $x = 0$, Equation 2.23 is,

$$\frac{dy}{dx} = b = g_1 \tag{2.24}$$

The second result for Equation 2.22 is the rate of change for the slope and is shown by,

$$\frac{d^2y}{dx^2} = 2a \tag{2.25}$$

The rate of change of slope shown in Equation 2.25 can also be shown

$$\frac{d^2y}{dx^2} = \frac{g_2 - g_1}{L} \tag{2.26}$$

Equation 2.25 and Equation 2.26 can be simplified while calculating for a yield,

$$a = \frac{g_2 - g_1}{2L} \tag{2.27}$$

Replacing Equation 2.27 along with 2.24 in Equation 2.22 while letting $c = y_o$ = elevation within PVC, results as:

$$y = \left(\frac{g_2 - g_1}{2L}\right) x^2 + g_1\, x + y_o \tag{2.28}$$

Previously, g_2-g_1 is equivalent to the geometric difference in grades. *A*, along with the design guides defining '*K*' factor that differentiates vertical curve compared to the rate of change in slope along with length as

$$K = \frac{L}{g_2 - g_1} = \frac{L}{A} \tag{2.29}$$

Replacing Equation 2.29 within 2.28 gives

$$y = \left(\frac{x^2}{2K}\right) + g_1\, x + y_o \tag{2.30}$$

Choosing a minimum curve length for *K* factor of a specific condition presents geometric control of vertical curves. Major situations can have vertical acceleration comfort, aesthetics or sight distance. In certain cases where multifaceted vertical alignment restraints do not ease the use for unsymmetrical or traditional vertical curves, what are then beneficial are the three-arc curves. The three-arc vertical curve was developed by Easa (1999), where three separate parabolic arcs are connected to the point for common curvature. It was also determined that the equivalent arc unsymmetrical vertical curve for the three-arc version was a special case. Traditional vertical curves were compared to the three-arc vertical curves and it showed that the three-arc curves were more accommodating in assuring difficult vertical clearance requirements and helped with sight distance (Easa, 1998).

Vertical curves deal with traditional parabolic arc positioned within two vertical transitions. Transitioned vertical curve within vertical alignment is similar to using spiral transitions on a horizontal curve within a horizontal curve with the mathematical calculation being different (Easa and Hassan, 2000). The transitioned vertical curve formulae were developed to explain the rate of curvature, instantaneous elevation and

geometry. The transitioned vertical curve is "especially useful for sharp vertical alignments" and was developed to maintain driver comfort.

2.1.2.2 EAU Vertical Curve Equations

Easa (1994) developed a new unsymmetrical vertical curve (EAU), with uneven projection for the tangents; however equivalent component parabolic arcs, providing improved clearance and sight distance versus traditional unsymmetrical vertical curves (TA). Additionally, in the EAU curve the rate of change of grade is minimized which increases the comfort of the rider thus resulting in higher aesthetics. Easa (1994) discusses a traditional unsymmetrical crest vertical curve, as shown in Figure 2.6. The curve has two parabolic arcs which have a common tangent by the point of common curvature (PCC). The intersection of the two tangents is where the PCC lies, also known as the point of vertical intersection (PVI). The two points of the vertical curve (BVC and EVC) are the beginning and end points having tangents with grades g_1 and g_2. The geometric difference with Grade A equals $|g_2\text{-}g_1|$. For sag vertical curves ($g_2\text{-}g_1$) is positive and for crest vertical curves, it is negative. The Absolute value for ($g_2\text{-}g_1$) then is used where A is positive for sag vertical and crest vertical curves. Hickerson (1964) provides the rate of change of grades for the two arcs.

$$r_1 = \frac{AL_2}{100\,L\,L_1} \tag{2.31}$$

$$r_2 = \frac{AL_1}{100\,L\,L_2} \tag{2.32}$$

where,

r_1 = rate of change of grades for the first arc,

r_2 = rate of change of grades for the second arc,

A = algebraic difference in grad (in percent),

L_1 = length for the first arc,

L_2 = length for the second arc, and

L = total length for the curve ($L_1 + L_2$).

r_1 and r_2 for both sag vertical curves and crest vertical curves will be positive. When L_1 = L_2 = *L*/2, Equations 2.31 and 2.32 present r_1= r_2 =*A*/100*L*, the rate of change of grades for a symmetrical curve, r. In regards to an unsymmetrical vertical curve where L_1<L_2 , r_1>*r* and r_2<*r*. This formula shows the first arc has a curvature that is larger (is sharper) than that of the symmetrical vertical curve, and the second arc has a curvature smaller (is flatter) than that of the symmetrical vertical curve. *R* is a parameter that describes the unsymmetrical vertical curve. It is characterized as the ratio for the length of the shorter tangent (or a shorter arc when dealing with a traditional curve) in regards to the total curve length.

$$R = \frac{L_1}{L} \tag{2.33}$$

Conveying Equations 2.31 and 2.32, in terms of *R* equals:

$$r_1 = \frac{A(1-R)}{100\,L\,R} \tag{2.34}$$

$$r_2 = \frac{AR}{100\,L\,(1-R)} \tag{2.35}$$

For R = 0.5 Equations 2.34 and 2.35 provide: $r_1 = r_2 = A/100\,L$, as the traditional curve diminishes to a symmetrical vertical curve. The EAU curve is derived from a common unsymmetrical vertical curve where the location of PCC is at a random point.

Easa (1994) provided an EAU curve for a larger vertical clearance, illustrated in Figure 2.6. The vertical clearance has the maximum difference appearing between the second arc for the traditional curve and the first arc for the EAU curve. The maximum difference of derivation for a crest vertical curve along with its location follows. Easa (1994) shows the r_1, r_2 for the EAU curve can be explained as:

$$r_1 = \frac{A(3-4R)}{100\,L}, \; L_1 < L_2 \tag{2.36}$$

$$r_2 = \frac{A(-1+4R)}{100\,L}, L_1 < L_2 \tag{2.37}$$

the first arc and the second arc elevations for the EAU curve can be calculated from Equation (2.38) and (2.39), respectively:

$$y_1 = y_{BVC} + \frac{g_1\,x}{100} - \frac{r_1\,x^2}{2} \tag{2.38}$$

$$y_2 = y_{EVC} - \frac{g_2\,(L-x)}{100} - \frac{r_2\,(L-x)^2}{2} \tag{2.39}$$

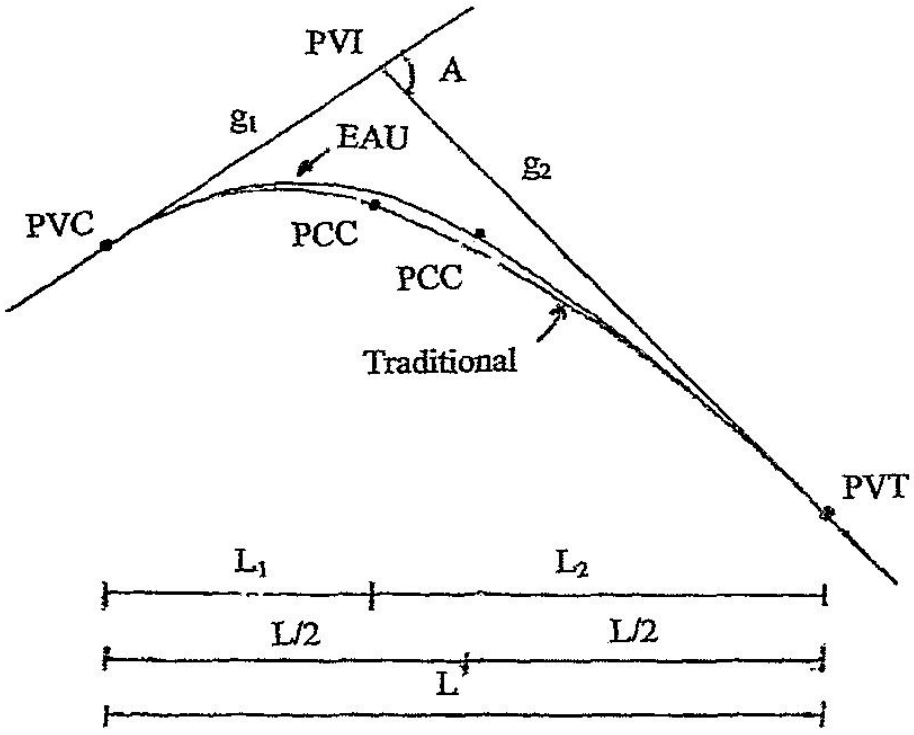

Figure 2. 6 Traditional unsymmetrical and equal-arc unsymmetrical (EAU) vertical curves (Easa, 2007)

2.1.2.3 SAU Vertical Curve Equations

Easa (2007) developed a new single-arc unsymmetrical curve (SAU) similar to the traditional (TA) and (EAU) unsymmetrical curves. The new single-arc unsymmetrical curve attaches two tangents within grades g_1, and g_2 as well as tangent lengths L_1, along with L_2. Consider 2D, where the horizontal direction for the road is along with the x-axis and the vertical direction passing through PVC is alone with the y-axis, as shown in Figure 2.7. Easa (2007) proposes the development of the SAU curve by considering a crest vertical curve, although the results are also applicable towards sag vertical curves.

To determine curve constrains the universal equation of SAU curve is known by the consequent cubic polynomial:

$$y = a + bx + cx^2 + dx^3 \quad (2.40)$$

Where a, b, c, and d are the determined constraints, and *x*, *y* are coordinates to any point (x, y) lying on the curve.

h_{PVC} = The elevation of PVC and

h_{PVT} = The elevation of PVT, is calculated as

$$h_{PVT} = h_{PVC} + g_1 L_1 + g_2 L_2 \quad (2.41)$$

To establish the curve constraints, let us consider the elevations at the curve as limits, where $y = h_{PVC}$ at $x = 0$ and $y = h_{PVT}$ at $x = L$. Then,

$$h_{PVC} = a \quad (2.42)$$

$$h_{PVT} = a + bL + cL^2 + dL^3 \quad (2.43)$$

The curve slope at any point (x, y) is known through the first derivative for *y* within *x* of Equation (2.40),

$$\frac{dy}{dx} = b + 2cx + 3dx^2 \quad (2.44)$$

While $\frac{dy}{dx} = g_1$, at $x = 0$ and $\frac{dy}{dx} = g_2$ at $x = L$, consequently, from Equation (2.44)

$$g_1 = b \tag{2.45}$$

$$g_2 = b + 2cL + 3dL^2 \tag{2.46}$$

The grade (rate of change of the slope) is known from the second derivative for y as:

$$\frac{d^2y}{dx^2} = 2c + 6dx \tag{2.47}$$

Consent to grade (the rates of change of the slope) at x = 0 and x = L are indicated by r_{PVC} , and r_{PVT}, correspondingly. Subsequently,

$$r_{PVC} = 2c \tag{2.48}$$

$$r_{PVT} = 2c + 6dL \tag{2.49}$$

The third derivative for y from Equation (2.40) is specified by

$$\frac{d^3y}{dx^3} = 6d = t \tag{2.50}$$

where, t is a constant. The second derivative of the parabola is constant, frequently referred to the rate of change in grade. The rates of change in grade for the existing unsymmetrical curve (TA) along each parabolic arc, r_1, and r_2,or r_{1t} and r_{2t}, are constant.

Based on the Equations (2.42), (2.45), (2.48), and (2.50), the SAU curve constraints can be resolved and the SAU curve equation becomes

$$y = h_{PVC} + g_1 x + \frac{r_{PVC}}{2} x^2 + \frac{t}{6} x^3 \tag{2.51}$$

The constraints r_{PVC} and t can be resolved as functions for the given curve geometric variables. Writing the Equations (2.43) and (2.46), correspondingly, as

$$t = \frac{6}{L^3} \left(h_{PVT} - h_{PVC} - g_1 L - \left(\frac{r_{PVC}}{2}\right) L^2\right) \tag{2.52}$$

$$t = \frac{2}{L^2} \left(g_2 - g_1 - r_{PVC}\, L\right) \tag{2.53}$$

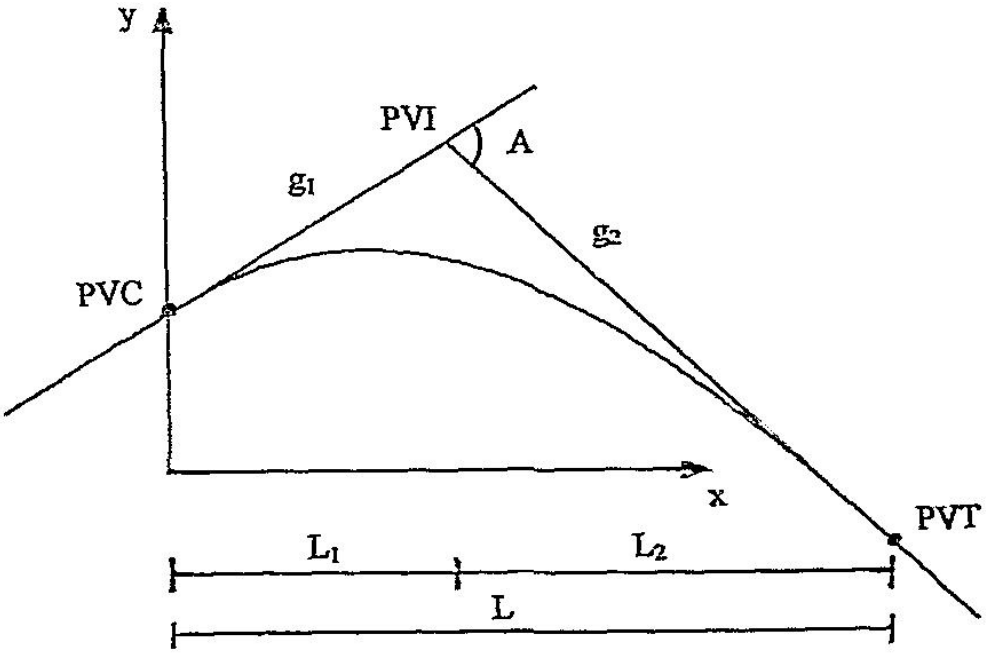

Figure 2. 7 Geometry of the new single-arc unsymmetrical vertical curve (SAU); (Easa, 2007).

and solving Equations (2.52) and (2.53) of r_{PVC} and t, subsequently

$$r_{PVC} = \left(\frac{-2A}{L^2}\right)(L_1 - 2\,L_2) \tag{2.54}$$

$$t = \left(\frac{6A}{L^3}\right)(L_1 - L_2) \tag{2.55}$$

based on Equation (2.49),

$$r_{PVT} = \left(\frac{-2A}{L^2}\right)(L_2 - 2\,L_1) \tag{2.56}$$

The SAU curve is attractive since it generates the symmetrical parabolic curve as a particular case. Representing a symmetrical curve, where $L_1 = L_2 = L/2$, Equations (2.54)-(2.56) defer $t = 0$ and $r_{PVC} = r_{PVT} = A/L = r$, as predictable. Since the equation for the SAU curve is cubic, it is important to guarantee that the curve is convex among PVC and PVT of a crest curve (or concave of a sag curve). This requirement involves that the inflection point of Equation (2.51) does not remain between PVC and PVT. The distance between PVC along with the inflection point can be resolved by associating the second derivative from Equation (2.46) to zero. This distance corresponds to replacement for c and d, subsequently

$$L_{max} = \frac{-r_{PVC}}{t} \tag{2.57}$$

The requirement of convexity (or concavity) is

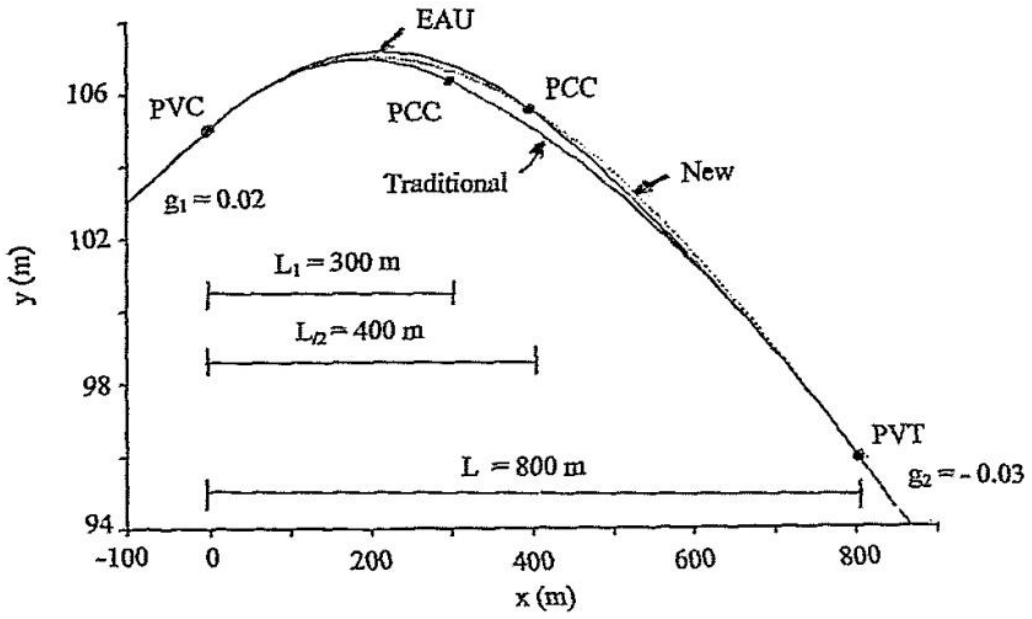

Figure 2. 8 Comparison of new and existing unsymmetrical vertical curves (Easa, 2007).

$$L \leq \frac{-r_{PVC}}{t} \qquad (2.58)$$

Replacement for r_{PVC} and t of Equations (2.54) and (2.55) to Equation (2.58) and substitute L_2 by L - L_1, the requirement becomes

$$\frac{L_1}{L} \geq 0.33 \qquad (2.59)$$

2.1.3 Cross Section along with Superelevation

The cross section is one of the principal elements within alignment and suitable consideration for this element absolutely contributes towards vehicle stability. Cross sectional design deals with several roadway features containing clearance with roadside

obstructions, when there is a median width, shoulder width and lane features of drainage and superelevation to change little. Careful consideration is required by the designer, but this discussion will be focused on the topic of superelevation.

When vehicle stability is on horizontal or else combined alignments, superelevation and side friction factors are the most significant characteristic of cross section. On tangents, the duration of superelevation is identical with cross slope or cross fall. Cross slope is basically provided to guarantee tolerable drainage, for even if it presents a longitudinal slope on the roadway, there is no assurance that water will move around and pass through the segment of the lane into the shoulder along with ditch or gutter.

Superelevation can be utilized on circular curves to minimize the magnitude for the centripetal force that proceeds on the vehicle (Lamm et al., 1999). Concededly, the vehicle travels on a horizontal curve that is subjected to the centripetal acceleration which is comparative with the vehicle speed. When the pavement surface is rotated to the curve center, it maximizes the vehicle stability and affords favourable pavement surface conditions.

The section of suitable superelevation rates is significant and all kinds of probable environment conditions should be considered when choosing this rate. When a rate that is higher or sudden is preferred, it may delay vehicle safety within icy curves at awfully low speeds. Lamm et al.(1999) stated that maximum superelevation, minimum superelevation rates should also be within the limitation to guarantee vehicle stability along with safety

because higher rates can affect a vehicle to slide across a highway while a vehicle makes an effort to accelerate for a complete stop, or stop in icy conditions (Lamm et al., 1999).

An assessment for the point mass equation associated along with maximum superelevation is required so that the variability depending on the type of terrain is taken into consideration along with predictable current environmental conditions. Superelevation higher rates reduce the side friction factor required to ensure vehicle stability at a certain design speed construction costs. Furthermore, when the horizontal radius curve is large, it can be very costly and unpractical to accomplish within mountainous terrain.

There is positive superelevation when the surface of pavement is rotated to the center of the curve, and negative superelevation but less effect resting on vehicle stability. Negative superelevation explains the continuance of a normal crown for the pavement surface resting on a horizontal curve either if it is gone from the curve centerline, it is utilized "…as a sound solution for road surface drainage in terms of economics and environmental compatibility." (Lamm et al.,1999).

2.2 Superelevation Distribution Methods

Superelevation is the rotation or tilting for a highway within a horizontal curve to defy certain lateral forces occurring within weight, speed, motion and directional change for the vehicle. In addition, the superelevation is defined as the vertical distance between height points of the inner and outer edges belonging to railroad rails or highway

pavement. The relationship belonging to friction forces and speed between the pavement and tires, the curve radius along with the superelevation rate was developed as a distribution method used within the design formulation for a horizontal curve from the 1940s. This will be the basis for the vertical curve equation illustrated early in this chapter.

A highway is superelevated when one side is raised within this way. The banking or rotation for the highway can be used for motor sports racing on speedways and also can be used in both urban and rural highways. A highway can rotate around a centerline as well as an inner edge or outer edge of the profile, otherwise a part of the cross slope of the highway can be rotated around the outer edge (ASHTTO, 2001). Then, the question arises: How much must the highway rotate in order to maintain the vehicles safety while crossing the horizontal curve within a highway that is close to a certain design speed without a slower vehicle sliding down a slope within a superelevated roadway?

AASHTO recommends the maximum rates for superelevation for a highway can be controlled within four factors (more details in Chapter 3). The various maximum superelevation rates (e_{max}), based on NCHRP439, present another situation, such as violation for driver's expectancy. It is due to these alternative maximum superelevation rates, an analysis from AASHTO states there are various superelevation rates that apply to each maximum superelevation rate required within the similar design speed. Therefore, the need to present a method for distributing superelevation rates to solve this dilemma is imperative.

2.2.1 AASHTO Methods

In 1965, the Association of State Highway and Transportation Officials (AASHTO) published Geometric Design of Rural Highway. This guideline highlights 5 methods for superelevation distributions that have been used with curve designs over the past 40 years. To allow the stability for this study, the 5 methods that are contained within AASHTO (2004), are stated as follows:

Method 1

Superelevation along with side friction is directly in proportion with the opposite radius (for example, a straight line connection is between $1/R = 1/R_{min}$ illustrated with curve 1 within Figure 2.9.A.)

The AASHTO (2004) as well offers the following information with regards to the first method.

A relationship for a straight-line involving superelevation along with an inverse for the curve radius found within Method 1 find that there are related relationships with both side frictions along with the radius of traveling vehicles that are within average running speed or the design speed. This method contains simplicity, logic and value. For a given highway, horizontal alignment has curves and tangents with different radii that are either equal to or greater than the allotted minimum radius of design speed (R_{min}). Application for superelevation that has quantities that are precisely proportional with the inverse for the radius could, for vehicles that are driving at consistent speed, conclude that side

friction factors pertaining to straight-line deviation involving zero within tangents (not including cross slope) toward maximum side friction within minimum radius.

This method could materialize to be the means for distributing side friction factor; however, its suitability varies with travel at constant speeds from each vehicle within a traffic stream, despite whether travel will be within a curve, intermediate design, an intermediate degree curve, and a design speed curve with minimum radius or a tangent. Consistent speed is always the goal for most drivers, which can be achieved within highways that are well designed with no heavy volumes; there becomes a focus that certain drivers will travel faster within flatter curves and tangents rather than within curves that are sharp, especially when being delayed without the opportunity for slower passing moving vehicles. This tends to show the desire for presenting superelevation rates of intermediate curves within excess for the results with Method 1.

From the previous information, Method 1 deals with the variation within friction factor and with relation to the change within speed; conversely, the vehicles should drive and maintain a constant speed. This may not be possible because speed variations transpire repeatedly since drivers typically do not maintain a constant speed. As well, Method 1 shows the physical state of a vehicle navigating through a superelevated curve. Nicholson (1998) shows Method 1 is expressed mathematically this way:

$$e_1 = \frac{R_{min}}{R} e_{max} \; ; f_1 = \frac{V^2}{gR} - \frac{R_{min}}{R} e_{max} \; ; (R_{min} \leq R \leq \infty) \qquad (2.60)$$

It can also be expressed:

$$e_1 = \frac{e_{max}}{(e_{max}+f_{max})} \frac{V^2}{gR}\,;\; f_1 = \frac{f_{max}}{(e_{max}+f_{max})} \frac{V^2}{gR}\,;\; (R_{min} \leq R \leq \infty) \qquad (2.61)$$

It is shown, Method 1 contains the suggestion which states the centrifugal force that arises from both the superelevation and side friction when *R* is larger than R_{min} is similar as when $R = R_{min}$ (Nicholson, 1998).

Method 2

Regarding Method 2, side friction states when a vehicle that is traveling within design speed has lateral acceleration constant within side friction on the curves up toward requiring f_{max} superelevation is applied until *e* reaches e_{max}. Within this method, first *f* then *e* is increased within inverse proportion into the radius of curvature, as illustrated with curve 3 in Figure 2.9.B.

AASHTO (2004) provides the following information in Method 2:

Method 2 utilizes side friction for sustaining lateral acceleration up toward the curvature that correlates within maximum side friction factor; hence sharper curves deal with maximum side friction factor. Concerning Method 2, superelevation is established once maximum side friction is used. Consequently, superelevation is not required for curves that are flat which require less maximum side friction regarding vehicles that travel with the designed speed (curve 2 within Figure 2.9A). Whenever superelevation is required, swift increases within maximum side friction and curves grow. Method 2 depends fully

on side friction availability, so it is to be utilized with highways and low-speed streets. This method is beneficial for urban streets with lower speeds where, due to certain limitations, frequent superelevation is not presented.

This method has been implemented within the design for urban streets that contain low speed. This method is not capable of being used with higher speed of sharper curves due to its dependency for available friction. Dealing with high speed, drivers surpass the maximum friction with ease; the danger of skidding coupled with the loss of control will become higher when the curve becomes sharper. Nicholson (1998) shows Method 2 is mathematically illustrated by the following:

$$e_2 = \frac{V^2}{gR} - f_{max} \; ; \; f_2 = f_{max} \; ; (R_{min} \leq R \leq R_{fo}) \tag{2.62}$$

$$e_2 = 0 \; ; \; f_2 = \frac{V^2}{gR} \; ; \quad (R_{fo} \leq R \leq \infty) \tag{2.63}$$

With the radius that is the smallest relying by side friction is:

$$R_{fo} = \frac{V^2}{g \, f_{max}} \tag{2.64}$$

Method 3

Superelevation states that when a vehicle is traveling at design speed, it has lateral forces that are constant with superelevation on curves toward requiring e_{max}. Regarding sharper curves, *e* remains e_{max} whereas side friction can then be used to maintain lateral

acceleration until f reaches f_{max}. Within this method, first e followed by f is increased within inverse proportion of the radius for the curvature. Nicholson (1998) shows Method 3 is expressed mathematically:

$$e_3 = e_{max} \; ; f_3 = \frac{V^2}{gR} - e_{max}; (R_{min} \leq R \leq R_{eo}) \tag{2.65}$$

and

$$e_3 = \frac{V^2}{gR}; \quad f_3 = 0 \; ; \quad (R_{eo} \leq R \leq \infty) \tag{2.66}$$

With the radius that is the smallest relying on superelevation is:

$$R_{eo} = \frac{V^2}{g \, e_{max}} \tag{2.67}$$

AASHTO (2004) provides the following discussion on Method 3.

Regarding Method 3 that has been carried out for many years, sustaining lateral acceleration regarding superelevation when a vehicle is traveling within design speed can be presented for all curves that require maximum realistic superelevation, where maximum superelevation within sharp curves is present. Within this method, side friction within flat curves is not provided less than the vehicles travelling at both design speed and maximum superelevation, as illustrated within Curve 3 for Figure 2.9.B, along with suitable side friction increasing quickly when curves that have maximum superelevation become sharper. Furthermore, illustrated by Curve 3 in Figure 2.9.C, regarding vehicles that are traveling within average running speed, negative friction results from this with curves that have extremely flat radii to middle range for curve radii; once curves are

sharper, side friction then increases tremendously to the maximum equivalency of the curvature of the minimum radius. The difference within side friction regarding different curves may not be rational and could end up with irregular driving, with the average running speed or the design speed.

The main issues regarding this method derive from the different curves having various side frictions dependent on how sharp the curve is. It also is not true physically, which states that there will be no side friction in between the pavement and the tires. Side friction is present within the tires due to it being a function for the weight of a car that is normal within the surface of the pavement. Friction allows a vehicle to corner, it allows it to brake, and allows the acceleration forces to transfer the forces to the pavement from the tires. Instead of using "coefficient of friction" for dynamics, highway engineers will instead use ratios for lateral forces where the pavement resists. This type of lateral ratio is also known as "friction factor." (AASHTO, 1984).

The friction factor needed to counter centrifugal forces can be reduced with vehicle braking (both accelerating and decelerating). When friction is utilized for sudden stopping, there will be little friction left to corner. Antilock Braking Systems (ABS) has helped improve this situation. The friction factor can also be dependent on any number of variables, such as, weight, vehicle speed, tire condition (tire pressure, tire temperature, wear), suspension, tire design (rubber compound, tread, sidewall stiffness, contact patch); pavement, along with any substance that is between the pavement and tire. As the friction factor starts to decrease when speed increases, several friction factor studies have been

conducted for various speeds (AASHTO, 2001). Friction factor decreases drastically once the tires begin to spin either slower and faster than that of the speed of the vehicle (for example, within a skid, tires spinning while trying to either accelerate or come to a full stop on the ice, as well, during a “peel out” or “burn out”).

Consequently, an improved method of the distribution method will take into account that the concurrent effect for the superelevation along with side friction within the vehicle passing a curve. The approach for Method 3 ends up with irregular driving done at the running speed and the design speed. This corresponding effect for the friction along with superelevation effects and the speed variation are illustrated in section 2.1.1.2 of this chapter.

Method 4

Method 4 is similar to Method 3, with the exception that Method 4 deals with running speed average instead of dealing with design speed.

The AASHTO (2004) offers the following consideration regarding method 4.

With Method 4, permeating the inefficiencies of Method 3 is the purpose, by utilizing superelevation at lower speeds than that of design speed. Method 4 has been utilized for average running speeds of which lateral acceleration can be constant by superelevation for curves that are flatter then superelevation for maximum rate. The average running speed presented in Table 2.1 is approximate, fluctuates at 78 to 100 [80 to 100] % for design speed. Curve 4 within Figure 2.9.A illustrates when utilizing this method,

maximum superelevation can be attained within the curvature range middle. Figure 2.9.C illustrates with average running speed that no side friction at this curvature is required, while side friction quickly increases within direct proportion of sharper curves. However, Method 4 has similar disadvantages to Method 3, yet those apply at smaller degrees.

Similar comments within Method 3 are provided in Method 4 through the use for lower speed than that of design speeds; whereas this case shows the running speed average. In the two cases, physical friction effects, superelevation and speed variation are not done together. Results are all the same as with Method 3, irregular driving can arise with the running speed average along with the design speed.

Table 2. 1 Average Running Speeds (AASHTO ,2004)

Metric		US Customary	
Design speed (km/h)	Average running speed (km/h)	Design speed (mph)	Average running speed (mph)
20	20	15	15
30	30	20	20
40	40	25	24
50	47	30	28
60	55	35	32
70	63	40	36
80	70	45	40
90	77	50	44
100	85	55	48
110	91	60	52
120	98	65	55
130	102	70	58
		75	61
		80	64

Method 2 Modified

For the four methods of determining the superelevation and side friction, the second one only involves zero superelevation on infinite radius curves. In addition, the second method is also–capable of modification to guarantee that a minimum superelevation is expressed. Nicholson (1998) shows how modified Method 2 mathematically can be explained:

$$e_{2m} = \frac{V^2}{gR} - f_{max} \; ; \; f_{2m} = f_{max} \; ; \; (R_{min} \leq R \leq R_{me}) \tag{2.68}$$

$$e_{2m} = e_{min} \; ; \; f_{2m} = \frac{V^2}{gR} - e_{min} ; \; (R_{me} \leq R \leq \infty) \tag{2.69}$$

where, 2m = "modified method 2."

where the smallest potential radius to be used and minimum superelevation applied is e_{min}

$$R_{me} = \frac{V^2}{g\,(e_{min}+f_{max})} \tag{2.70}$$

Method 5

Superelevation along with side friction has a curvilinear relationship with the opposite for the curve radius, within values between that for Methods 1 and 3. Method 5 utilizes a method of curvilinear distribution that depends upon the unsymmetrical parabolic curve of distribution of f which is tangent into two legs that define Method 4. Subtracting the value of *f* from design values for $(e + f)$ to make the curve equation less complex for e,

the final e distribution is obtained. The AASHTO clearly states the Method 5 mathematical formulation. However, the comparison of the Method 5 results is included in chapter 5. AASHTO (1990) discusses that e, related with the degree for curvature (D) for both the curve along with side friction, needs to assure 3 conditions which will be discussed in detail in chapter 3. Easa (1999) shows how Method 5 can be mathematically explained:

$$R_{PI} = \frac{V^2}{g\, e_{max}} \tag{2.71}$$

$$f_5 = f_{max}\ \frac{R_{min}\, R_{PI}}{2\, R^2};\ 1/R \leq 1/R_{PI} \tag{2.72}$$

$$f_5 = f_{max}\left[\frac{R_{min}}{R}\left(\frac{R_{PI}-R}{R_{PI}-R_{min}}\right) + \frac{R_{min}R_{PI}}{2\, R^2}\left(\frac{R-R_{min}}{R_{PI}-R_{min}}\right)^2\right];\ 1/R>1/R_{PI} \tag{2.73}$$

$$e_5 = \frac{V^2}{g\, R} - f_5 \tag{2.74}$$

The AASHTO (2004) provides the discussion of Method 5.

To deal with overdriving, likely occurring within intermediate to flat curves, the approximate superelevation can be acquired by Method 4. Overdriving within certain curves deals with low risk where drivers may lose the control of their vehicle due to superelevation being maintained with lateral acceleration within average running speed, along with side friction available at greater speeds. Method 1, which eludes utilizing maximum superelevation of a significant part for the curve radii range. Regarding Method 5, involving curved lines (Curve 5 illustrated within a range for the triangle that ranges from curve 1 along with 4 within Figure 2.9.A) represent both superelevation

along with side friction distribution practically maintaining the advantages for Method 1 and Method 4. Curve 5 has a practical distribution of superelevation along with having an unsymmetrical parabolic form within a range for curvature.

Method 5 integrates the advantages for both Method 4 and Method 1 to generate a feasible superelevation distribution over a range for curvature with simply illustrating the best fit curve above a considerable region of space that is both practical and reasonable. Even though this provides a preferred result, the calculation is awkward, inflexible and is not easily utilized in practice; therefore, 14 different equations require solving to produce a design curve distribution. So, 10 tables and charts which are provided within the AASHTO are used for design.

2.2.3 Fundamental subject within Superelevation Design

There are two fundamental approaches related to superelevation distribution:

(1) Superelevation within a limited way is used by friction factor for cornering similar to Method 2

(2) Heavy dependency for superelevation and minimum friction factor required to deal with faster drivers, whereas slower drivers utilize superelevation for safety purposes. This prevents negative friction that could force drivers into steering against directions within the curve that may be risky and could result in irregular driving (NCHRP 439).

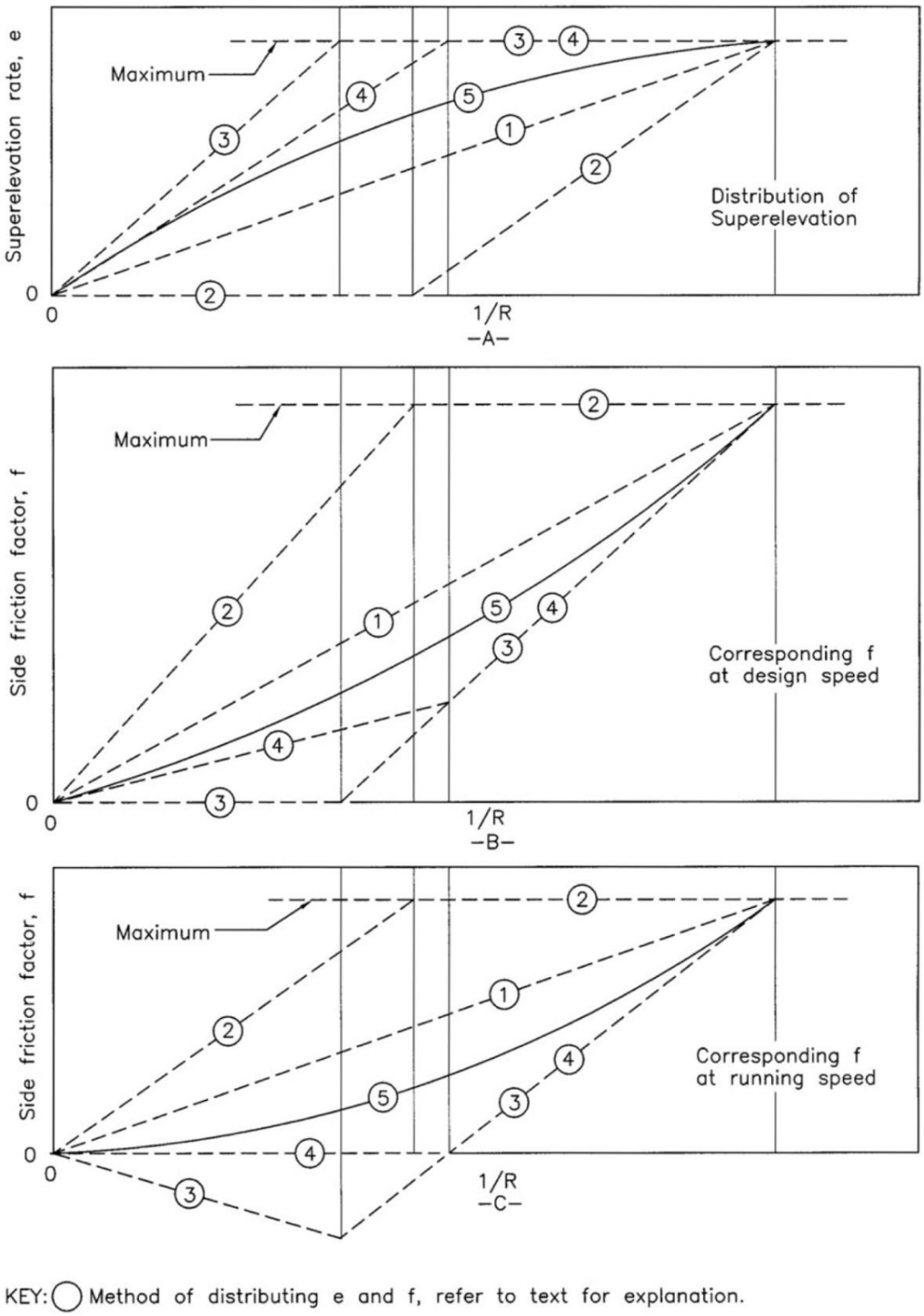

Figure 2. 9 Methods of Distributing Superelevation and Side Friction (AASHTO,2004)

This research presents a straightforward and proper approach towards superelevation distribution with the utilization for EAU Method and SAU Method. This combines advantages with Method 5 along with EAU and SAU curve, respectively, that accounts for speed variation within a vehicle passing through horizontal curve.

2.2.4 Superelevation Distribution Approach by Other International Agencies

NCHRP439 incorporates a review with 6 agencies internationally and noted that of the 6 agencies, 4 have distribution methods capable of providing constant mathematical relationships between radius, design speed and superelevation or an equal plan. The areas are Canada, France, Germany, and the United Kingdom. Figures below (based on NCHRP439) illustrates a similarity with mathematical relationships between Canada and the United States.

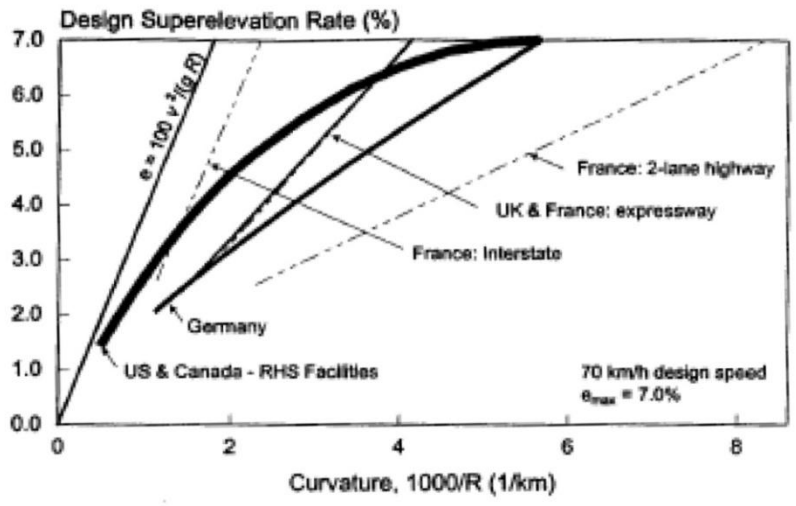

Figure 2. 10 Superelevation distribution methods recommended by several international agencies for high-speed facilities

The first line within the left side of the graph (Figure 2.10) shows the superelevation amount needed to connect centripetal acceleration that is associated within travel for a given curved path thus acting within upper limit control. With the exception of Canada and the United States, which use unsymmetrical parabolic curves, others then use linear relationships from superelevation rate and curvature.

2.3 Highway Consistency

Over half of the fatalities are connected to collisions on rural highways that are located on curved sections (Lamm et al., 1992). Therefore, corresponding transition sections and the curves represent the most critical regions for safety improvements. One of the main objectives that can improve safety on a highway, by considering a system for curves, should be geometric design consistency. Design consistency guarantees that successful geometric elements act in a coordinated way, so they produce coordinated driver performance consistent within driver expectations (Lunenfeld & Alexander, 1990; Krammes et al., 1995).

Evaluating the methods for highway design consistency is classified in three categories: performance, speed, and safety (Gibreel et al., 1999). The performance section includes methods such as driver anticipation, driver workload, and other areas that influence driver performance (e.g., interchange design and aesthetics). Regarding the speed section, evaluating different geometric design consistency elements depends on operating speed. In the safety section, special attention is focused on the effects of superelevation design and side friction and vehicle stability.

2.3.1 Choices for Design Speed

2.3.1.1 Traditional Design Speed Method

The goal is to avoid any geometric inconsistencies by including consistency within the design speed right through the road section. The minimum radius is fixed once a design speed is chosen; AASHTO (Policy 1954) affirmed "there should be no restriction to the use of flatter horizontal curves ... where (they) can be introduced as part of an economic design." Conversely, Barnett (1936) saw "if a driver is encouraged to speed up on a few successive comparatively flat curves, the danger point will be the beginning of the next sharp curve," along with the AASHTO (Policy 1990) cautioned against having a continuous set of flatter curves, for drivers are willing to increase driver speed.

Krammes et al. (1995) voiced concern towards design speed selection within the AASHTO guidelines, citing the 85^{th} percentile operating speeds are usually both greater and less than the design speed once the design speed was both lower and higher than 100 km/h. Krammes et al. recommended as well that another concern was the traditional design speed concept only relates to both horizontal and vertical curves, while not applying to tangents. Krammes et al. (1995) finished with this: "the design speed concept . . . can ensure operating speed consistency only when the design speed exceeds the desired speed of a high percentile of drivers."

Krammes et al. (1995) re-examined both the geometric design consistency practices and policies for a range of countries, those including five European countries, Canada,

Australia and the United States and recognized two very different approaches to improving design consistency. The most familiar is the speed-profile evaluation technique, which is utilized in Germany, Switzerland and France and which Krammes et al. (1995) also suggest utilizing within the United States. The other speed profile is the Australian speed-environment approach that is also utilized within New Zealand; it is the subsequent analysis basis for the effect on different methods in choosing superelevation along with side friction, within the highway alignment consistency.

2.3.1.2 Speed-Environment Approach

The speed-environment method by Rural (1993) entails calculating the 85^{th} percentile desired speed that can also be defined as a "speed environment." Both long and level tangents can be seen as desired speeds, with low traffic concentration where drivers do not have to deal with many other vehicles. McLean (1979) discovered that desired speeds were managed from the driver's opinion within the overall standard for the road section comprising of:

1) The entire geometric standard (particularly horizontal curves).
2) The road environment (mainly the terrain).

Different from traditional design speed that connects with particular geometric elements, it is the speed environment that connects with the substantial road length containing both several tangents and curves and is steady within a segment of the road. A speed environment is measured within an existing section of the road that needs to be calculated

for newer roads that take into account both the range and the terrain for the horizontal curve radii in the road section (Rural, 1993).

The design speed can be defined as "not less than the estimated 85th percentile operating speed on a particular element within a given speed environment" and then utilized similarly to traditional design speed for the coordination of superelevation, side friction, radius and sight distance. Design speed of a given curve radius, calculated utilizing Figure 2.11 , is seen to differ within the speed environment. The design speed approaches the speed environment as the radius increases.

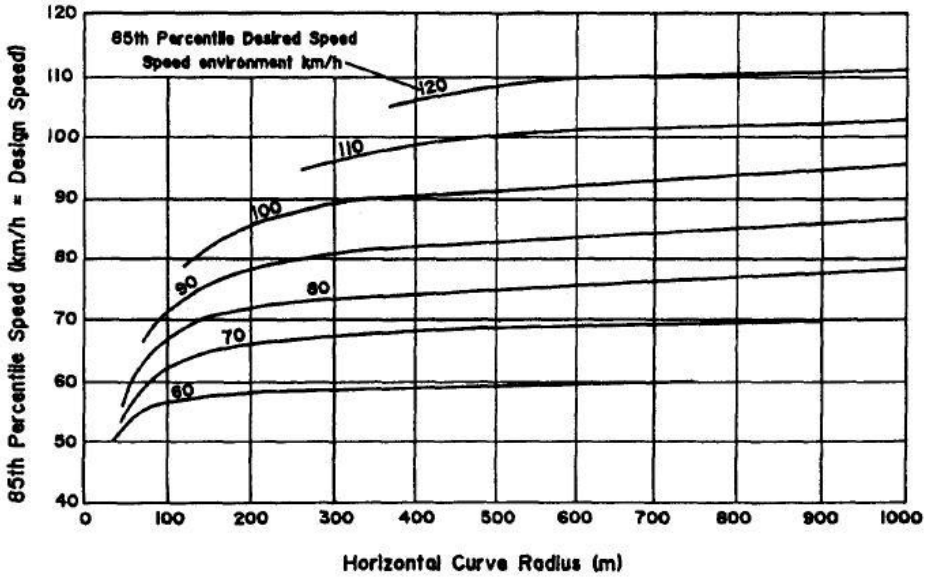

Figure 2. 11 Estimation of design speed (Rural,1993)

Figure 2.12 shows the relationship between both the speed environments of a road section along with the design speeds of the alignment elements in that section. This illustrates the operating speed frequency distributions of a tangent, a low radius curve and a medium

radius curve. The operating speed distribution of the tangent can also be the desired speed distribution (presuming low traffic concentration). Once radius decreases, drivers become more controlled by the geometry, therefore the operating speed distribution variance decreases. For the condition illustrated within Figure 2.12, the speed environment is 109 km/h, when the design speeds (for example, the 85th percentile operating speeds) of the low radius curve, medium radius curve and the tangent are 66, 87, and 109 km/h, respectively. The methods for speed-environment involve the design speed concept for tangents; this is merely the approximate 85th percentile operating speed within the downstream tangent end. To make sure a practical level for consistency between consecutive alignment elements, Austroads (Rural, 1993) suggests that the curve design speed should not be higher than 10 km/h below the design speed for the previous tangent.

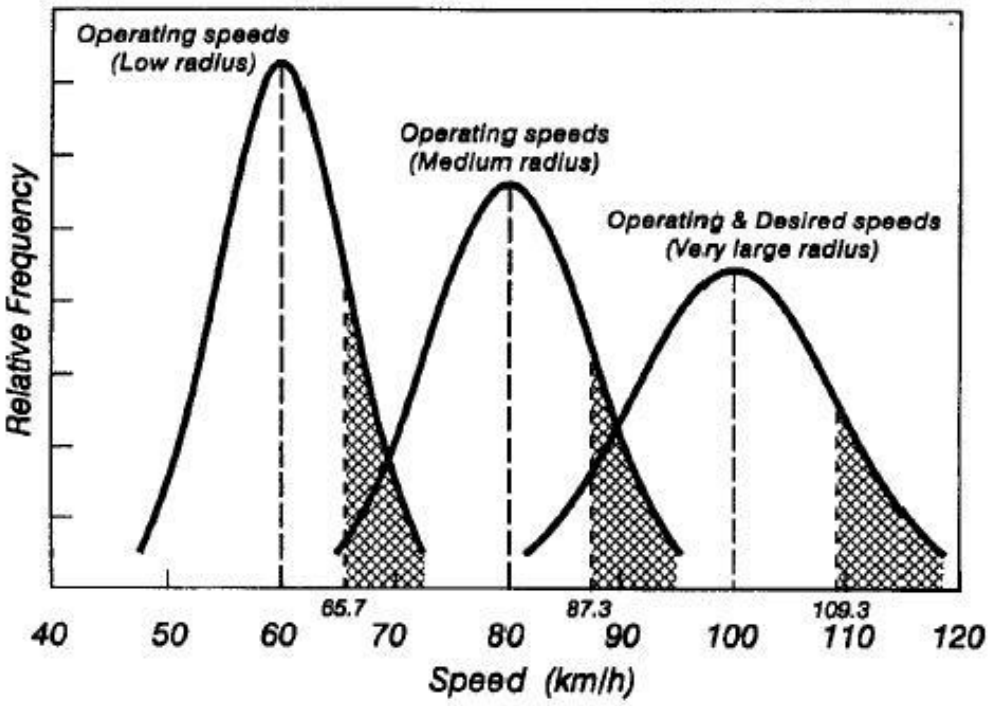

Figure 2. 12 Representative Operating Speed Distribution (Nicholson, 1998)

2.3.2 Superelevation Distribution to Maximize Design Consistency of Highway

Given that AASHTO methods are mainly supported with subjective analysis, Easa (2003) provided an objective approach that distributes superelevation utilizing mathematical optimization in maximizing design consistency. The difference between the design speed and the maximum limiting speed that corresponds to f_{max} is the definition of safety margin. Two analysis types are utilized:

1. Aggregate analysis,
2. Disaggregate analysis.

Aggregate analysis is described as the objective function for the model minimizing total safety margin variation on the highway. Within disaggregate analysis; it is explained as the objective function for the model minimizing individual safety margin variations among adjacent curves. The definition of safety margin stems from Nicholson (1998) where he defines safety margin as "the difference between the speed at which maximum permissible design side friction is being called upon by the driver (sometimes called safe speed) and the design speed". Easa presented an optimization model that eliminates trial and error when determining the necessary *e* by examining the total *e* distribution area among AASHTO Method 2 along with 3 in determining the best *e*. Even though the model provides results that are approximately similar with Method 5, which is the ideal AASHTO distribution method, the method can be utilized for professional practice. However, required influential optimization computer software is needed to present a solution. Furthermore, a complex calculation method presents higher f than that of

Method 5 and utilizes a discrete function that is different from the dynamic equation of vehicle motion within a horizontal curve.

2.4 Summary

Below are important points regarding the literature review of the three main sections, highway geometric design, superelevation distribution methods and highway consistency:

- Highway geometric design:
    - In the horizontal alignment element, the focus is on vehicle motion dynamics within superelevated horizontal curves.
    - In the vertical alignment element, the benefit is to discuss the derivative of EAU and SAU curve equations.
    - In the cross section element along with superelevation, the emphasis contributes toward vehicle stability.
- Superelevation distribution is based on the AASHTO Methods: AASHTO Method 2 is suitable for low speed urban streets and AASHTO Method 5 is suitable for high speed urban streets.
- Highway Consistency:
    - In highway geometric design consistency, the objective is to improve highway safety, by considering a system for curves.
    - In choice of design speed, the goal for traditional design speed method is to avoid any geometric inconsistencies by including consistency within the design speed right through the road section; in addition, the goal for the

speed environment approach involves calculating the 85th percentile desired speed that can also be defined as “speed environment.”

- In safety margin, the objective is to maximize design consistency of the highway using superelevation distribution.

Chapter 3: Existing Methodology for Superelevation Design

This chapter provides the methodology for superelevation design considerations and the superelevation for AASHTO Method 5. Furthermore, a description for superelevation of a system of curves and safety margin are also presented.

3.1 Superelevation Design Considerations

Superelevation rates applied towards a range of curvature of each design speed are used within highway design. One extreme is maximum superelevation rate created to determine the maximum curvature of each design speed, which may be different for various highway conditions. Regarding the other extreme, superelevation is not needed for tangent highways or highways with flatter horizontal curves. For curvature between both extremes along with a specified design speed, the superelevation (*e*) should be selected in a proper manner where there is a sensible relation between the applied superelevation rate and the side friction factor.

3.1.1 Maximum Superelevation

AASHTO recommends that maximum rates for superelevation assumed for highways can be controlled with four factors:

1) Climate conditions – deals with the quantity and the frequency of ice and snow.
2) Terrain Condition - deals with whether or not the terrain will be rolling, mountainous or flat.

3) Determining the area – determining whether it is either urban or rural.
4) Frequency for extremely slow moving vehicles – there are vehicles that may be affected by high superelevation rates. Slow moving vehicles that are on a very icy road may slide down a slope with a superelevated road that is high, while a vehicle that is moving fast along a rural road could turn over within a superelevated road that is low.

Significance for these factors leads to the conclusion that there is no one maximum superelevation rate that is commonly relevant. Thus, utilizing one maximum superelevation rate in a region with comparable climate conditions along with land use being attractive promotes design consistency. Furthermore, AASHTO has concluded, there is "no single maximum superelevation rate that is universally applicable and that a range of values should be used". However, there are some recommendations regarding maximum superelevation rates provided:

1) 4% to 6% of design for urban highways within areas has no constraints.
2) 8% of areas have both snow and have ice.
3) 10% to 12% of areas have no snow or no ice.

Design consistency deals with the consistency for highway alignment along with its related design element dimensions. This consistency allows for drivers to increase their awareness-reaction skills to develop expectancies. Non-consistent design elements with related types of roadways might counteract a driver’s expectancy, and thus will result in a higher driver workload. Rationally, there is a comparison between driver workload,

design consistency along with motorist safety having “consistent” designs that are related with safer highways and lower workloads.

3.1.2 Minimum Superelevation

According to the AASHTO (Policy 1990) guide, "no superelevation is needed for tangent highways or highways with extremely long-radius curves." Furthermore, the Austroads (Rural 1993) guide affirms "it will usually be found desirable to superelevate all curves at least to a value equal to the normal crossfall on straights, unless the radius of an individual curve is so great that it can be regarded as a straight, and normal crossfalls (or adverse superelevation) used."

If normal crossfall in the tangent is maintained within a circular curve, outside of the curve could experience steady superelevation. The issue may exist for those that are inside the curve; when a vehicle is driving very fast, the driver may cross the centerline and experience a change within superelevation to an opposing superelevation. This could explain the likelihood for a driver not maintaining control by increasing a significant condition that may not be reliable within a lenient street. One way to avoid this is to have minimum superelevation $e_{min} > 0$.

3.1.3 Maximum Side Friction Factors

Due to the maximum available side friction factor, horizontal curves are unable to be designed. As an alternative, when used in design, there should be a ratio where maximum

side friction factor is used for both comfort and safety of most drivers. Side friction factor levels that represent bleeding, lacking skid-resistant traits or glazed pavements should not influence design because these conditions that are avoidable regarding geometric design based within a suitable surface condition capable of being achieved is done at reasonable cost (AASHTO, 2004).

Based on both experience and data, AASHTO has developed reliable side friction factor values, which can be used concerning highway curvature design. These values tend to typically be dependent on improved relationships involving both side friction factor and design speed (Alberta Infrastructure, 1999). Maximum safe values for each design speed are illustrated within the Table 3.1.

3.1.4 Minimum Radius

The minimum radius can be a limiting value for curvature of a certain design speed that is calculated based on the maximum side friction factor for design (limiting value for *f*) and the maximum rate for superelevation. Utilizing sharper curvature for a design speed could mean superelevation past the considerable limit or could mean operation within tire friction along with lateral acceleration past the considered comfort area by many drivers. The minimum radius for curvature is a very important control value to determine superelevation rates involving flatter curves (AASHTO, 2004). The minimum radius for curvature, R_{min}, is calculated precisely from the shortened curve formula as shown within section 2.1.1.3 (Equation 2.18). This calculation can determine R_{min}:

$$R_{min} = \frac{V^2}{127\,(0.01\,e_{max}+f_{max})} \quad (3.1)$$

Where,

V = vehicle speed (Km/h)

e = superelevation rate (percentage)

f = side friction factor (no unit)

R_{min} = minimum radius for horizontal curve

3.1.5 Choice of Design Superelevation and Side Friction

Easa et al. (2003) explain the variables utilized within the calculation for the minimum horizontal curve radius adopting the PM model, which include vehicle speed (V), minimum curve radius (R_{min}), maximum side friction (f_{max}), acceleration of gravity (g) and maximum superelevation (e_{max}) along with the side friction, and can all be defined within the design guides between the vertical and horizontal forces. Moreover, it is this ratio between the component for the vehicle weight and the side (or radial) friction force that is perpendicular with the pavement.

Easa et al. (2003) discusses the effect for superelevation that needs raising the radius. As illustrated, regarding e_{max} = 0.06 was shown to be typically more than what was required for e_{max} = 0.04, particularly for lower speeds. It can be explained regarding the conservative rates for side friction utilized within the design guides, particularly for low speeds. It is those conservative rates that could result in unlikely design radii related with higher superelevation. To provide an example, for e_{max} = 0.04 and with V = 60 km/h, the

understood f_{max} = 0.15 (TAC, 1999), along with R_{min} =150 m. Conversely, for e_{max} = 0.06 along with the similar design speed, R_{min} = 130 m (86.7% of R_{min} needed for e_{max} = 0.04). If the definite side friction (keeping the similar safety margin) was higher than f_{max} (0.18), then R_{min} can be 130 along with 120 m for e_{max} = 0.04 and 0.06, in that order, for similar V = 60 km/h. Therefore, R_{min} needed for e_{max} = 0.06 is 92.3% for the required e_{max} = 0.04. The variation within load distribution for different tires increases with a similar increase within superelevation, whereas the load increases within the inner tires then decreases within the outer tires. The difference within load distribution ends up with more disparity within side friction demands for certain truck tires.

3.2 Superelevation Distribution based on AASHTO Method 5

AASHTO (2004) discussed urban highways, rural freeways and high-speed urban streets that account for speed being reasonably uniform and high, horizontal curves tend to be superelevated with successive curves usually balanced to make for a transition that is smooth-riding from one particular curve to the next. The drivers with higher speed are not as comfortable within lateral acceleration in curves. Varying radii involving a series of curves with a balanced design are presented with the suitable distribution for both e along with f values, for selecting a suitable superelevation rate within the range of the maximum superelevation to the normal cross slope.

Figure 3.1 illustrates the suggested side friction factors of urban and rural highways along with highways and high-speed urban streets. They present a practical safety margin of the

various speeds. Maximum side friction factors differ precisely with design speed with a range of 0.40 at 15 km/h to 0.08 at 130 km/h. Dealing with the maximum allowable side friction factors based on Figure 3.1, Table 3.1 provides the minimum radius of each five maximum superelevation rates. Method 5, as explained before, is suggested for the distribution of e and f of all curves that have radii higher than the minimum radius for curvature in urban highways and rural highways along with high-speed urban streets. Uses for Method 5 are explained within the following text and Figure 3.2.

The procedure of development for Method 5 superelevation distribution is illustrated and the side friction factors depicted as a solid line within Figure 3.1, which symbolize maximum f values chosen as design of each speed. When these particular values are used within combination with the suggested Method 5, it determines f distribution curves of the various speeds. Deducting the computed value of ($0.01\ e + f$) from the computed f values within design speed (V), the confirmed e distribution is then attained (Figure 3.2).

Figure 3.2 elaborates on the different methods for distribution involving e along with f over a set of curve ranges available. Even though Method 5 is currently used by AASHTO, this does not mean other methods do not apply or else there is no room to maneuver. An example of the developed superelevation using Method 5 is shown in Figure 3.3 for e = 10%.

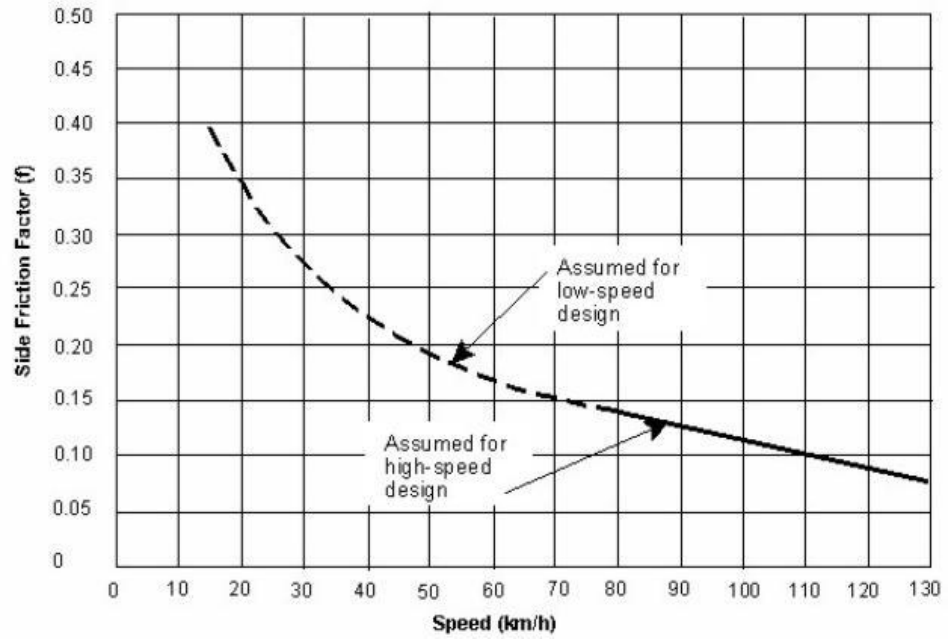

Figure 3. 1 Side Friction Factors based on Design (AASHTO, 2004)

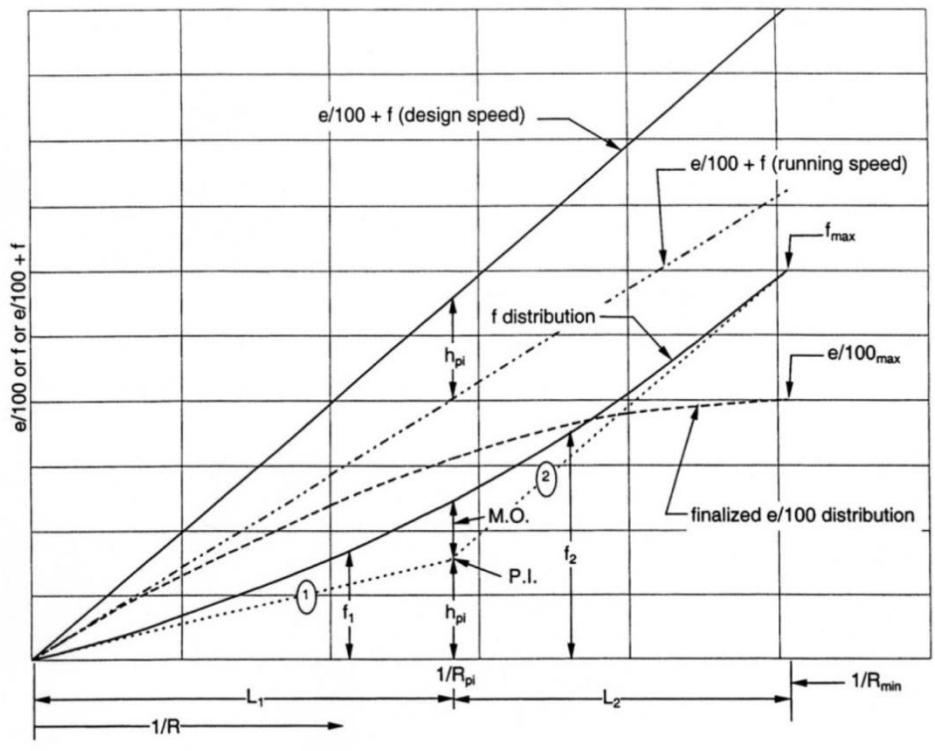

Figure 3. 2 Method 5 Procedure for Development for Superelevation Distribution (AASHTO, 2004)

Table 3. 1 Minimum Radius that use Limiting Values for both e and f (AASHTO, 2004)

METRIC						US Customary					
Design Speed (km/h)	Maximum *e* (%)	Maximum *f*	Total (*e*/100 + *f*)	Calculated Radius (m)	Rounded Radius (m)	Design Speed (mph)	Maximum *e* (%)	Maximum *f*	Total (*e*/100 + *f*)	Calculated Radius (ft)	Rounded Radius (ft)
15	4.0	0.40	0.44	4.0	4	10	4.0	0.38	0.42	15.9	16
20	4.0	0.35	0.39	8.1	8	15	4.0	0.32	0.36	41.7	42
30	4.0	0.28	0.32	22.1	22	20	4.0	0.27	0.31	86.0	86
40	4.0	0.23	0.27	46.7	47	25	4.0	0.23	0.27	154.3	154
50	4.0	0.19	0.23	85.6	86	30	4.0	0.20	0.24	250.0	250
60	4.0	0.17	0.21	135.0	135	35	4.0	0.18	0.22	371.2	371
70	4.0	0.15	0.19	203.1	203	40	4.0	0.16	0.20	533.3	533
80	4.0	0.14	0.18	280.0	280	45	4.0	0.15	0.19	710.5	711
90	4.0	0.13	0.17	375.2	375	50	4.0	0.14	0.18	925.9	926
100	4.0	0.12	0.16	492.1	492	55	4.0	0.13	0.17	1186.3	1190
						60	4.0	0.12	0.16	1500.0	1500
15	6.0	0.40	0.46	3.9	4	10	6.0	0.38	0.44	15.2	15
20	6.0	0.35	0.41	7.7	8	15	6.0	0.32	0.38	39.5	39
30	6.0	0.28	0.34	20.8	21	20	6.0	0.27	0.33	80.8	81
40	6.0	0.23	0.29	43.4	43	25	6.0	0.23	0.29	143.7	144
50	6.0	0.19	0.25	78.7	79	30	6.0	0.20	0.26	230.8	231
60	6.0	0.17	0.23	123.2	123	35	6.0	0.18	0.24	340.3	340
70	6.0	0.15	0.21	183.7	184	40	6.0	0.16	0.22	484.8	485
80	6.0	0.14	0.20	252.0	252	45	6.0	0.15	0.21	642.9	643
90	6.0	0.13	0.19	335.7	336	50	6.0	0.14	0.20	833.3	833
100	6.0	0.12	0.18	437.4	437	55	6.0	0.13	0.19	1061.4	1060
110	6.0	0.11	0.17	560.4	560	60	6.0	0.12	0.18	1333.3	1330
120	6.0	0.09	0.15	755.9	756	65	6.0	0.11	0.17	1656.9	1660
130	6.0	0.08	0.14	950.5	951	70	6.0	0.10	0.16	2041.7	2040
						75	6.0	0.09	0.15	2500.0	2500
						80	6.0	0.08	0.14	3047.6	3050
15	8.0	0.40	0.48	3.7	4	10	8.0	0.38	0.46	14.5	14
20	8.0	0.35	0.43	7.3	7	15	8.0	0.32	0.40	37.5	38
30	8.0	0.28	0.36	19.7	20	20	8.0	0.27	0.35	76.2	76
40	8.0	0.23	0.31	40.6	41	25	8.0	0.23	0.31	134.4	134
50	8.0	0.19	0.27	72.9	73	30	8.0	0.20	0.28	214.3	214
60	8.0	0.17	0.25	113.4	113	35	8.0	0.18	0.26	314.1	314
70	8.0	0.15	0.23	167.8	168	40	8.0	0.16	0.24	444.4	444
80	8.0	0.14	0.22	229.1	229	45	8.0	0.15	0.23	587.0	587
90	8.0	0.13	0.21	303.7	304	50	8.0	0.14	0.22	757.6	758
100	8.0	0.12	0.20	393.7	394	55	8.0	0.13	0.21	960.3	960
110	8.0	0.11	0.19	501.5	501	60	8.0	0.12	0.20	1200.0	1200
120	8.0	0.09	0.17	667.0	667	65	8.0	0.11	0.19	1482.5	1480
130	8.0	0.08	0.16	831.7	832	70	8.0	0.10	0.18	1814.8	1810
						75	8.0	0.09	0.17	2205.9	2210
						80	8.0	0.08	0.16	2666.7	2670
15	10.0	0.40	0.50	3.5	4	10	10.0	0.38	0.48	13.9	14
20	10.0	0.35	0.45	7.0	7	15	10.0	0.32	0.42	35.7	36
30	10.0	0.28	0.38	18.6	19	20	10.0	0.27	0.37	72.1	72
40	10.0	0.23	0.33	38.2	38	25	10.0	0.23	0.33	126.3	126
50	10.0	0.19	0.29	67.9	68	30	10.0	0.20	0.30	200.0	200
60	10.0	0.17	0.27	105.0	105	35	10.0	0.18	0.28	291.7	292
70	10.0	0.15	0.25	154.3	154	40	10.0	0.16	0.26	410.3	410
80	10.0	0.14	0.24	210.0	210	45	10.0	0.15	0.25	540.0	540
90	10.0	0.13	0.23	277.3	277	50	10.0	0.14	0.24	694.4	694
100	10.0	0.12	0.22	357.9	358	55	10.0	0.13	0.23	876.8	877
110	10.0	0.11	0.21	453.7	454	60	10.0	0.12	0.22	1090.9	1090
120	10.0	0.09	0.19	596.8	597	65	10.0	0.11	0.21	1341.3	1340
130	10.0	0.08	0.18	739.3	739	70	10.0	0.10	0.20	1633.3	1630
						75	10.0	0.09	0.19	1973.7	1970
						80	10.0	0.08	0.18	2370.4	2370
15	12.0	0.40	0.52	3.4	3	10	12.0	0.38	0.50	13.3	13
20	12.0	0.35	0.47	6.7	7	15	12.0	0.32	0.44	34.1	34
30	12.0	0.28	0.40	17.7	18	20	12.0	0.27	0.39	68.4	68
40	12.0	0.23	0.35	36.0	36	25	12.0	0.23	0.35	119.0	119
50	12.0	0.19	0.31	63.5	64	30	12.0	0.20	0.32	187.5	188
60	12.0	0.17	0.29	97.7	98	35	12.0	0.18	0.30	272.2	272
70	12.0	0.15	0.27	142.9	143	40	12.0	0.16	0.28	381.0	381
80	12.0	0.14	0.26	193.8	194	45	12.0	0.15	0.27	500.0	500
90	12.0	0.13	0.25	255.1	255	50	12.0	0.14	0.26	641.0	641
100	12.0	0.12	0.24	328.1	328	55	12.0	0.13	0.25	806.7	807
110	12.0	0.11	0.23	414.2	414	60	12.0	0.12	0.24	1000.0	1000
120	12.0	0.09	0.21	539.9	540	65	12.0	0.11	0.23	1224.6	1220
130	12.0	0.08	0.20	665.4	665	70	12.0	0.10	0.22	1484.8	1480
						75	12.0	0.09	0.21	1785.7	1790
						80	12.0	0.08	0.20	2133.3	2130

Note: In recognition of safety considerations, use of e_{max} = 4.0% should be limited to urban conditions.

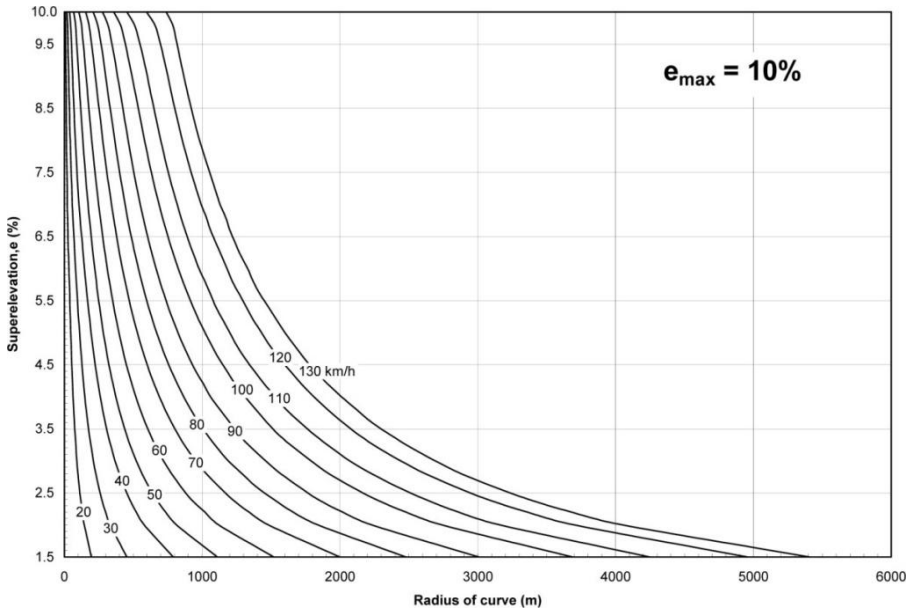

Figure 3. 3 Design Superelevation Rates for Maximum Superelevation Rate of 10 Percent (AASHTO, 2004)

Table 3. 2 Minimum Radii for Design Superelevation Rates, Design Speeds, and e_{max} = 10% (AASHTO, 2004)

e (%)	V_d = 20 km/h R (m)	V_d = 30 km/h R (m)	V_d = 40 km/h R (m)	V_d = 50 km/h R (m)	V_d = 60 km/h R (m)	V_d = 70 km/h R (m)	V_d = 80 km/h R (m)	V_d = 90 km/h R (m)	V_d = 100 km/h R (m)	V_d = 110 km/h R (m)	V_d = 120 km/h R (m)	V_d = 130 km/h R (m)
1.5	197	454	790	1110	1520	2000	2480	3010	3690	4250	4960	5410
2.0	145	333	580	815	1120	1480	1840	2230	2740	3160	3700	4050
2.2	130	300	522	735	1020	1340	1660	2020	2480	2860	3360	3680
2.4	118	272	474	669	920	1220	1520	1840	2260	2620	3070	3370
2.6	108	249	434	612	844	1120	1390	1700	2080	2410	2830	3110
2.8	99	229	399	564	778	1030	1290	1570	1920	2230	2620	2880
3.0	91	211	368	522	720	952	1190	1460	1790	2070	2440	2690
3.2	85	196	342	485	670	887	1110	1360	1670	1940	2280	2520
3.4	79	182	318	453	626	829	1040	1270	1560	1820	2140	2370
3.6	73	170	297	424	586	777	974	1200	1470	1710	2020	2230
3.8	68	159	278	398	551	731	917	1130	1390	1610	1910	2120
4.0	64	149	261	374	519	690	866	1060	1310	1530	1810	2010
4.2	60	140	245	353	490	652	820	1010	1240	1450	1720	1910
4.4	56	132	231	333	464	617	777	953	1180	1380	1640	1820
4.6	53	124	218	315	439	586	738	907	1120	1310	1560	1740
4.8	50	117	206	299	417	557	703	864	1070	1250	1490	1670
5.0	47	111	194	283	396	530	670	824	1020	1200	1430	1600
5.2	44	104	184	269	377	505	640	788	975	1150	1370	1540
5.4	41	98	174	256	359	482	611	754	934	1100	1320	1480
5.6	39	93	164	243	343	461	585	723	896	1060	1270	1420
5.8	36	88	155	232	327	441	561	693	860	1020	1220	1370
6.0	33	82	146	221	312	422	538	666	827	976	1180	1330
6.2	31	77	138	210	298	404	516	640	795	941	1140	1280
6.4	28	72	130	200	285	387	496	616	766	907	1100	1240
6.6	26	67	121	191	273	372	476	593	738	876	1060	1200
6.8	24	62	114	181	261	357	458	571	712	846	1030	1170
7.0	22	58	107	172	249	342	441	551	688	819	993	1130
7.2	21	55	101	164	238	329	425	532	664	792	963	1100
7.4	20	51	95	156	228	315	409	513	642	767	934	1070
7.6	18	48	90	148	218	303	394	496	621	743	907	1040
7.8	17	45	85	141	208	291	380	479	601	721	882	1010
8.0	16	43	80	135	199	279	366	463	582	699	857	981
8.2	15	40	76	128	190	268	353	448	564	679	834	956
8.4	14	38	72	122	182	257	339	432	546	660	812	932
8.6	14	36	68	116	174	246	326	417	528	641	790	910
8.8	13	34	64	110	166	236	313	402	509	621	770	888
9.0	12	32	61	105	158	225	300	386	491	602	751	867
9.2	11	30	57	99	150	215	287	371	472	582	731	847
9.4	11	28	54	94	142	204	274	354	453	560	709	828
9.6	10	26	50	88	133	192	259	337	432	537	685	809
9.8	9	24	46	81	124	179	242	316	407	509	656	786
10.0	7	19	38	68	105	154	210	277	358	454	597	739

3.3 Analytical Formulas

AASHTO (2004) explains that both *e* and *f* distributions involving Method 5 can result in a basic curve formula, ignoring the (1 – 0.01*ef*) term mentioned earlier within this chapter, utilizing the following series of equations:

$$0.01e + f = \frac{V^2}{127\ R} \tag{3.2}$$

Where,

V_D = V = design speed, km/h;

e_{max} = e = maximum superelevation (percent);

f_{max} = f = maximum allowable side friction factor;

R_{min} = R = minimum radius, meters;

R_{PI} = R = radius at the Point of Intersection, PI, with legs (1) and (2) for the f distribution; parabolic curve (R within the point for intersection of 0.01 e_{max} along with (0.01e + f) R);

V_R = running speed, km/h

then:

$$R_{min} = \frac{V_D^2}{127\ (0.01\ e_{max} + f_{max})} \tag{3.3}$$

and

$$R_{PI} = \frac{V_R^2}{1.27\ e_{max}} \tag{3.4}$$

Because $(0.01e\ +\ f\ )_D - (0.01e\ +\ f\ )_R = h$, at point R_{PI} the calculations diminish to the following:

$$h_{PI} = \left(\frac{(0.01\ e_{max})V_D^2}{V_R^2}\right) - 0.01\ e_{max} \tag{3.5}$$

whereas, h_{PI} = PI counterbalance from the 1/*R* axis.

Also,

$$S_1 = h_{PI}\ (R_{PI}) \tag{3.6}$$

whereas, S_1 = slope for leg 1 and

$$S_2 = \frac{f_{max} - h_{PI}}{\frac{1}{R_{min}} - \frac{1}{R_{PI}}} \tag{3.7}$$

where, S_2 = slope for leg 2.

The calculation of the middle ordinate (*MO*) for an unsymmetrical vertical curve is as follows:

$$MO = \frac{L_1 L_2 (S_2 - S_1)}{2(L_1 + L_2)} \tag{3.8}$$

where, $L_1 = 1/R_{PI}$ and $L_2 = 1/R_{min} - 1/R_{PI}$.

Then:

$$MO = \frac{1}{R_{PI}} \left(\frac{1}{R_{min}} - \frac{1}{R_{PI}} \right) \left(\frac{S_2 - S_1}{2} \right) R_{min} \quad (3.9)$$

whereas, *MO* = middle ordinate for the *f* distribution curve, and

$$(0.01\ e + f)_D = \frac{(0.01\ e_{max} + f_{max}) R_{min}}{R} \quad (3.10)$$

in which *R* = radius at any point.

Utilizes the general vertical curve equation:

$$\frac{Y}{MO} = \left(\frac{x}{L} \right)^2 \quad (3.11)$$

with 1/R measured from the vertical axis.

with $1/R \leq 1/R_{PI}$,

$$f_1 = MO \left(\frac{R_{PI}}{R} \right)^2 + \frac{S_1}{R} \quad (3.12)$$

where, f_1 = *f* distribution at any given point $1/R \leq 1/R_{PI}$; and

$$0.01\ e_1 = (0.01\ e + f)_D - f_1 \quad (3.13)$$

Where, 0.01 e_1 = 0.01 e distribution at any given point $1/R \leq 1/R_{PI}$.

For $1/R > 1/R_{PI}$,

$$f_2 = MO\left(\frac{\frac{1}{R_{min}}-\frac{1}{R}}{\frac{1}{R_{min}}-\frac{1}{R_{PI}}}\right)^2 + h_{PI} + S_2\left(\frac{1}{R}-\frac{1}{R_{PI}}\right) \quad (3.14)$$

where, f_2 = f distribution at any given point $1/R > 1/R_{PI}$; and

$$0.01\ e_2 = (0.01\ e + f)_D - f_2 \quad (3.15)$$

where, 0.01 e_2 = 0.01 e distribution at any given point $1/R > 1/R_{PI}$.

3.4 Evaluation of the AASHTO methods

Side friction and superelevation regarding Above-Minimum Radius Curves, it is stated from Austroads (Rural, 1993) that "it is usual to adopt radii greater than (the minimum values) and to reduce superelevation and side friction below their maximum values," however, no advice was given regarding the proportions for the centripetal force, which could be offered from sideways friction and superelevation (Nicholson, 1998).

With radii that are greater than minimum radius, design superelevation along with side friction is less than its maximum values. Regarding a certain design speed (e_{max}, f_{max}, and R_{min}), AASHTO provided five methods of neutralizing the centrifugal force with the use for e along with f, or both (AASHTO, 2004). These five methods include:

1) Side friction and superelevation are precisely proportional with the inverse for radius *R* (otherwise, the curve degree). That is, *e* depends linearly beginning at 0 from $R = \infty$ (curve degree equals zero) to e_{max} by *R* = (maximum curve degree), and also for *f*;
2) For a vehicle driving within the design speed, the centrifugal force can be offset within the direct proportion with side friction upon curves to those needing f_{max}. Involving sharper curves, *f* stays at f_{max} while e then is utilized within direct proportion involving the increase within curvature until $e = e_{max}$;
3) For a vehicle driving within the design speed, the centrifugal force can be offset within direct proportion with superelevation upon curves to those needing e_{max} . Involving sharper curves, *e* stays at e_{max} while *f* then is utilized within direct proportion involving the increase within curvature until $f = f_{max}$.
4) It similar to Method 3, apart from it being based on running speed average as opposed to design speed; as well as
5) The side friction and superelevation differ with the opposite of the radius within a curvilinear method, providing values between both Methods 1 and 3.

AASHTO suggests utilizing Method 5.

The AASHTO guideline offers a difference between those methods that are based on running speed average that is basically the distance traveled that is divided by the average running time (the time that the vehicle is within motion), along with the methods that are based on design speed. If design speed is determined to be the 85^{th} percentile operating speed within the circular curve, little validation, if any, is needed for sustaining the difference between those methods that are based on speed unspecified for design

purposes along with the definite operating speeds, therefore, there are the five methods discussed by Nicholson(1998) .

3.4.1 Method 5 Evaluated by Nicholson

AASHTO (1990) discusses that *e*, related with the degree for curvature (*D*) for both the curve along with side friction, needs to assure 3 conditions:

1) $e = 0$ when $D = 0$ (or $R = \infty$);
2) $e = e_{max}$ when $D = D_{max}$ (or $R = R_{min}$); and
3) $\frac{\partial e}{\partial D} = 0$ when $D = D_{max}$ (or $R = R_{min}$);

Nicholson (1998) described that the degree of curvature *D* is inversely proportional to the radius *R*, such that their product equals 5,729.58, and is thus subject to an upper bound

$$D_{max} = \frac{5{,}729.58\ g(e_{max}+f_{max})}{V^2} \tag{3.16}$$

Nicholson (1998) explained that both the *e* and *f* distributions involving Method 5 can result in the symmetrical vertical curve formula, utilizing the following series of Equations:

For ($R_{min} \leq R \leq \infty$)

$$e_5 = e_{max}\ \frac{R_{min}}{R}\left(2 - \frac{R_{min}}{R}\right) \tag{3.17}$$

$$f_5 = \frac{V^2}{gR} - e_{max}\ \frac{R_{min}}{R}\left(2 - \frac{R_{min}}{R}\right) \tag{3.18}$$

The assumption of the symmetrical vertical curve of AASHTO Method 5 superelevation distribution is not correct. The equation should be an unsymmetrical vertical curve equation (Easa, 1999).

3.4.2 Method 5 Evaluated by Easa

Easa (1999) explains that both the *e* and *f* distributions involving Method 5 can result in the unsymmetrical vertical curve formula. The reproduction for ‘‘AASHTO Method 5’’ provided in Nicholson (1998) is not actually that of the AASHTO Method 5. This debate portrays the reproduction of AASHTO Method 5 (that distributes superelevation, *e*, along with side friction, *f*, utilizing an unsymmetrical parabolic curve) and observes the conclusion where this method is not as good as Method 1 (which is a linear distribution).

Nicholson (1998) affirmed that the e versus D relationship that was presented within Figure III-6 (*A*) within the 1990 AASHTO guide (Policy 1990), and Figure III-7 (*A*) within the 1994 AASHTO guide (Policy 1994), assures three conditions as discussed in section 3.4.1. Based on these conditions, Equations (3.17 & 3.18) were both correct. However, these calculations suggest a symmetrical parabolic curve involving the e distribution having a midpoint at $D_{max}/2$ along with a slope that is equivalent to zero where $D = D_{max}$. This varies from AASHTO Method 5 that is characterized with an unsymmetrical (two-arc) parabolic curve guaranteeing the *e* curve be tangent with the ($e + f$) line within $R = \infty$ ($D = 0$).

The symmetrical description could result within the *e* curve lying on top of the (e + f) line thus producing negative values for *f*. This is notably true as the ratio $t = e_{max}/(e_{max} + f_{max})$ becomes greater than 0.5 and *R* becomes larger than 2 R_{min}. Involving t = 0.5, Equations (3.17 & 3.18) are exact due to the unsymmetrical curve being lessened to a symmetrical curve. Regarding t = 0.5, problems regarding negative values for *f* may not occur, thus the symmetrical curve may not digress from that of the unsymmetrical curve.

Within AASHTO Method 5, the unsymmetrical (US) curve was first created for the *f* distribution, where the *e* distribution can be seen (Figure 3.2). The unsymmetrical curve deals with two parabolic arcs associated within the point of intersection ($1/R_{PI}$), whereas R_{PI} is the radius analyzed utilizing Equation (3.19) where $e = e_{max}$ and f = 0. Disregarding the difference between average running speed and design speed, and utilizing the basic principles for unsymmetrical vertical curves (Hickerson, 1964), side friction, *f*, can result in:

$$e + f = \frac{V^2}{gR} \tag{3.19}$$

$$R_{PI} = \frac{V^2}{g\, e_{max}} \tag{3.20}$$

For $1/R \leq 1/R_{PI}$

$$f_5 = f_{max}\ \frac{R_{min}\, R_{PI}}{2\, R^2} \tag{3.21}$$

For $1/R > 1/R_{PI}$

$$f_5 = f_{max}\left[\frac{R_{min}}{R}\left(\frac{R_{PI}-R}{R_{PI}-R_{min}}\right) + \frac{R_{min}R_{PI}}{2\,R^2}\left(\frac{R-R_{min}}{R_{PI}-R_{min}}\right)^2\right] \quad (3.22)$$

Then, the superelevation, e_5, is set by

$$e_5 = \frac{V^2}{g\,R} - f_5 \quad (3.23)$$

For $e_{max} = f_{max}$, is shown that f_5 along with e_5 for Equation (3.19)–(3.23) is decreased to f_5 along with e_5 within the symmetrical curve for Equation (3.17 & 3.18).

3.5 Superelevation Design based on Safety Margin

Nicholson (1998) defined safety margin as the difference involving design speed (V) and the limiting speed (VL). The VL is the speed where f equals f_{max} as well as the e variable is the design superelevation. In regards to a circular curve that contains radius R along with design superelevation e, limiting speed is shown by

$$VL = \sqrt{\frac{R(e+f_{max})}{0.00787}} \quad (3.24)$$

where, *VL*= limiting speed (Km/h), *R*= radius of a curve (m)

Nicholson (1998) contemplates a vehicle driving along a curve for constant radius *R*, with specified superelevation *e*. If the design speed (V) is more that the vehicle's speed, design

maximum side friction factor f_{max} would be more than the friction f, and as f approaches f_{max} then the travel speed approaches V. The speed by which f is equal to f_{max} is deemed a limiting speed (represented by VL), thus, the side friction factor will exceed f_{max} when a vehicle is traveling in excess of VL.

The limiting speed of a particular radius R along with superelevation e is evidently equal to or greater than the design speed (equal only when design $f = f_{max}$). The limiting speed VL can be projected with the ball-bank indicator and can frequently be termed as a "safe speed" (Policy 1990), however this is not a suitable term, as it means that it is not safe to surpass VL , when actually it is quite possible to surpass VL safely. This is due to the value for f_{max} being utilized, for design tends to be typically less than the available side friction factor, so when a speed larger than VL will involve requiring a side friction factor larger than f_{max}, the available side friction factor might not be exceeded. The amount where limiting speed exceeds design speed indicates a lower bound of safety margin alongside the demanded friction that exceeds the friction available. Therefore, the design safety margin equals $VL - V$.

The available side friction may differ both temporally (for example, from one time towards another time, within the same curve) to spatially (for example, from one curve towards another, within the same time). Temporal differences within the available side friction factor are frequently due to changes within weather patterns and are therefore predictable, and the most realistic way towards minimizing the whole difference is to reduce the spatial differences by offering a spatially consistent road surface.

Safety margin variation occurs from the differences between friction demanded by drivers and within the available friction. The geometric design may slightly affect the available side friction, however, it may affect the friction demand (and therefore the safety margin), by changing the behaviour of drivers (especially their speed preference). Provided the tendency of certain drivers to drive similarly as fast as possible, the function of expectancies within affecting driver behaviour, along with the effect that current experiences have towards those expectancies, the objective is to maximize the consistency based on the safety margin $VL - V$ from the one curve to the next. This will reduce any driver tendency of increasing speed, as previous curves were passed with increasing speeds without having any feeling towards losing control, and to reduce the likelihood of expectations being breached.

For example, consider a series of four curves that are equal with comparable design speeds (V_1, V_2, V_3, along with V_4) along with limiting speeds (VL_1, VL_2 , VL_3, along with VL_4), where $VL_1 < VL_2 < VL_3$ however $VL_4 < VL_3$. There may involve driver discomfort when the design speed increases. There is usually little outlook for loss of control; it is only when the speed exceeds the limiting speed, that there is a real outlook for loss of control within various situations. Certain drivers might be equipped to deal with a little discomfort, as long as they sense not having any loss of control, then certain drivers may decide to increase speeds once they proceed during the initial three curves that are in line within an increase in limiting speeds of those curves. They may also presume the limiting speed for the fourth and remaining curve (VL_4) which is either greater than (or is equal

to) the third curve, and then select a speed that is greater than VL_4. As a result, there could be a loss of control within the fourth curve.

As the previous situation illustrates, containing comparable design speeds of consecutive curves is not adequate; the margins (and therefore the limiting speeds) within consecutive curves need to be similar. Wherever curve radii are larger than that of the minimum radius, the side friction and superelevation are selected so the safety margin becomes balanced (for example, the difference for the margin among the curves becomes small).

Easa (2003) developed an Optimization Model which, assuming a highway section under consideration, deals with N circular horizontal curves having different radii, the curves are combined to K groups having similar radii. Group i contains a radius R_i , curve frequency q_i, design speed V_i, maximum side-friction $f\ maxi_i$, design superelevation e_i , design side friction f_i and minimum radius $R\ min_i$, where i = 1,2,...,K. Both the minimum along with maximum superelevations for the highway segment become designated with e_{min} and e_{max} . In order to resolve both e_i and f_i (decision variables), it is necessary to know R_i , q_i, V_i, $f\ max_i$, e_{min}, e_{max} and $R\ min_i$.

It should be kept in mind that the previous rotation symbolizes the wide-scale case and that the maximum side friction and design speed (along with the minimum radius) differ within the curve radius of a certain speed environment, based on the Australian design standards (Rural, 1993). Regarding AASHTO standards, such that f_{max}, R_{min} and V are

similar for a certain highway section and $f\ max_i = f_{max}$, $R\ min_i = R_{min}$ and $V_i = V$, for every i.

3.5.1 Aggregate Analysis

Regarding highway design consistency, it is attractive to reduce the variance for the safety margin. Given that the variance is nonlinear within the decision variables, including it precisely within the objective function is not possible. As an alternative, the maximum safety margin becomes reduced and this could minimize the variance. Thus, the objective function can be displayed as:

$$\text{Minimize } Z = M \tag{3.25}$$

where Z = objective function along with M = maximum safety margin. The mean safety margin m is equal to or greater than an attractive minimum value, S_{min} . Stated as,

$$m \geq S_{min} \tag{3.26}$$

other constraints related within the objective function:

$$m_i \leq M\ , \forall_i \tag{3.27}$$

$$m = \frac{\sum_{i=1}^{k} q_i\ m_i}{\sum_{i=1}^{k} q_i} \tag{3.28}$$

$$m_i = VL_i - V_i, \forall_i \tag{3.29}$$

where, m_i= safety margin for Curve Group; V_i = design speed for Curve Group i ; along with the sum for $q_i = N$. The constraints for Equation (3.29) includes the limiting speed for Curve Group, VL_i . The limiting speed formula was provided initially from Equation (3.24), however, it cannot be used directly within the optimization model due to Equation (3.24) being a nonlinear function for the decision variables e and VL. To alleviate this concern, Equation (3.24) is linearized. Thus, considering for Curve Group i, Equation (3.24) is shown as:

$$VL = \sqrt{\frac{R_i \, f\,max_i}{0.00787}} \left(1 + \frac{e_i}{f\,max_i}\right)^{1/2} \tag{3.30}$$

Observing that $(1+x)^{1/2} \cong [1+(x/2)]$ for small x, then

$$VL = \sqrt{\frac{R_i \, f\,max_i}{0.00787}} \left(1 + \frac{e_i}{2\,f\,max_i}\right), \forall_i \tag{3.31}$$

Table 3. 3 Accuracy of Approximation of Equation (3.31) for Practical Parameter Values of AASHTO (Easa, 2003)

	f_{max}		$x = e_{max}/f_{max}$		Difference[a]	
e_{max}	V = 30 km/h	V = 120 km/h	V = 30 km/h	V = 120 km/h	V = 30 km/h	V = 120 km/h
0.04	0.17	0.09	0.24	0.44	0.6%	1.7%
0.06	0.17	0.09	0.35	0.67	1.1%	3.3%
0.08	0.17	0.09	0.47	0.89	1.9%	5.1%
0.10	0.17	0.09	0.59	1.11	2.7%	7.0%
0.12	0.17	0.09	0.71	1.33	3.6%	9.1%

[a]Difference (%) = $100\{[1+(x/2)]-(1+x)^{1/2}\}/(1+x)^{1/2}$.

that is linear within the decision variables e_i and VL_i . The approximation for Equation (3.31) accurate as the ratio (e_i / $f\ max_i$) is less than 1.5. For instance, a ratio that equal 1.5, the value in brackets in Equation (3.31) =1.75 related with the precise value of 1.58 (with a difference of a value of 10.7%). Table 3.3 illustrates the realistic values for the ratio (e_{max} /f_{max}) from Table III-6 AASHTO 2001). The major difference is 9.1%, thus the estimate will be correct for all the real cases. Within Table 3.3, the ratios symbolize (e_{max} /f_{max}) corresponding to R_{min}, thus flatter curves having e_i, e_{max} will contain ratios that are smaller and thus a more accurate reading for Equation (3.31). Design superelevation e_i , based on Equation (3.5), is shown

$$e_i = \frac{0.00787\ V_i^2}{R_i} - f_i\ , \forall_i \tag{3.32}$$

The last constraints are related within the maximum side friction $f\ max_i$ along with the maximum and minimum superelevation e_{max} and e_{min}

$$f_i \leq f\ max_i\ , \forall_i \tag{3.33}$$

$$e_i \geq e_{min}\ , \forall_i \tag{3.34}$$

$$e_i \leq e_{max}\ , \forall_i \tag{3.35}$$

The objective function for Equation (3.25) along with the constraints for Equation (3.26)-(3.35) symbolizes a linear optimization model. A model summary is provided within Table 3.4. The model contains (7K+2) constraints, embodied by all the values that apply

to seven constraints for i along with the two constraints of m. The model contains (4K+2) decision variables, categorized by four variables having a subscript i (f_i , e_i VL_i, and m_i) as well as two variables, M and m. The linear optimization model for Table 3.4 can be solved utilizing existing optimization software, one being LINDO (Schrage, 1991a, b). This software deals with large problems, connecting 800 constraints and 4,500 variables.

Table 3. 4 Linear Optimization Model (Discrete $\boldsymbol{e_i}$); (Easa, 2003)

Minimize $Z = M$
Subjectto $m_i \leq M, \quad \forall i$
$m_i = VL_i - V_i, \quad \forall i$
$m = \dfrac{\sum_{i=1}^{K} q_i m_i}{\sum_{i=1}^{K} q_i}$
$m \geq S_{\min}$
$VL_i = \sqrt{\dfrac{R_i f\max_i}{0.00787}}\left(1 + \dfrac{e_i}{2 f\max_i}\right), \quad \forall i$
$e_i = \dfrac{0.00787 V_i^2}{R_i} - f_i, \quad \forall i$
$f_i \leq f\max_i, \quad \forall i$
$e_i \geq e_{\min}, \quad \forall i$
$e_i \leq e_{\max}, \quad \forall i$
$VL_i, e_i, f_i, m_i, , M, m \geq 0$

3.5.2 Disaggregate Analysis

The optimization model for Table 3.4 minimizes the maximum deviation focusing on the system for horizontal curves in total, including curve radii along with the frequencies of occurrence. These models could be helpful when designing superelevation within the aggregate level, particularly once the highway segment contains many curves. To effectively maximize highway consistency within the disaggregate level, considering individual horizontal curves is important along the series on the highway. This information allows modeling for the safety margin variations between adjacent curves, along with finding superelevation distribution which minimize these variations.

The horizontal curves on the highway segment are signified by 1, 2,..., N, where the value of N is defined by the amount of curves. Then, the variation difference between both the safety margins for curve j and the initial curve j = 1, is shown:

$$d_j = m_j - m_{j-1}, \forall_j \quad (3.36)$$

whereas, j = 2, 3,..., N. Since dj can be either negative or positive, the objective function can be displayed where it minimizes the maximum absolute variation considering the horizontal curve system.

The associated constraints and objective function for the relative variation model is:

$$\text{Minimize } Z = D \quad (3.37)$$

subjected to

$$d_j^+ \leq D \ , \forall_j \tag{3.38}$$

$$d_j^- \leq D \ , \forall_j \tag{3.39}$$

$$m_j - m_{j-1} + d_j^- - d_j^+ = 0 \ , \forall_j \tag{3.40}$$

whereas, D = maximum variation for safety margin. As stated within Equation (3.40), for any particular d_j, either d_j^+ equals zero (if $m_j < m_{j-1}$) or d_j^- equals zero (if $m_j > m_{j-1}$) while the other will be positive. The relative variation model constraints are similar in Table 3.4, except Equation (3.25) that is replaced with Equations (3.37)–(3.40).

Chapter 4: Development of New Methods and Model for Superelevation Distribution

This chapter presents the development of two new categories for superelevation and side friction distribution; the first category is a single curve, which focuses on two proposed methods: superelevation distribution based on EAU and SAU curve equations, respectively. The second category is a system of curves which concentrates on two proposed methods and a model, superelevation distribution based on EAU, SAU curve equations, and parametric cubic curve, respectively. Furthermore, an analysis of the safety margin is provided for the second category, which is the system of curves.

4.1 Introduction

EAU equal parabolic arc unsymmetrical curve equations and SAU single arc unsymmetrical curve equations form the basis of EAU and SAU Methods, respectively, and together combine to define the proposed methods, which improve highway design consistency based on the safety margin. Furthermore, it describes the e and f distributions considering a cubic distribution of f values with specific mathematical shape that follow a general cubic curve with a constraint determined by the optimization model. The optimization model for design consistency of highway is a mathematical procedure consisting of three parts: objective function, decision variables, and constraints. This is accomplished using the design speed of a horizontal curve, while

factoring in the extent for the curve which maximizes highway design consistency, based on the safety margin.

The terminology of the two categories is based on the "single curve" and "system of curves", as shown in Figure 4.1. The "single curve" elements are:

- Superelevation distribution based on EAU curve equations
- Superelevation distribution based on SAU curve equations

The "system of curves" elements are:

- Superelevation distribution based on EAU curve equations and safety margin analysis presented.
- Superelevation distribution based on SAU curve equations and safety margin analysis presented.
- Superelevation distribution based on parametric cubic curve model and safety margin analysis presented.

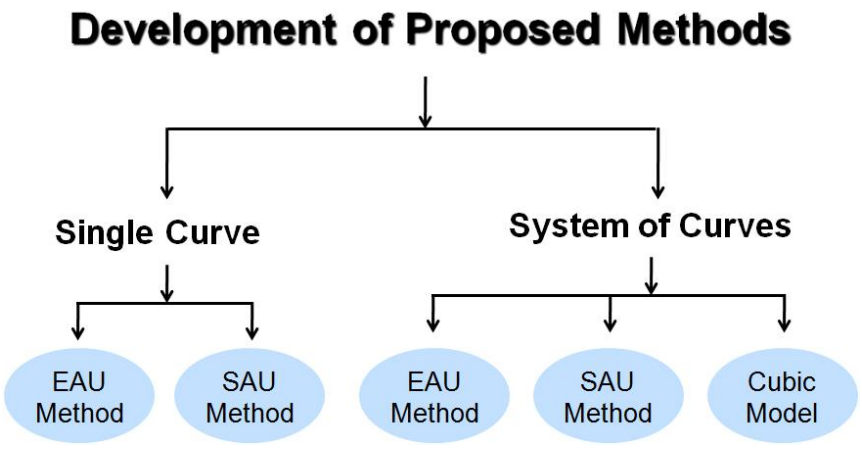

Figure 4. 1 Development of Proposed Methods

Additionally, the EAU and SAU vertical curve Equations have been explained in Chapter 2, the basis for both the EAU and the SAU curves which were developed by Easa (1994) and Easa (2007), respectively.

Since the beginning of superelevation distribution, the distribution methods have been a complex concern requiring an alternative procedure of design and evaluation. The development of superelevation is meant to maximize highway consistency, based on the safety margin, affording an excellent opportunity to develop better techniques of superelevation distribution. Furthermore, the proposed methods can be solved by mathematical software, such as Lingo. Pertaining to the Parametric Cubic Model, Lingo is one of the programming systems utilized to resolve decision variables subjected to assured constraints for a specified objective function. The objective function maximizes design consistency based on the safety margin, which affects safety as well as performance in terms of superelevation distribution. The safety margin depends on the superelevation distribution. The decision variables are represented within four variables and a subscript i (f_i , e_i , VL_i , and m_i) along with the two variables c and d to satisfy the constraint.

4.2 Improved Superelevation Distribution for a Single Curve

4.2.1 Distribution Using Fixed Curves (EAU Method)

The proposed method is a mathematical procedure for superelevation distribution based on Method 5 by AASHTO (2004) and EAU curve Equations developed earlier by Easa

(1994), as illustrated in Figure 4.2. This section describes the derivation of the proposed method. Side friction factors and superelevation distribution rates are all very important when designing appropriate horizontal highway alignments. Dealing with laws of mechanics, superelevation rates, *e*, needed by drivers to cope with turning along a horizontal curve, are formulated as:

$$0.01e = \frac{V^2}{127\,R} - f \tag{4.1}$$

whereas, R = turning radius (m), V = vehicle speeds (km/h), and f = side friction factor. Practical design values exist regarding upper limits for e and, for example, e_{max} along with f_{max}, taking into account many conditions associated with driving comfort, safety, pavement, traffic and weather. In accordance with AASHTO, traveling at an accurate design speed, the minimum turning radius, for example, R_{min} (m) can be resolved such that both e_{max} and f_{max} are chosen according to AASHTO (2004):

$$R_{min} = \frac{V_D^2}{127\,(0.01\,e_{max}+f_{max})} \tag{4.2}$$

whereas, V_D = design speed of curve (km/h). This value functions as a maximum value of limiting both side friction factors and superelevation rates past what is considered realistic for either comfort or the operation by drivers, conversely, utilizing radius larger than R_{min} permits both superelevation rates and side friction factors in having design

values that are beneath their upper limits. The radius of the point at the intersection, R_{PI} , can be obtained from Equation (4.3) according to AASHTO (2004),

$$R_{PI} = \frac{V_R^2}{1.27\, e_{max}} \tag{4.3}$$

where, PI is the Point of Intersection, with legs (1) and (2) for the *f* distribution parabolic curve, and V_R = running speed (km/h), the *PI* counterbalance from 1/*R* axis is shown in Figure 4.2 can be obtained from Equation (4.4) according to AASHTO (2004)

$$h_{PI} = \left(\frac{(0.01\, e_{max})V_D^2}{V_R^2}\right) - 0.01\, e_{max} \tag{4.4}$$

The slope for leg (1), $g_1 = S_1$ in AASHTO can be obtained from the Equation (4.5)

$$g_1 = h_{PI} * R_{PI} \tag{4.5}$$

And the slope for leg (2), $g_2 = S_2$ in AASHTO can be obtained from the Equation (4.6)

$$g_2 = \frac{f_{max} - h_{PI}}{\frac{1}{R_{min}} - \frac{1}{R_{PI}}} \tag{4.6}$$

The algebraic difference in grade (in percent), *A*, the length for the first arc, L_1, the length for the second arc, L_2 , and the total length for the curve, L ,which can be obtained from Equations (4.7) to (4.10) , respectively.

$$A = g_2 - g_1 \quad (4.7)$$

$$L_1 = \frac{1}{R_{PI}} \quad (4.8)$$

$$L_2 = \frac{1}{R_{min}} - \frac{1}{R_{PI}} \quad (4.9)$$

$$L = L_1 + L_2 \quad (4.10)$$

Using the EAU vertical curve equations:

The curve parameters of the proposed EAU vertical curve equations:

$$X = \frac{1}{R} \quad (4.11)$$

The parameter that describes the unsymmetrical curve, R_{EAU} , can be obtained from Equation (4.12) which was developed by Easa (1994):

$$R_{EAU} = \frac{L_1}{L} \quad (4.12)$$

R_{EAU} is characterized as the ratio for the length of the shorter tangent (or a shorter arc when dealing with a traditional curve) in regards to the total curve length. The rate of change of grades for the first arc, r_1 , the rate of change of grades for the second arc, r_2 , for the EAU curve, can be determined from Equations (4.13) , and (4.14), respectively (Easa, 1994):

$$r_1 = \frac{A(3-4R_{EAU})}{L}, \qquad L_1 < L_2 \quad (4.13)$$

$$r_2 = \frac{A(-1+4R_{EAU})}{L}, \qquad L_1 < L_2 \tag{4.14}$$

where, x value is measured from the vertical axis, and when $x \leq L/2$, the first arc elevations for the EAU Curve, as $y_1 = f_1$ can be determined as follows (Easa, 1994):

$$f_1 = g_1 x + \frac{r_1 x^2}{2} \tag{4.15}$$

noting that $y_{BVC} = 0$ for f_1;

$f_1 = f$ distribution at any given point $x \leq L/2$; and

$$e_1 = \frac{V^2}{127 R} - f_1 \tag{4.16}$$

where, $e_1 = e$ distribution at any given point $x \leq L/2$.

when $x > L/2$, the second arc elevations for the EAU curve, such as $y_2 = f_2$ can be obtained by the following (Easa, 1994):

$$f_2 = f_{max} - g_2 (L - x) + \frac{r_2 (L-x)^2}{2} \tag{4.17}$$

noting that $y_{EVC} = f_{max}$ for f_2;

where, $f_2 = f$ distribution at any given point $x > L/2$; and

$$e_2 = \frac{V^2}{127 R} - f_2 \tag{4.18}$$

where, e_2 = e distribution at any given point $x > L/2$.

The summary of EAU Method is given in Table D.1 (Appendix D) and can be solved by mathematical software such as Lingo.

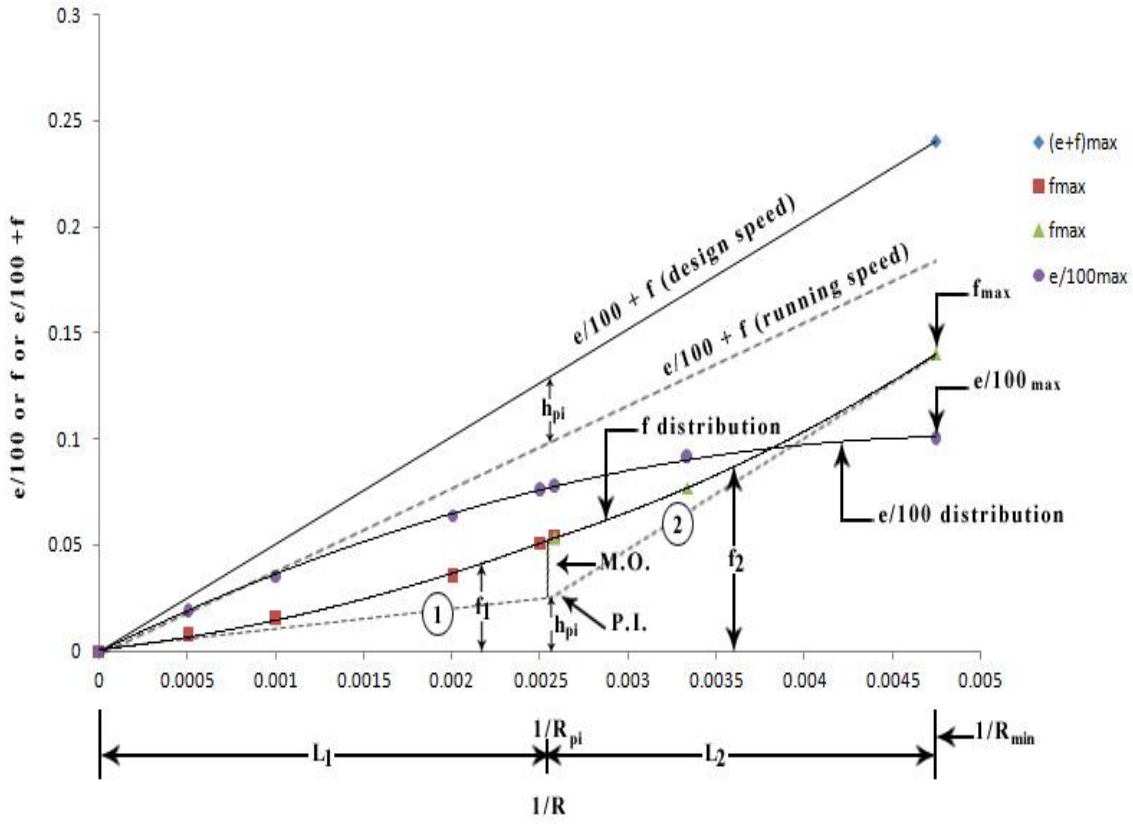

Figure 4. 2 Development Procedures for Superelevation Distribution of EAU Method (e_{max} = 8%)

4.2.2 Distribution Using Fixed Curves (SAU Method)

The proposed method is a mathematical procedure for superelevation distribution based on Method 5 by AASHTO (2004) and SAU curve equations developed earlier by Easa (2007), as shown in Figure 4.3. This section describes the derivation of the proposed

method. When designing suitable horizontal alignment of highways, superelevation rate distribution (or the equivalent turning radii/curvatures) along with side friction factors are all very important. Dealing with laws of mechanics, superelevation rates, e are needed by drivers to cope with turning along a horizontal curve. The SAU Method of superelevation, using Equations (4.2) to (4.10), determines the curve parameters, such as: R_{min} , R_{PI} , h_{PI} , g_1 , g_2 , A , L_1 , L_2 , L, and x from Equation (4.11). Using the SAU vertical curve equations:

The parameter that describes the single-arc unsymmetrical curve (SAU) t equally to a constant, and the rate of change of the slope, r_{PVC} can be obtained from the Equations (4.19) and (4.20), respectively, which were developed by Easa (2007):

$$r_{PVC} = \left(\frac{-2A}{L^2}\right)(L_1 - 2\,L_2) \tag{4.19}$$

$$t = \left(\frac{6A}{L^3}\right)(L_1 - L_2) \tag{4.20}$$

where, x value is measured from the vertical axis, and when $x \leq 1/R_{PI}$, or $x > 1/R_{PI}$ the arc elevations for the SAU curve, as $y = f$, can be determined following Easa (2007) as :

$$f = g_1 x + \frac{r_{PVC}}{2} x^2 + \frac{t}{6} x^3 \tag{4.21}$$

Noting that $h_{PVC} = 0$ for f;

where, h_{PVC} = The elevation of PVC,

f = distribution at any given point $x \leq 1/R_{PI}$, or $x > 1/R_{PI}$, and

$$e = \frac{V^2}{127\,R} - f \qquad (4.22)$$

where, e = distribution at any given point $x \leq 1/R_{PI}$, or $x > 1/R_{PI}$.

The summary for the SAU Method is given in Table D.2 (Appendix D) and can be solved by mathematical software such as Lingo.

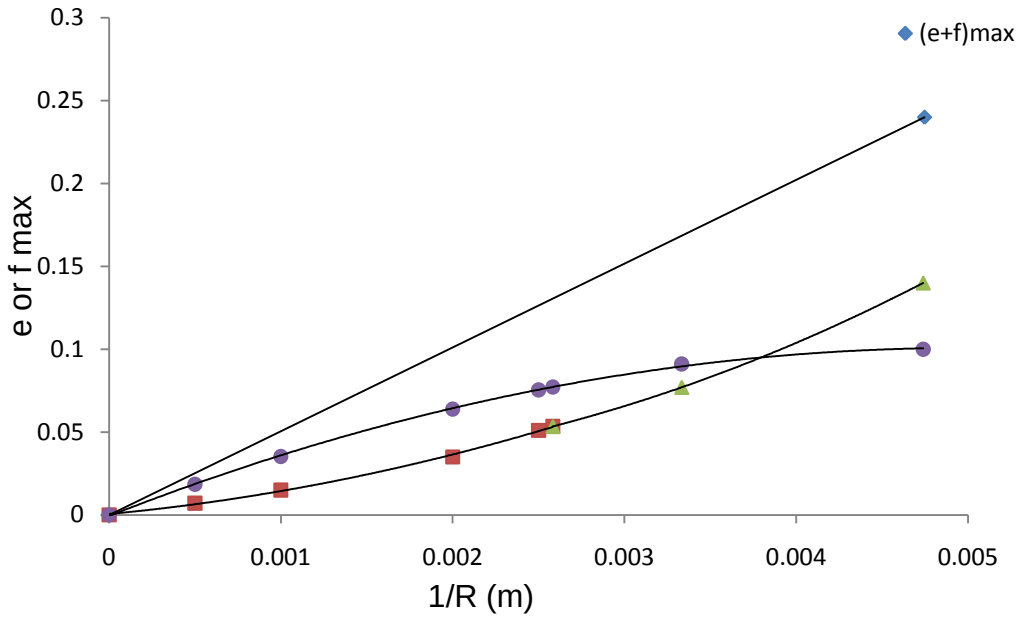

Figure 4. 3 Development Procedures for Superelevation Distribution of SAU Method ($\mathbf{e_{max}}$ = 8%)

4.3 Improved Superelevation Distribution for a System of Curves

Following Easa's (2003) research, assuming a highway section is under consideration, and deals with N circular horizontal curves having different radii, the curves are combined to K groups having similar radii. Group i contains a radius R_i , curve frequency q_i, design speed V_i, maximum side friction $f\ maxi_i$, design superelevation e_i,

design side friction f_i and minimum radius $R\,min_i$, where i = 1,2,...,K. Both the minimum and maximum superelevations for the highway segment become designated with e_{min} and e_{max} . In order to resolve both e_i and f_i, variables R_i , q_i, V_i, $f\,max_i$, e_{min}, e_{max} and $R\,min_i$ need to be known.

It should be kept in mind that the previous rotation symbolizes the wide scale case and that the maximum side friction and design speed (along with the minimum radius) differ within the curve radius of a certain speed environment based on the Australian design standards (Rural, 1993). Regarding AASHTO standards, f_{max}, R_{min} and V are similar for a certain highway section and $f\,max_i = f_{max}$, $R\,min_i = R_{min}$ and $V_i = V$, for every i.

4.3.1 Distribution Using System of Curves (EAU Method)

The proposed method is a mathematical procedure for superelevation distribution based on Method 5 by AASHTO (2004) and EAU curve Equations developed earlier by Easa (1994). This section describes the proposed method. When designing suitable horizontal alignment of highways, superelevation rate distribution (or the equivalent turning radii/curvatures) along with side friction factors are all very important. Dealing with laws of mechanics, superelevation rates e are needed by drivers to cope with turning along a horizontal curve. The EAU Method of superelevation, using Equations (4.2) to (4.18) , determines the curve parameters, such as: R_{min} , R_{PI} , h_{PI} , g_1 , g_2 , L_1 , L_2 , L, A, x, R_{EAU} , r_1 , r_2 , f_1 , e_1 , f_2 , and e_2. The summary for the EAU Method of system of

curves is given in Table D.3 (Appendix D) and can be solved by mathematical software such as Lingo.

4.3.2 Distribution Using System of Curves (SAU Method)

The proposed method is a mathematical procedure for superelevation distribution based on Method 5 by AASHTO (2004) and SAU curve Equations developed earlier by Easa (2007). When designing suitable horizontal alignment of highways, superelevation rate distribution (or the equivalent turning radii/curvatures) along with side friction factors are all very important. Dealing with the laws of mechanics, superelevation rates e are needed by drivers to cope with turning along a horizontal curve. The SAU Method of superelevation, using Equations (4.2) to (4.11) , determines the curve parameters, such as: R_{min} , R_{PI} , h_{PI} , g_1 , g_2 , L_1 , L_2 , L, A, x, and using Equations (4.19) to (4.22) , determines the curve parameters, such as: r_{PVC} , t , f , and e. The summary for the SAU Method of system of curves is given in Table D.4 (Appendix D) and can be solved by mathematical software such as Lingo.

4.3.3 Safety Margin Computation

Based on Nicolson (1998), VL is the speed where f equals f_{max} as well as the e variable is the design superelevation. In regards to a circular curve that contains radius R along with design superelevation e, the limiting speed is shown in Equation (3.24), which is based on the constant development by AASHTO (1/127 $\cong$ 0.00787). Based on Nicholson (1998), the safety margin can be calculated in Equation (4.23).

$$m_i = VL_i - VD_i, \forall_i \quad (4.23)$$

where, m_i= safety margin for curve Group ; VD_i = design speed for Curve Group i ; the limiting speed (VL); the sum for $q_i = N$; Easa (2003) discusses the constraints for Equation (4.23) and includes the limiting speed for Curve Group, VL_i , and Equation (3.18) is linearized. Therefore, Curve Group i, is shown as:

$$VL = \sqrt{\frac{R_i \, f\,max_i}{0.00787}} \left(1 + \frac{e_i}{2\, f\,max_i}\right), \forall_i \quad (4.24)$$

The Mean of safety margin for EAU Method can be calculated following Easa (1999; 2003):

$$Mean = \frac{\sum_{i=1}^{k} q_i \, m_i}{\sum_{i=1}^{k} q_i} \quad (4.25)$$

$$Variance = \frac{\sum_{i=1}^{k} q_i \, (m_i - Mean)^2}{\sum_{i=1}^{k} q_i - 1} \quad (4.26)$$

$$SD = \sqrt{Variance} \quad (4.27)$$

$$CV = SD \,/\, Mean \quad (4.28)$$

where, $Mean$ = Mean of the safety margin; $Variance$ = Variance of the safety margin ; SD = Standard Deviation of the safety margin, CV = Coefficient of Variation of the safety margin. The CV thus has no units. It can be displayed as a decimal or a percentage. If the value of SD for a given dataset is small, then the values are clustered together resulting in a small CV. However, if the dataset SD is high, the values become dispersed and provide a high value for the CV. The coefficient of variation (as shown in Equation 4.28), *CV*, is

utilized as a measure reflecting safety and consistency. Therefore, a smaller *CV* involves a larger mean (improved safety) as well as a smaller standard deviation (improved consistency). The EAU Method improves the design consistency by focusing on the system for horizontal curves in total, including curve radii along with the frequencies of occurrence. The summary of EAU Method is given in Table D.3 (Appendix D), which can be solved by mathematical software such as Lingo.

The SAU Method could be helpful when designing superelevation within the SAU curve Equation, particularly if the highway segment contains many curves. To effectively improve highway consistency within the SAU Method and to consider the SAU curve Equation, it is important to determine first the cubic polynomial Equation finding and then the best superelevation distribution, followed by the many horizontal curves on the highway. This information allows for representation of the safety margin along with horizontal curves in total which improves the design consistency. The horizontal curves on the highway segment are signified by 1, 2,..., N, where the value of N is defined by the number of curves. Then, the limiting speed (VL_i), can be determined from Equation (4.24) which was developed earlier by Easa (2003), but safety margin (m_i) can be determined from Equation (4.23) which was developed earlier by Nicolson (1998). The Mean, Variance, Standard Deviation, and Coefficient of Variation of safety margin can be calculated in Equation (4.25)-(4.28). The proposed methods improve the design consistency, based on the safety margin. The summary of SAU Method is given in Table D.4 (Appendix D), which can be solved by mathematical software such as Lingo.

4.3.4 Distribution Using Parametric Cubic Model

The general cubic curve is designed for the f distribution along with a component of the aggregate analysis (Quadratic Model), which is provided by Easa (2003), forms the Parametric Cubic Optimization Model of the safety margin. Similar to Easa's research (2003) regarding highway design consistency, it is attractive to reduce the variance for the safety margin. Given that the variance is nonlinear within the decision variables, including it precisely within the objective function is possible. As an alternative, minimizing the maximum safety margin could minimize the variance. Thus, the objective function can be displayed as:

$$\text{Minimize } Z = M \tag{4.29}$$

where Z = objective function and M = maximum safety margin. The mean safety margin is equal to or greater than an attractive minimum value, S_{min} stated as,

$$mean \geq S_{min} \tag{4.30}$$

other constraints related within the objective function:

$$m_i \leq M \text{ , } \forall_i \tag{4.31}$$

where, m_i= safety margin for Curve Group; The m_i formula was provided in Equation (4.23); V_i = design speed for Curve Group i; along with the sum for $q_i = N$. The constraints for Equation (4.23) includes the limiting speed for Curve Group, VL_i . The limiting speed formula was provided in Equation (4.24).

Design side friction factor f_i (the derivation is described in Appendix B) and superelevation e_i , can be calculated as:

$$f_i = fmax_i \left(\frac{R\ min_i}{R_i}\right) - c \left(\frac{R_i - R\ min_i}{R\ min_i}\right) \left(\frac{1000}{R_i}\right)^2 - d \left(\frac{{R_i}^2 - {R\ min_i}^2}{{R\ min_i}^2}\right) \left(\frac{1000}{R_i}\right)^3, \forall i \quad (4.32)$$

$$e_i = \frac{0.00787\ V_i^2}{R_i} - f_i\ , \forall_i \quad (4.33)$$

The last constraints are related within the maximum side friction $f\ max_i$ along with the maximum and minimum superelevation e_{max} and e_{min}

$$f_i \leq f\ max_i\ , \forall_i \quad (4.34)$$

$$e_i \geq e_{min}\ ;\ \forall_i \quad (4.35)$$

$$e_i \leq e_{max}\ , \forall_i \quad (4.36)$$

The Mean, Variance, Standard Deviation, and Coefficient of Variation of the safety margin can be calculated from Equations (4.25)-(4.28). The objective function for Equation (4.29) along with the constraints for Equations (4.30)-(4.36) symbolizes a nonlinear optimization model. The model contains (92) constraints. The model contains (6) decision variables, categorized by four variables having a subscript i (f_i , e_i VL_i, and m_i) as well as two variables, c and d. A summary of the nonlinear optimization model in Table 4.1 can be solved utilizing existing optimization software like Lingo.

Table 4. 1 Optimazation Model for Superelevation Distribution Using Parametric Cubic Curve

$Minimize\ Z = \ M$	(1)
$f_i = f max_i \left(\frac{R\ min_i}{R_i}\right) - c \left(\frac{R_i - R\ min_i}{R\ min_i}\right)\left(\frac{1000}{R_i}\right)^2 - d \left(\frac{{R_i}^2 - {R\ min_i}^2}{{R\ min_i}^2}\right)\left(\frac{1000}{R_i}\right)^3, \forall i$	(2)
$e_i = \frac{0.00787\ V_i^2}{R_i} - f_i\ , \forall_i$	(3)
$VL_i = \sqrt{\frac{R_i\ f\ max_i}{0.00787}}\left(1 + \frac{e_i}{2\ f\ max_i}\right), \forall_i$	(4)
$m_i = \ VL_i - V_i, \forall_i$	(5)
$mean \geq \ S_{min}$	(6)
$m_i \leq \ M\ , \forall_i$	(7)
$f_i \leq \ f\ max_i\ \ , \forall_i$	(8)
$e_i \geq \ e_{min}\ \ , \forall_i$	(9)
$e_i \leq \ e_{max}\ \ , \forall_i$	(10)
$VL_i, e_i, f_i, m_i \geq 0$	(11)
$M, Mean\ \geq 0$	(12)
$Mean = \ \frac{\sum_{i=1}^{k} q_i\ m_i}{\sum_{i=1}^{k} q_i}$	(13)
$Variance = \ \frac{\sum_{i=1}^{k} q_i\ (m_i - Mean)^2}{\sum_{i=1}^{k} q_i - 1}$	(14)

4.4 Lingo Program (Optimization Software)

According to the Lingo user manual (2010), Lingo is a thorough tool that is designed to make, solve and build mathematical optimization models more efficiently and easily. Lingo offers a fully integrated suite that provides an influential language to express optimization models, a full-suite for editing along with building problems, besides a set of quick in suite problem solvers able to easily solve most classes for optimization models. Lingo has many solvers for both nonlinear and linear (nonconvex & convex), quadratically constrained, quadratic and integer optimization. In this study, the following solvers have been used. Lingo provides both a broad nonlinear solver along with

nonlinear/integer means. The nonlinear choice is needed to utilize the nonlinear capabilities for LINDO API.

The global solver merges a sequence for range bounding (for example, convex analysis and interval analysis) along with range reduction techniques (for example, constraint propagation and linear programming) with a branch-and-bound outline to determine established global solutions towards non-convex non-linear programs. Conventional nonlinear solvers can get caught at both local and suboptimal solutions. Utilizing the global solver alleviates this.

4.5 Summary

Below are important points regarding the development of proposed methods and an optimization model for superelevation distribution:

- Improved superelevation distribution for single curve:
    - The single curve category is based on two methods, the first method is superelevation distribution based on EAU curve equations, which is illustrated in the Table D.1.
    - The second method is superelevation distribution based on SAU curve equations, shown in the Table D.2.
- Improved superelevation distribution for a system of curves:

- The system of curves category is based on two methods and a model, the first method is superelevation distribution based on EAU curve equations and safety margin analysis, depicted within the Table D.3.
- The second method is superelevation distribution based on SAU curve equations and safety margin analysis, illustrated in the Table D.4.
- The model is the superelevation distribution based on parametric Model model, shown in the Table 4.1.

Chapter 5: Applications and Results

When designing suitable horizontal alignment of highways, both the distribution of side friction factors and superelevation rates (or equivalent turning radii/curvatures) are critical. The purpose of this chapter is to illustrate the numerical examples and results that highlight two significant categories. The first category is a single curve, which demonstrates an improvement regarding the distribution of side friction factor and superelevation rates based on two methods, the EAU and SAU Methods. The second category is a system of curves that will illustrate the side friction factor and superelevation distribution of two proposed methods and an optimization model (the EAU Method, SAU Method and the Parametric Cubic Model), to improve the design consistency based on the safety margin. For evaluation purposes of a single curve, the percentage change in superelevation and side friction for a single value of horizontal curve radius exists between the two methods, the EAU and SAU Methods, and AASHTO Method 5. When evaluating a system of curves, all the methods apply Means (μ), Standard Deviation (*SD*) and Coefficient of Variation (*CV*) of the safety margin in determining the best superelevation distribution design that can be utilized as a measure reflecting both the safety and consistency.

5.1 Data Selection

The horizontal curve radius (centreline of the roadway) was obtained as the curve radii. To determine the distribution of superelevation, calculations are illustrated in the following examples.

- Examples 1, 2 and 3 show the distribution of superelevation rate results based on AASHTO Method 5, the EAU Method and SAU Method, respectively highlighted in this chapter. A review for the input data is illustrated in Table 5.1.

Table 5.1 Parameters for Developing of Superelevation Distribution used for Examples 1, 2 and 3

VD km/h	**VR** km/h	**e_{max}** %	**f_{max}**	**R_{min}** (m)	**R_{PI}** (m)	**h_{PI}**	**L_1**	**L_2**	**g_1**	**g_2**	**M.O.**
20	20	8	0.18	12.11	39.35	0.000	0.025	0.057	0.000	3.148	0.028
30	30	8	0.17	28.33	88.54	0.000	0.011	0.024	0.000	7.083	0.027
40	40	8	0.17	50.37	157.40	0.000	0.006	0.014	0.000	12.592	0.027
50	47	8	0.16	81.98	217.31	0.011	0.005	0.008	2.290	19.675	0.025
60	55	8	0.15	123.18	297.58	0.015	0.003	0.005	4.525	28.332	0.023
70	63	8	0.14	175.29	390.45	0.019	0.003	0.003	7.327	38.563	0.022
80	70	8	0.14	228.95	482.04	0.024	0.002	0.002	11.805	50.368	0.021
90	77	8	0.13	303.56	583.27	0.029	0.002	0.002	17.086	63.747	0.019
100	85	8	0.12	393.50	710.76	0.031	0.001	0.001	21.839	78.700	0.018
110	91	8	0.11	501.19	814.64	0.037	0.001	0.001	30.056	95.227	0.015
120	98	8	0.09	666.64	944.79	0.040	0.001	0.000	37.745	113.328	0.012
130	102	8	0.08	831.27	1023.49	0.050	0.001	0.000	51.124	133.003	0.008

- Examples 4, 5, 6 and 7 are similar to the examples utilized by Nicholson (1998), Easa (1999) and Easa (2003) in terms of the best resolution focusing on the results from the AASHTO methods. It contains a single carriageway rural highway within rolling terrain expected to contain 20 circular horizontal curves, having radii R_i = 100, 150, 200, 250, 300, 350 m along with equivalent frequencies q_i = 3, 4, 6, 4, 2, 1. The design guide of Australia recommends a 90 km/h speed environment having design speeds V_i = 71, 76, 78, 80, 81, along with 82 km/h. The e_{min} and e_{max} values then are both 0.02 and 0.10, respectively. The $f\ max_i$

values are all 0.30, 0.28, 0.27, 0.26, 0.25, and 0.24. Minimum radius, R_{min}, is determined utilizing Equation (4.2).

Table 5. 2 Input data for examples 4, 5, 6 and 7 [a]

Curve No.	***R*** (m)	***q***	***V*** (km/h)	***VR*** (km/h)	e_{max}	f_{max}	R_{min}	***V2/gR***	e_{min}	R_{me}	R_{fo}	R_{eo}
1	100	3	71	63.90	0.1	0.3	99	0.40	0.02	124.04	132.31	396.93
2	150	4	76	66.50	0.1	0.28	120	0.30	0.02	151.60	162.43	454.80
3	200	6	78	68.25	0.1	0.27	129	0.24	0.02	165.19	177.43	479.06
4	250	4	80	70.00	0.1	0.26	140	0.20	0.02	179.98	193.82	503.94
5	300	2	81	70.88	0.1	0.25	148	0.17	0.02	191.34	206.65	516.61
6	350	1	82	71.75	0.1	0.24	156	0.15	0.02	203.63	220.60	529.45

[a] Minimum mean of safety margin, S_{min} = 10 km/h

For the purposes of simplicity, the curve and path radius are equal. Supposing a minimum superelevation valued at 0.02, the lowest radii utilizing minimum superelevation, R_{me} , is determined utilizing Equation (2.70), where the lowest radii that depends on friction solely, R_{fo} , along with superelevation solely, R_{eo} , is analyzed utilizing both Equations (2.64) and (2.67) respectively, providing the values highlighted within Table 5.2. For each radius greater than 100 m, the radius surpasses the minimum radius; consequently, there is flexibility within the proportions for the centripetal force given by side friction and superelevation. The input data mentioned in Table 5.2 is used to illustrate the results for AASHTO methods, the EAU Method, the SAU Method and the Parametric Cubic model (optimization model).

5.2 Superelevation Distribution for Single Curve

5.2.1 Numerical Example 1 (AASHTO Method 5 – Single Curve)

Similarly to AASHTO (2004), here are examples for Method 5 where the procedures for calculating e with a design speed of 80 km/h along with an e_{max} of 8 percent is, V_R = 70 km/h, f_{max} = 0.14 (highest allotted side friction factor). The results are as follows: R_{min} = 228.945, R_{PI} = 482.038, h_{PI} = 0.02449, S_1 = 11.805, S_2 = 50.368, L_1 = 0.00207, L_2 = 0.00229, L = 0.00437. The middle ordinate (MO) is 0.02090. The e distribution value of a radius can be determined by obtaining the $(0.01\ e + f)_D$ value and deducting either the f_1 or f_2 value (Figure 5.1). Therefore, the e distribution value of $R = R_{PI}$ would result in $(0.01\ e + f)_D = V_D^2/127\ R$ = 0.1045 minus an f_1 = 0.045, which gets e_1= 0.059. This value multiplied by 100 (converting the value to a percent) would be e_1= 5.9 %, then rounded up to the nearest 2/10ths, relates to an e value of 6.0 %. The e value is calculated for R = 482.038 m at 80 km/h design speed within Table 5.3. Table 5.3 shows all the calculations of the distribution of the superelevation based on AASHTO Method 5 using e_{max} 8% with speed ranges from 40 km/h to 130 km/h.

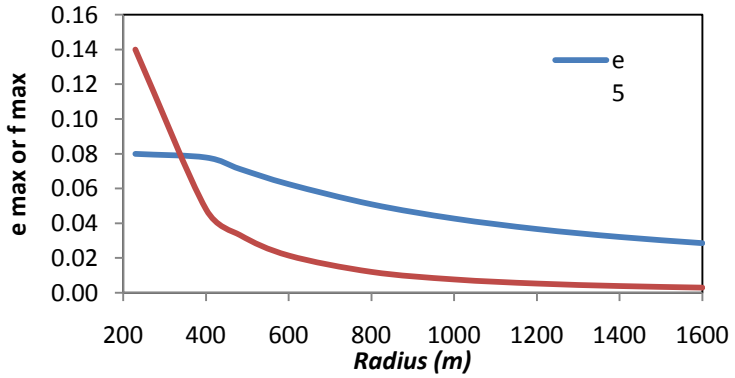

Figure 5. 1 Design Side Friction Factor and Superelevation Rate for Method 5 (e_{max} = 8%)

Table 5. 3 Method 5 of Design Superelevation Rates for Different Radii (e_{max} = 8%)

Design Speed (km/h)	**40**	**50**	**60**	**70**	**80**	**90**	**100**	**110**	**120**	**130**
Radius (m)	**e**	**e**	**e**	**e**	**e**	**e**	**e**	**e**	**e**	**e**
7000	0.2	0.2	0.3	0.4	0.5	0.7	0.8	0.9	1.1	1.2
5000	0.3	0.3	0.5	0.6	0.8	0.9	1.1	1.3	1.5	1.6
3000	0.4	0.6	0.8	1.0	1.2	1.5	1.8	2.1	2.4	2.7
2500	0.5	0.7	0.9	1.2	1.5	1.8	2.1	2.5	2.9	3.2
2000	0.6	0.8	1.1	1.5	1.8	2.2	2.6	3.0	3.5	3.9
1500	0.8	1.1	1.5	1.9	2.4	2.8	3.4	3.9	4.6	5.1
1400	0.9	1.2	1.6	2.1	2.5	3.0	3.6	4.1	4.9	5.5
1300	0.9	1.3	1.7	2.2	2.7	3.2	3.9	4.4	5.2	5.9
1200	1.0	1.4	1.8	2.4	2.9	3.4	4.1	4.7	5.6	6.3
1000	1.2	1.6	2.2	2.8	3.4	4.0	4.8	5.5	6.5	7.4
900	1.3	1.8	2.4	3.1	3.7	4.4	5.2	6.0	7.1	7.9
800	1.5	2.0	2.7	3.4	4.1	4.8	5.7	6.6	7.6	8.0
700	1.7	2.3	3.0	3.8	4.5	5.3	6.3	7.2	8.0	
600	1.9	2.6	3.4	4.3	5.1	6.0	7.0	7.7		
500	2.3	3.0	3.9	4.9	5.8	6.7	7.6	8.0		
400	2.7	3.6	4.7	5.7	6.6	7.5	8.0			
300	3.5	4.5	5.6	6.8	7.6	8.0				
250	4.0	5.1	6.3	7.4	8.0					
200	4.6	5.8	7.0	7.9						
175	5.0	6.2	7.4	8.0						
150	5.4	6.7	7.8							
140	5.6	6.9	7.9							
130	5.8	7.1	8.0							
120	6.0	7.4	8.0							
110	6.3	7.6								
100	6.6	7.8								
90	6.9	8.0								
80	7.2	8.0								
70	7.5									
60	7.9									
50	8.0									
40										
30										
20										

5.2.2 Numerical Example 2 (EAU Method – Single Curve)

Based on the equations in Table D.1 (Appendix D), the EAU Method applies the following input data where the procedures for calculating e with a design speed of 80 km/h along with an e_{max} of 8 percent is, V_R = 70 km/h, f_{max} = 0.14 (highest allotted side friction factor). The results are as follows, R_{min} = 228.945, R_{PI} = 482.038, h_{PI} = 0.02449, g_1 = 11.805, g_2 = 50.368, A = 38.563, L_1 = 0.00207, L_2 = 0.00229, L = 0.00437, R_{EAU} = 0.47495, r_1 = 9713.344, r_2 = 7944.303. The e distribution value of a radius can be determined by obtaining e_1 and e_2 values and deducting either the f_1 or f_2 values, respectively (Figure 5.2). Therefore, the e distribution value is determined when $R = R_{PI}$ resulting in f_1 = 0.045 and e_1 = 0.059. This value multiplied by 100 (converting value to a percent) then rounded up to the nearest 2/10ths becomes 5.91 %. Table 5.4 shows all the calculation of the distribution of the superelevation based on EAU Method using e_{max} 8% with speed ranges from 40 km/h to 130 km/h.

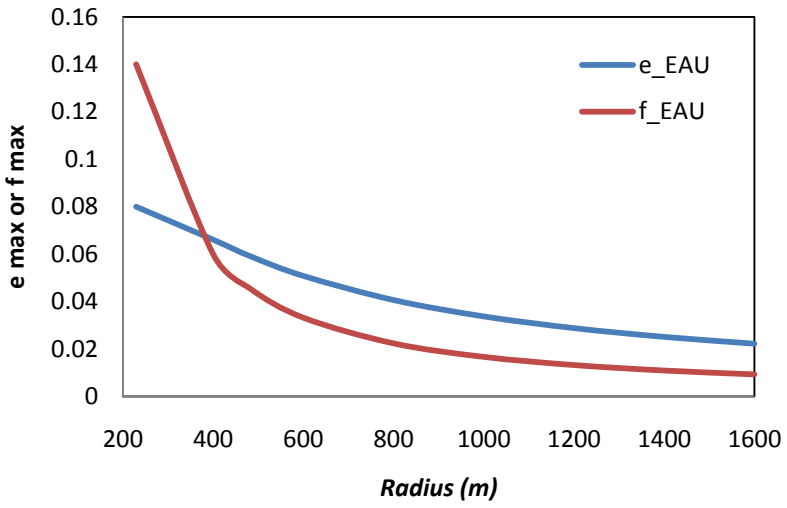

Figure 5. 2 Design Side Friction Factor and Superelevation Rate for EAU Method (e_{max} = 8%)

Table 5. 4 EAU Method of Design Superelevation Rates for Different Radii (e_{max} = 8%)

Design Speed (km/h)	**40**	**50**	**60**	**70**	**80**	**90**	**100**	**110**	**120**	**130**
Radius (m)	**e**	**e**	**e**	**e**	**e**	**e**	**e**	**e**	**e**	**e**
7000	0.2	0.2	0.4	0.4	0.5	0.7	0.8	0.9	1.1	1.2
5000	0.2	0.3	0.6	0.6	0.8	0.9	1.1	1.3	2.3	1.7
3000	0.4	0.6	0.9	1.0	1.2	1.5	1.8	2.1	3.7	2.8
2500	0.5	0.7	1.1	1.2	1.5	1.8	2.1	2.5	4.5	3.4
2000	0.6	0.8	1.4	1.5	1.8	2.2	2.6	3.0	5.6	4.3
1500	0.8	1.1	1.8	1.9	2.4	2.8	3.4	4.0	7.4	5.8
1400	0.9	1.2	1.9	2.1	2.5	3.0	3.6	4.2	7.9	6.3
1300	0.9	1.3	2.1	2.2	2.7	3.2	3.9	4.5	8.5	6.8
1200	1.0	1.4	2.2	2.4	2.9	3.4	4.1	4.8		
1000	1.2	1.6	2.6	2.8	3.4	4.0	4.8	5.6		
900	1.3	1.8	2.9	3.1	3.7	4.4	5.2	6.2		
800	1.5	2.0	3.2	3.4	4.1	4.8	5.7	6.8		
700	1.7	2.3	3.6	3.8	4.5	5.3	6.3	7.5		
600	1.9	2.6	4.2	4.3	5.1	6.0	7.0			
500	2.3	3.1	4.9	4.9	5.8	6.7	7.9			
400	2.8	3.7	5.8	5.7	6.6	7.6				
300	3.6	4.6	7.2	6.7	7.5	8.3				
250	4.2	5.3	8.2	7.2	7.7					
200	4.9	6.0								
175	5.4	6.5								
150	6.0	6.9								
140	6.2	7.0								
130	6.5	7.1								
120	6.7	7.1								
110	6.9									
100	7.1									
90	7.3									
80										
70										
60										
50										
40										
30										
20										

5.2.3 Numerical Example 3 (SAU Method – Single Curve)

Based on the equations in Table D.2 (Appendix D), the SAU Method applies the following input data where the procedures for calculating e with a design speed of 80 km/h along with an e_{max} of 8 percent is, V_R = 70 km/h, f_{max} = 0.14 (highest allotted side friction factor). The results are as follows, R_{min} = 228.945, R_{PI} = 482.038, h_{PI} = 0.02449, g_1 = 11.805, g_2 = 50.368, A = 38.563, L_1 = 0.00207, L_2 = 0.00229, r_{PVC} = 10155.604, t = -607520.746. The e distribution value of a radius can be determined by obtaining e value and deducting the f value, respectively (Figure 5.3). Therefore, the e distribution value is determined when $R = R_{PI}$ resulting in f = 0.045 and e = 0.059. This value multiplied by 100 (converting the value to a percent) then rounded up to the nearest 2/10ths becomes 5.9 %. Table 5.5 shows all the calculation of the distribution of the superelevation based on SAU Method using e_{max} 8% with speed ranges from 40 km/h to 130 km/h.

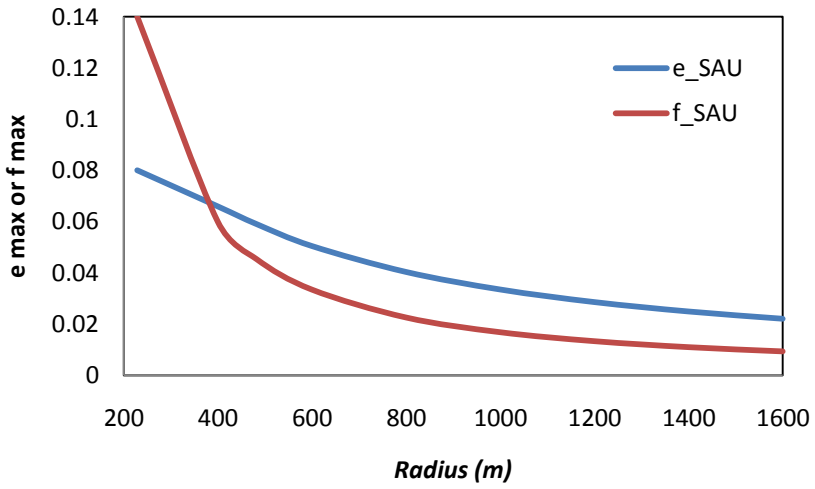

Figure 5. 3 Design Side Friction Factor and Superelevation Rate for SAU Method (e_{max} = 8%)

Table 5. 5 SAU Method of Design Superelevation Rates for Different Radii (e_{max} = 8%)

Design Speed (km/h)	**40**	**50**	**60**	**70**	**80**	**90**	**100**	**110**	**120**	**130**
Radius (m)	**e**	**e**	**e**	**e**	**e**	**e**	**e**	**e**	**e**	**e**
7000	0.2	0.2	0.3	0.4	0.5	0.7	0.8	0.9	1.1	1.2
5000	0.2	0.3	0.5	0.6	0.7	0.9	1.1	1.3	1.5	1.7
3000	0.4	0.6	0.8	1.0	1.2	1.5	1.8	2.1	2.5	2.9
2500	0.5	0.7	0.9	1.2	1.5	1.8	2.1	2.5	3.0	3.5
2000	0.6	0.8	1.1	1.5	1.8	2.2	2.6	3.1	3.7	4.4
1500	0.8	1.1	1.5	1.9	2.3	2.8	3.4	4.0	4.9	5.7
1400	0.9	1.2	1.6	2.0	2.5	3.0	3.6	4.2	5.2	6.1
1300	0.9	1.3	1.7	2.2	2.7	3.2	3.9	4.5	5.5	6.4
1200	1.0	1.4	1.8	2.4	2.9	3.4	4.1	4.8	5.9	6.8
1000	1.2	1.6	2.2	2.8	3.4	4.0	4.8	5.6	6.7	7.6
900	1.3	1.8	2.4	3.0	3.7	4.4	5.2	6.1	7.2	7.9
800	1.5	2.0	2.6	3.4	4.0	4.8	5.7	6.6	7.6	7.9
700	1.7	2.2	3.0	3.8	4.5	5.3	6.3	7.1	7.9	
600	1.9	2.6	3.4	4.2	5.0	5.9	6.9	7.7		
500	2.3	3.0	3.9	4.9	5.7	6.7	7.5	7.9		
400	2.8	3.6	4.6	5.7	6.6	7.5	7.9			
300	3.5	4.5	5.7	6.8	7.5	7.9				
250	4.0	5.1	6.3	7.4	7.9					
200	4.8	5.9	7.1	7.8						
175	5.2	6.4	7.5	7.9						
150	5.8	6.9	7.8							
140	6.0	7.1	7.9							
130	6.3	7.3	7.9							
120	6.6	7.5	7.9							
110	6.8	7.7								
100	7.1	7.8								
90	7.4	7.9								
80	7.6	7.9								
70	7.8	7.8								
60	7.9	7.8								
50	7.9	8.1								
40	8.1									
30										
20										

5.3 Superelevation Distribution for System of Curves

5.3.1 Numerical Example 4 (AASHTO Methods – System of Curves)

Table 5.6 illustrates all the results for AASHTO five methods, based on the input data that is shown in Table 5.2. The values for both *e* and *f* can be determined utilizing Equation (2.60), Method 1; Equations (2.62) and (2.63), Method 2; Equations (2.65) and (2.66), Method 3; Equations (2.68) and (2.69), Modified Method 2; and Equations (2.72), (2.73) and (2.74), Method 5. Regarding each radius, the design safety margin *VL*-*V* can be anticipated and the limiting speed *VL* can be determined utilizing (3.24). Utilizing the frequency information for each curve radius (Table 5.2), the mean, standard deviation and coefficient of variation of the design safety margin can be determined with each method (Table 5.7).

The effect for the above minimum design speeds was noted by Krammes et al. (1995), indicating that traditional design speed methodology "controls only minimum (design speed) values and encourages the use of above-minimum values." In the previous example, the design speed values were determined utilizing Figure 2.11. When the design speed of the 200 m curves is established at 85 km/h rather than 78 km/h, then for those curves f_{max}, R_{min}, along with the centripetal ratio (V^2/gR) results in 0.22, 178 m, along with 0.284, respectively, as opposed to 0.27, 129 m, along with 0.239 respectively (Table 5.2). Utilizing Method 5, the *e*, *f*, *VL* and *VL*-*V* value is from 0.100, 0.297, 71.292, and 0.292, respectively, ending with 0.078, 0.073, 117.257 and 36.951 respectively (Table

5.6). The mean and standard deviation of the safety margin are 17.14 and 10.71 respectively (Table 5.7).

For AASHTO methods, as illustrated within Table 5.7, the largest mean of the safety margin occurs within Method 3 (followed by Method 5); however, the smallest standard deviation can be found in Method 2. Therefore, no single method is the best in either respect. Clearly, Method 5 provides a larger mean of the safety margin (17.14 km/h) in relation to Method 1 (13.8 km/h), Method 2 (6.35 km/h) and Method 2 modified (8.54 km/h), conversely, it is slightly smaller than Method 3 (18.44 km/h). Furthermore, Method 5 provides a smaller standard deviation of the safety margin (10.71) in relation to Method 3 (11.81), conversely larger than Method 1 (8.82), Method 2 (6.54) and Method 2 modified (8.01). Regarding the coefficient of variance, Method 5 (0.63) has the lowest value compared with Method 1 (0.64), Method 2 (1.03), Method 3 (0.64) and Method 2 modified (0.94). As a result, Method 5 provides a good balance within the three different measurements of statistics and thus is considered the best method.

Utilizing a design speed higher than the suggested value reduces the mean safety margin and then increases the standard deviation for the safety margin (e.g., inconsistency is increased between the curves), and the effects become unfavorable. This verifies the recommendation from Krammes et al. (1995) that utilizing "above-minimum values (of the design speed) ... may have a negative effect on consistency among alignment elements."

Table 5. 6 Safety Margins for Diffrence Methods and Optimization Model

Method	Variable	Radius (m)					
		100	**150**	**200**	**250**	**300**	**350**
1	e	0.099	0.080	0.065	0.056	0.049	0.044
	f	0.298	0.223	0.175	0.146	0.123	0.107
	VL(km/h)	71.219	82.805	92.227	100.185	106.792	112.477
	VL-V (km/h)	0.219	6.805	14.227	20.185	25.792	30.477
2	e	0.097	0.023	0.000	0.000	0.000	0.000
	f	0.300	0.280	0.239	0.201	0.172	0.151
	VL(km/h)	71.000	76.000	82.834	90.880	97.621	103.312
	VL-V (km/h)	0.000	0.000	4.834	10.880	16.621	21.312
3	e	0.100	0.100	0.100	0.100	0.100	0.100
	f	0.297	0.203	0.139	0.101	0.072	0.051
	VL(km/h)	71.292	85.104	96.968	106.939	115.507	122.966
	VL-V (km/h)	0.292	9.104	18.968	26.938	34.507	40.966
2 modified	e	0.097	0.023	0.020	0.020	0.020	0.020
	f	0.300	0.280	0.219	0.181	0.152	0.131
	VL(km/h)	71.000	76.000	85.847	94.311	101.451	107.531
	VL-V (km/h)	0.000	0.000	7.847	14.311	20.451	25.531
5	e	0.100	0.097	0.091	0.087	0.082	0.078
	f	0.297	0.206	0.148	0.115	0.090	0.073
	VL(km/h)	71.292	84.644	95.322	104.019	111.163	117.257
	VL-V (km/h)	0.292	8.792	17.843	24.926	31.484	36.951
EAU	e	0.100	0.098	0.093	0.088	0.083	0.078
	f	0.297	0.205	0.147	0.114	0.089	0.073
	VL(km/h)	72.031	85.806	97.059	106.250	113.814	120.121
	VL-V (km/h)	1.031	9.806	19.059	26.250	32.814	38.121
SAU	e	0.100	0.100	0.096	0.089	0.082	0.076
	f	0.298	0.204	0.145	0.113	0.091	0.076
	VL(km/h)	71.292	85.095	96.381	105.285	112.519	118.526
	VL-V (km/h)	0.292	9.095	18.381	25.285	31.519	36.526
Cubic Model	e	0.100	0.068	0.044	0.032	0.024	0.020
	f	0.297	0.235	0.195	0.170	0.148	0.131
	VL(km/h)	72.031	81.944	89.611	96.413	102.402	107.617
	VL-V (km/h)	1.031	5.944	11.611	16.413	21.402	25.617

Table 5. 7 Comparison of Means, Standard Deviation and Coefficient of Variation of Safety Margins for all Methods and Optimization Models

	Safety margin (km/h)		
Element	Mean	Standard Deviation	Coefficient of Variation
	AASHTO methods		
Method 1	13.80	8.82	0.64
Method 2	6.35	6.54	1.03
Method 3	18.44	11.81	0.64
Method 2m [b]	8.54	8.01	0.94
Method 5	17.14	10.71	0.63
	Fixed curve		
EAU Method	18.27	10.89	0.60
SAU Method	18.39	10.88	0.59
	Optimization models		
Discete [a]	10.70	6.50	0.61
Quadratic [a,c*]	10.30	7.30	0.71
Cubic [c,d]	11.53	7.05	0.61

[a] Based on Easa (2003).

[b] The modified Method 2m is the same as Method 2 except that e_{min}=0.02 instead of zero.

[c*] For the quadratic distribution, c=-0.000073.

[c] For the cubic distribution, c=-0.004658587.

[d] For the cubic distribution, c=-0.0002452192.

5.3.2 Numerical Example 5 (EAU Method – System of Curves)

The results of Table D.3 (Appendix D) of the EAU Method, e, f, VL and $VL - V$ values is from 0.100, 0.297, 72.031 and 1.031, respectively ending with 0.078, 0.073, 120.121 and 38.121, respectively (Table 5.6). The mean and standard deviation of the safety margin are 18.27 and 10.89, respectively (Table 5.7).

Table 5.7 illustrates the improved solution compared with the AASHTO methods for the safety margin of the mean, standard deviation and coefficient of variation. The mean of the EAU Method (18.27) has a margin of improvement from Method 1, 2, 2 modified and 5 respectively, (13.80, 6.35, 8.54 and 17.14 respectively). However, it has a slightly inferior margin compared with Method 3 (18.44), as shown in Table 5.7. The standard deviation of the EAU Method (10.89) has a margin of improvement from Method 3, (11.81); however, it has a slightly inferior margin compared with Method 1, 2, 2 modified and 5 (8.82, 6.54, 8.01 and 10.71 respectively), as shown in Table 5.7; the coefficient of variation of the EAU Method (0.60) has a margin of improvement from Method 1, 2, 3, 2 modified and 5 respectively, (0.64, 1.03, 0.64, 0.94 and 0.63 respectively). The performance of different methods was examined using e_{max}, f_{max}, and V_D, where those variables were the same for all curves, superior than the AASHTO Method, Discrete, Quadratic and Cubic model will belong to distribution e and f.

As a result, the EAU Method counterbalances the order of distributing e and f that is dependent upon the frequency of the curves and their radii, roadway restriction and the significance of the mean with variance of the safety margin and improving the design consistency. Consequently, the EAU Method provides a good balance within the three different measurements of statistics and is thus considered the better method, compared with AASHTO, for being used as a measure which reflects both safety and consistency.

5.3.3 Numerical Example 6 (SAU Method – System of Curves)

The results of Table D.4 (Appendix D) involving the SAU Method, the e, f, VL and $VL - V$ values are from 0.100, 0.298, 71.292 and 0.292, respectively ending with 0.076, 0.076, 118.526 and 36.526 respectively (Table 5.6). The mean, standard deviation and coefficient of variation of the safety margin are 18.39, 10.88 and (0.59), respectively (Table 5.7). Table 5.7 illustrates the improved solution compared with the AASHTO methods for the safety margin of the mean, standard deviation and coefficient of variation. The mean of the SAU Method has a margin of improvement from Method 1, 2, modified version of 2 and 5 respectively; however, it has a slightly inferior margin compared with Method 3, as shown in Table 5.7. The standard deviation of the SAU Method has a margin of improvement from Method 3; however, it has a slightly inferior margin compared with Method 1, 2, 2 modified and 5, as shown in Table 5.7. The coefficient of variation of the SAU Method has a margin of improvement from Method 1, 2, 3, 2 modified and 5 respectively.

The superelevations differ drastically between the improved method and AASHTO Method 5. While AASHTO superelevation distribution utilizes a parabolic formula for an asymmetrical curve, the SAU Method utilizes a cubic formula of the SAU curve. The performance belonging to different methods was examined using e_{max}, f_{max}, and V_D, where those variables were the same for all curves, and was superior than the AASHTO, the EAU Method, Discrete, Quadratic and Cubic model belonging to distribution e and f.

As a result, the SAU Method counterbalances the order of distributing e and f that are dependent upon the frequency of the curves and their radii, roadway restriction and the significance of the mean with variance belonging to the safety margin and improving the design consistency. Consequently, the SAU Method provides a good balance within the three different measurements of statistics and is thus considered the best method for use as a measure which reflects both safety and consistency.

5.3.4 Numerical Example 7 (Parametric Cubic Model – System of Curves)

The results of the optimization model for Table 4.1 are given in Table 5.6. Using the Lingo software based on the Global optimal solution, the objective function was obtained as 25.617, and the parameters of the optimization model determined that $c = -0.004658$, and $d = 0.000245$. Additionally, the *f* values calculated from the optimization model lie (*f* follows a cubic distribution curve) between Method 2 and Method 3 as shown in Figure 5.4. The range of the safety margin is from 1.03 to 25.62 km/h (Table 5.6) within an 11.53 km/h mean, 7.05 Standard Deviation and 0.61 Coefficient of Variation (Table 5.7). The optimization model presented another solution that is better than the AASHTO methods, which is the improved solution, based on the coefficient of variation for the safety margin as shown in Figure 5.11.

A comparison for both the superelevation e_i along with the safety margin m_i for AASHTO Method 5, along with the optimization model is illustrated in Table 5.6.

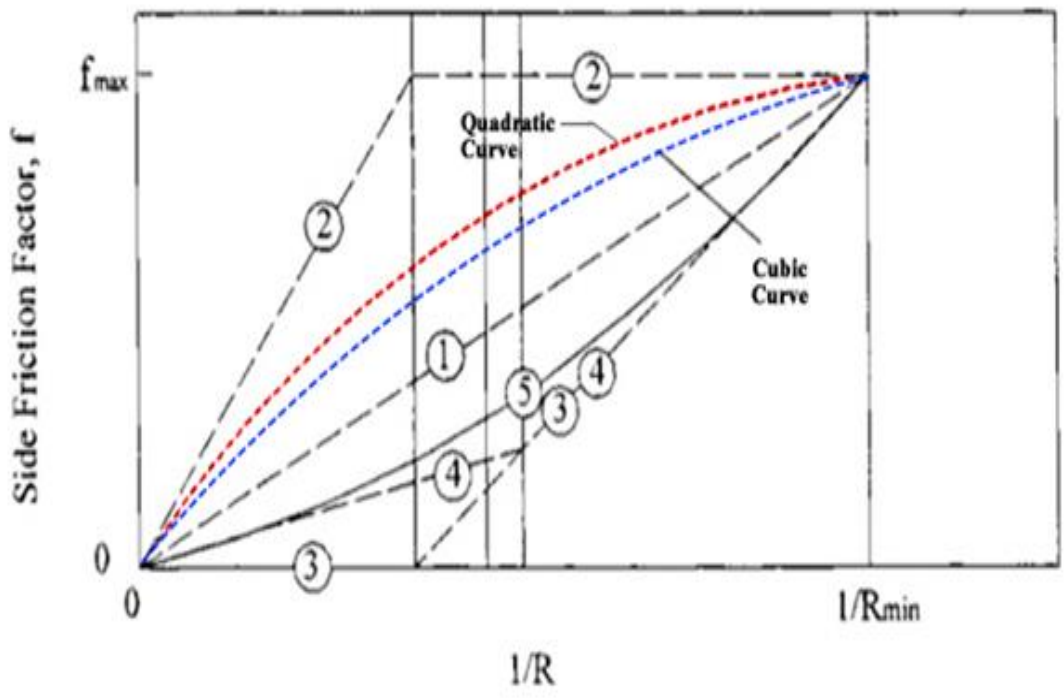

Figure 5. 4 Compare of Cubic Model, Quadratic Model, and AASHTO Methods (AASHTO 2001)

The superelevations differ drastically between the optimization model and AASHTO Method 5. While AASHTO superelevation distribution utilizes a parabolic formula for an asymmetrical curve, the optimization model utilizes a cubic formula of f distribution. The Optimization model, it minimizes the variation in safety margin of a specific highway segment. Clearly, the optimization model step function is significant only with this example, where usually the optimization model values might follow other patterns according to other examples.

5.4 Sensitivity Analysis

5.4.1 Single Curve

For sensitivity analysis purposes, based on V_D = 80 km/h, V_R = 70 km/h, e_{max} = 8%, and f_{max}= 0.14, the percentage reduction in superelevation and side friction for a single value of horizontal curve radius is between two methods, the EAU and SAU Methods respectively, and AASHTO Method 5 as illustrated in Figure 5.5 and Figure 5.6.

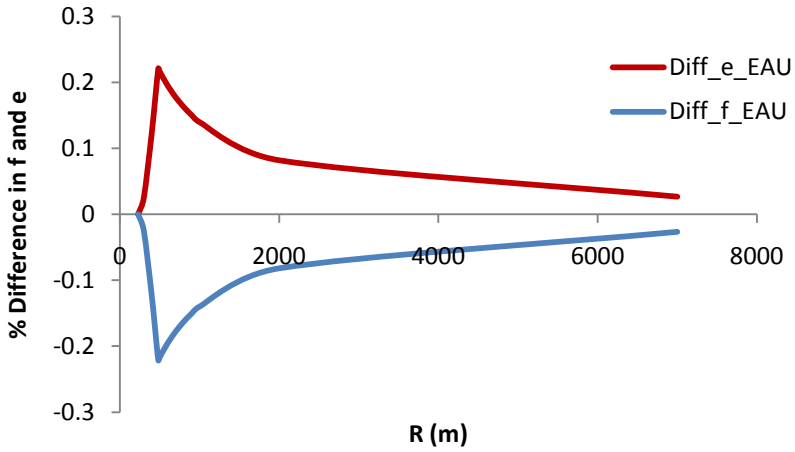

Figure 5. 5 The difference between AASHTO Method 5 and EAU Method (e_{max} = 8%)

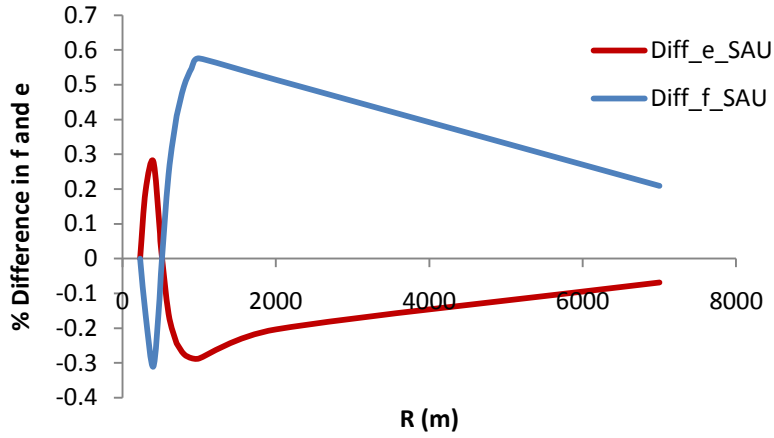

Figure 5. 6 The difference between AASHTO Method 5 and SAU Method (e_{max} = 8%)

This study focuses on the superelevation distribution based on the EAU and SAU curve equations, respectively. Regarding single curve analysis, Figure 5.5 shows the difference between the EAU Method and AASHTO Method 5 involving side friction (f) and superelevation (e). There is a decrease in f while an increase in e, however, the difference is substantially small between the two methods. Figure 5.6 illustrates the difference between the SAU Method and AASHTO Method 5 involving side friction (f) and superelevation (e). In this case, there is an increase in f while a decrease in e, with the difference being very small between the two methods. Appendix A illustrates design superelevation rates for e_{max} = 8% for AASHTO Method 5 along with EAU and SAU Methods for different speeds ranging from 40 to 130 km/h. Figure 5.7 shows the comparison of traditional curve, which is used by AASHTO Method 5 along with EAU and SAU curve, which is used by EAU and SAU Method, respectively.

Furthermore, for sensitivity analysis purposes, V_D = 100 km/h, V_R = 85 km/h, e_{max} = 10%, e_{min} = 0.02 and f_{max}= 0.12. The results of the example show that the rates of the superelevation for the EAU and SAU methods are greater than that of AASHTO Method 5 as illustrated in Figure 5.7 and Figure 5.8.

This study focuses on the superelevation distribution based on the EAU and SAU curve equations, respectively. Regarding single curve analysis, Figure 5.7 shows the difference between the EAU Method and AASHTO Method 5 involving side friction (f) and superelevation (e). There is a decrease in f while an increase in e, however, the difference is substantially small between the two methods.

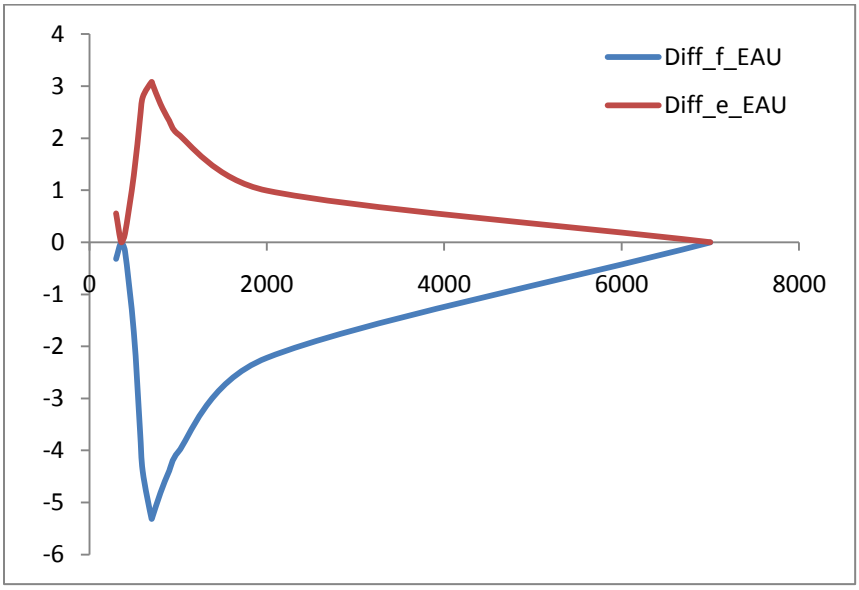

Figure 5. 7 The diffrence between Method 5 and EAU Method (e_{max}=10%)

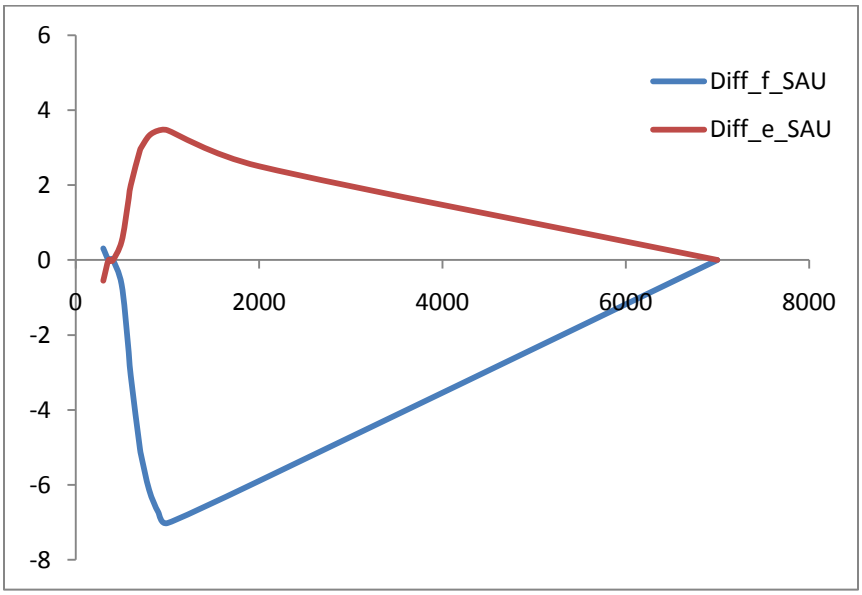

Figure 5. 8 The diffrence between Method 5 and SAU Method (e_{max}=10%)

Figure 5.8 illustrates the difference between the SAU Method and AASHTO Method 5 involving side friction (f) and superelevation (e). In this case, there is an decrease in f while a increase in e, with the difference being small between the two methods. Figure 5.9 shows the comparison of traditional curve, which is used by AASHTO Method 5 along with EAU and SAU curve, which is used by EAU and SAU Method, respectively.

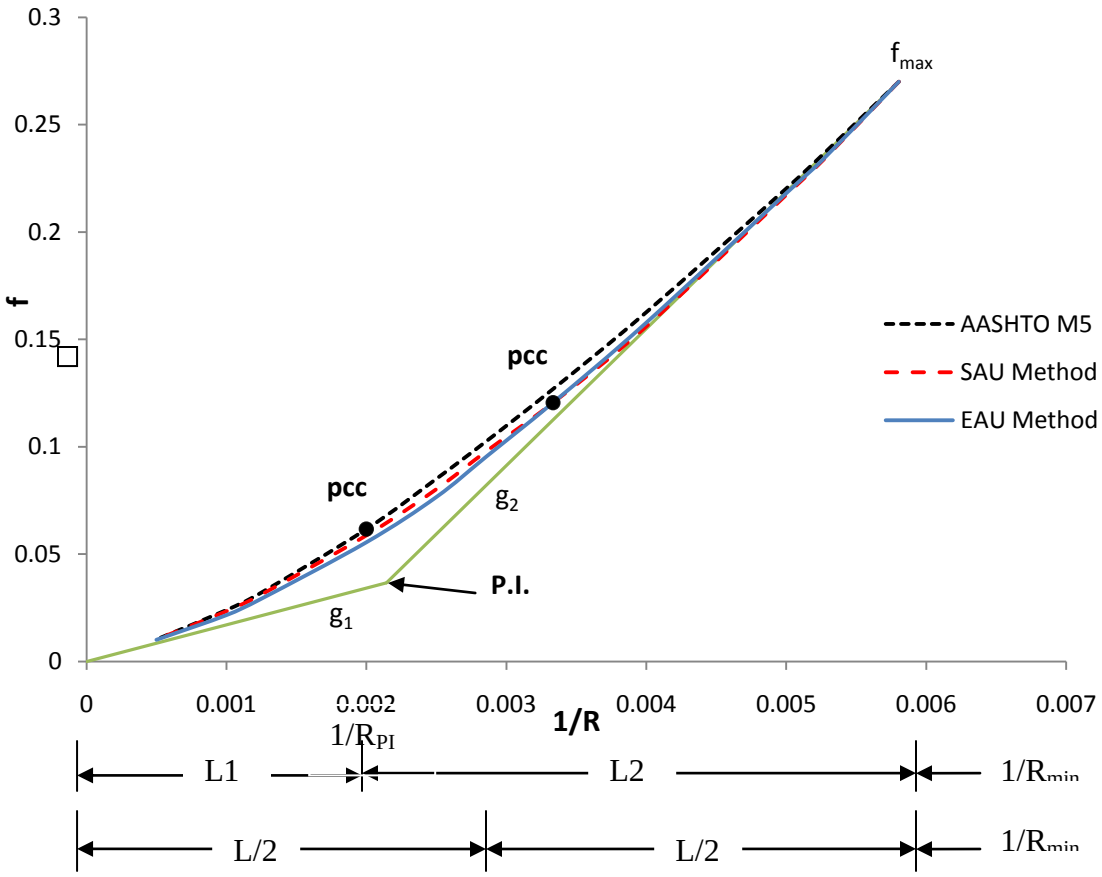

Figure 5. 9 Comparison of ***f*** between Method 5, EAU and SAU Methods

The differences in the AASHTO, EAU and SAU Methods, can be seen in Appendix C. The results show:

1) For Methods 1, 2, along with 2 (modified), f is larger than e regarding all radii.
2) For AASHTO Methods 3 and 5 along with EAU and SAU Methods, f is larger than e for all small radii while e is larger than f regarding large radii.
3) AASHTO Methods 1 and 5 along with EAU and SAU Methods provide a smooth change within both e along with f when the radius increases.
4) AASHTO Method 1 maintains the proportions for the centripetal force offered by the e and the f constant.

The utilization for a minimum superelevation (similarly in Method 2 Modified) involves having superelevation, wherever it may presently not be offered. This ends up increasing

construction costs however, it could lead to less loss-of-control situations dealing with vehicles going about the inside curve crossing the centerline then going from a difficult to favourable curvature. Therefore, a decision-making needed when a curve radius is very large, that the curve could be considered a normal crossfall and tangent utilized.

AASHTO has individually calculated the prior methods. The linear distribution for Method 1 is best only when all the vehicles travel within a constant speed despite whether the travel is within a curve with minimum radius, a flat curve or a tangent. Methods 5 is suggested by AASHTO of distribution for e along with f regarding all curves that have radii larger than minimum radius within urban high-speed streets and

rural highways. EAU and SAU Methods improve the distribution for e along with f regarding all curves that have radii larger than minimum radius within urban high-speed streets and rural highways. The curvilinear distribution for EAU and SAU Methods involves an equal parabolic arc unsymmetrical curve (EAU) and single arc unsymmetrical curve (SAU), respectively of the f distribution where a tangent for two legs defines Method 5. Deducting the f values with the design values for (e+f), a final e distribution can then be obtained. Appendix C shows superelevation and side friction versus Curve Radius for V_D = 100 km/h and e_{max} = 10% for AASHTO Methods along with EAU and SAU Methods. Furthermore, it also highlights the difference in percent involving e and f initially between AASHTO Method 5 and EAU Method, and then shows the difference in percent involving e and f between AASHTO Method 5 and SAU Method.

5.4.2 System of Curves

Pertaining to the system of curves, this involves two proposed methods and an optimization model, the EAU, SAU Methods and Parametric Cubic Model, respectively. According to the counterbalance of the mean, standard deviation and the coefficient of variation of the safety margin, the results demonstrated here appear in relation to the curvilinear distribution belonging to Method 5 that is recommended by AASHTO. Table 5.7 shows all the AASHTO, the EAU, SAU Methods along with the Discrete, Quadratic and Parametric Cubic Models, where the SAU Method improves e and f distribution that is dependent upon the frequency of the curves and their radii, roadway restriction and the

significance of the mean and standard deviation belonging to the safety margin and improving the design consistency.

When comparing the EAU Method with all methods and models, the results show a counterbalance where the EAU Method is superior to AASHTO Methods, Discrete, Quadratic and Parametric Cubic Model; however, it is inferior to the SAU Method in improving design consistency based on the safety margin. Considering the Parametric Cubic Model, it is the best in order of e and f distribution (Table 5.6), and it is superior to AASHTO Methods and the Quadratic model; however, it is slightly inferior to the SAU and EAU Methods and Discrete Model in maximizing design consistency based on the safety margin, and demonstrated through numerical examples in Figure 5.10 & Figure 5.11.

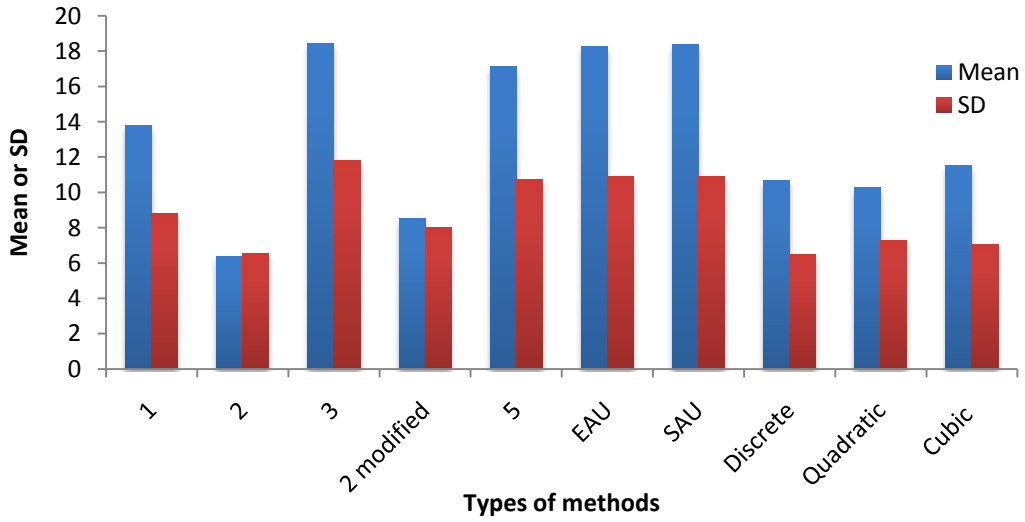

Figure 5. 10 Means and Standard Deviation of Safety Margins for all Methods and Optimization Models

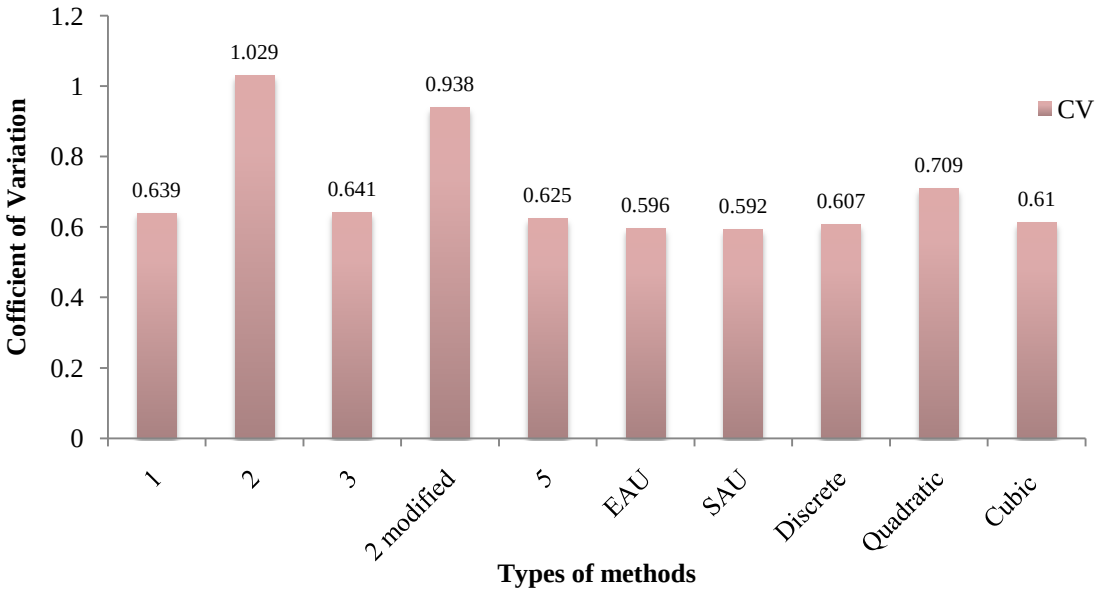

Figure 5. 11 Coefficient of Variation of Safety Margins for all Methods and Optimization Models

5.5 Summary

Considering a single curve, based on e_{max} of 8% and speed of 80 km/h, the percentage gets increased in reduction towards superelevation for a single value of horizontal curve radius between the SAU Method and AASHTO Method 5. For a horizontal curve with a large radius, the reduction will be high for superelevation design; conversely, the increase is low for side friction. Furthermore, for a horizontal curve with a small radius, the reduction is low for superelevation design; however, the increase is very low for side friction. Relating to a system of curves, based on e_{max} of 8% and speed of 80 km/h, the proposed methods and optimization model are extremely helpful because they give the superelevation distribution of different radii for design speed and horizontal curves.

For purposes of evaluation, these methods are utilized for improving the design consistency. This result certifies a superelevation design that will assist most drivers with a low level of uncertainty. Table 5.8 provides a methodology comparison of the different methods.

Table 5. 8 Distribution Method Comparisons for ***e*** and ***f*** within AASHTO, NCHRP439, Discrete, Quadratic, EAU, SAU, Cubic.

Methods	Advantages	Disadvantages
1	- e and f use a linear relationship with the radius inverse - Straightforward (*e* along with *f* is relative to 1/*R*) - Avoid utilizing *f*max and *e*max - Ideal and sensible to distribute *f* or *e*	- Uncertain once vehicle speeds are not consistent
2	- Suitable within low-speed urban streets as *e* is less possible	- Greatly dependent within available *f* where driving comfort can be an issue
3	- *f* is not required at flatter curves within design speeds	- Outcome within negative *f* in flatter curve going at average of running speeds - increasing the value of *f* sharply to *f*max on sharper curves, which could result in inconsistent driving
4	- *f* is not needed at flatter curve within average running speeds along with *f* that is retained for overdriving	- *f* rises towards *f*max at certain sharper curves that could result in inconsistent driving
5	- Suitable for high-speed urban streets - e and f uses a curvilinear relationship with the radius inverse - keep advantages for Method 1 and 4	- Using an unsymmetrical vertical curve equation -Very complicated to calculate, subjectively chosen distribution path
NCHRP439	Keep advantages for methods 1 and 4, reduce design inconsistency for different e of the same *v*d . exceptional radius	Stepped function utilized within design that is similar with discrete function. Needs speed decrease at 95th percentile speed. There is no difference with 85th percentile.

Discrete and Quadratic optimization model	Maximizes the design consistency within an analysis of single alignment-aggregate. Minimizes the variation within safety margin within a single alignment in a number of large curves no matter what their order. Within disaggregate analysis-sequence for horizontal curves within a single alignment are measured. Creates lower e than Method 5.	Required influential optimization computer software needed to present a solution. Complex calculation method presents higher f than that of Method 5. Utilizes discrete function that is different with the dynamic equation of vehicle motion within a horizontal curve.
EAU	- This Mathematical formula is superior to AASHTO. - Takes advantage of the benefits from Method 1, 4 and 5 - Maximizes the design consistency within an analysis of the EAU Vertical Curve Equation.	- Complicated to calculate, however, it will be simplified by incorporating and the using mathematical program software such as Lingo.
SAU	- This Mathematical formula is superior to AASHTO. Takes advantage of the benefits from Method 1, 4 and 5 - Maximizes the design consistency within an analysis of the SAU Vertical Curve Equation.	- Complicated to calculate, however, it will be simplified by incorporating and the using mathematical program software such as Lingo.
Cubic Optimization Model	Maximizes the design consistency within system of curves. Minimizes the variation within safety margin within alignment in a number of large curves regardless of their order. Creates lower e than Method 5.	Required influential optimization computer software needed to present a solution. Complex calculation method presents higher f than that of Method 5.

Chapter 6: Conclusions and Recommendations

6.1 Conclusions

This thesis presented the analysis of superelevation design approaching the proposed methods. For single curves, both EAU and SAU methods are valuable and theoretically parallel to AASHTO Method 5, by offering a smooth distribution of superelevation for highway curves. For system of curves, the proposed methods and the optimization model equations towards superelevation design are uncomplicated to apply and provide superelevation rates that are relatively comparable with AASHTO Method 5. As acknowledged earlier, the utilization of Method 5 signifies a mathematical analysis having little consideration towards the speed variation, along with an extensive process needed to attain the superelevation distribution.

For AASHTO methods, inconsistency within the safety margin could also arise from utilizing curves whose radii is more than the minimum radius; variation levels within the margin are dependent on the superelevation and side friction factor choices within some situations. The system of curves (EAU and SAU Methods) offers a reasonably high mean of safety margin (higher than Method 5) and lower value of coefficient of variation which provide a higher consistency level for the safety margin between curves (fairly higher than Method 5).

This thesis presents an optimization model considering the mean, standard deviation along with the coefficient for variation for the probability distribution for each variable (e and f) that is different from extreme values. The optimization model also accounts for the connection between variables. This thesis proposes a new technique to improve highway design consistency following the principles of the safety margin. Safety margin is defined by determining the difference between the design speed and maximum limiting speed.

In summary, the proposed methods and optimization model have advantages over AASHTO methods as follows:

1) Eliminate the requirement for the process of trial-and-error to evaluate all AASHTO methods to find the design of superelevations for any known set of data for highway curves. Moreover, it directly finds the best superelevations taking into account the complete design space (of which AASHTO curves are a division).
2) Present flexibility to determine both the mean and standard deviation of the safety margin concurrently. Furthermore, these proposed methods and optimization model are able to hold other limitations that are considered essential for specific practical cases.
3) Both the EAU and SAU methods are valuable when the highway section has numerous horizontal curves. However in this case, the proposed methods reduce the variation of the safety margin for a set of highway curves without taking into consideration their sequence. This increases better ad hoc expectancy for drivers

on a specific highway. This study is theoretically similar to AASHTO Method 5 (which offers an even distribution of e for highway curves) and succeeds analysis by Nicholson (1998) and Easa (2003). Consequently, this analysis presents clear deliberation for the safety margin in designing superelevations to improve highway consistency.

4) In consequence, the optimization model determines the superelevation rate and side friction factor that minimize the objective function of a certain highway segment.
5) Highway design consistency based on the safety margin approach assists other approaches that aim to support larger consistency into design speed selection.
6) Optimization is clearly a powerful and beneficial tool, and the method presented in this thesis will help increase its function in geometric design.

These results certify a superelevation design that will assist most drivers with a low level of uncertainty. The information provided will be helpful for both the evaluator and designer, especially when discussion with respect to design sufficiency comes into question. Integrating the safety index within the turning radius design, along with the superelevation distribution, promises a thorough proposed method analysis built within the design methodology.

6.2 Future recommendations

This study considers the superelevation distribution of horizontal curves within highway design in regard to the effect of several parameters, such as side friction factor, superelevation rate, limiting speed and safety margin. Based on the numerical examples provided in Chapter 5, it was determined that the EAU, SAU Methods and the Parametric Cubic Model were superior to that of the AASHTO Methods due to improving highway design consistency. However, this is not quite complete and the following will illustrate recommendations for future analysis along with numerical research:

1) To consider differences between design speeds and operating speeds as the safety margin for a horizontal curve on a highway.
2) To improve operational reliability conditions can be analyzed utilizing a reliability index as safety margin.
3) To develop the mathematical example utilizing data from North America.

References

American Association of State Highway and Transportation Officials.(1954). “A Policy on geometric design of highways and streets”. AASHTO, Washington, D.C.

American Association of State Highway and Transportation Officials.(1984). “A Policy on geometric design of highways and streets”. AASHTO, Washington, D.C.

American Association of State Highway and Transportation Officials.(1990). “A Policy on geometric design of highways and streets”. AASHTO, Washington, D.C.

American Association of State Highway and Transportation Officials.(1994). “A Policy on geometric design of highways and streets”. AASHTO, Washington, D.C.

American Association of State Highway and Transportation Officials.(2001). “A Policy on Geometric Design for Highways and Streets”. AASHTO, Washington, D. C., pp. 131 - 203.

American Association of State Highway and Transportation Officials.(2004). “A Policy on Geometric Design for Highways and Streets”. AASHTO, Washington, D. C.

Alberta Infrastructure.(1999).“Highway Geometric Design”. Alberta, Canada.

Barnett, J. (1936). "Safe side friction factors and superelevation design".Proc., Hwy. Res. Bd., Vol. 16, Washington, D.C., 69-80.

Bonneson, J. A.(2000). “Superelevation Distribution Methods and Transition Designs”. NCHRP

Project 439, Transportation Research Board, Washington, D.C.

Bonneson, James A. (2001). "Controls for Horizontal Curve Design". Transportation Research Record 1751, TRB, National Research Council, Washington, D.C., pp.82 - 89.

Chang, Tangr-Hsien (2001). "Effect of Vehicle's Suspension on Highway Horizontal Curve Design". Journal of Transportation Engineering, ASCE. Vol. 127, No. 1, pp. 89 - 91.

Easa, S.M., (1994). "New and Improved Unsymmetrical Vertical Curve for Highways". Transportation Research Record No. 1445, TRB, National Research Council, Waehington, D.C., pp. 94-100.

Easa, S.M. and Hassan, Y. (1998). “Design Requirements of Equal-Arc Unsymmetrical Vertical Curves”, Journal of Transportation Engineering, Vol.124, No. 5, pp. 404-410.

Easa, S. M. (1999). “Discussion of superelevation, side friction, and roadway consistency, by Alan Nicholson”. Journal of Transportation Engineering, 124(5), 411–418.

Easa, S.M. and Hassan, Y.(2000). “Transitioned vertical curves: I properties.” Transp. Res., 34A(6). 2000, PP. 481-496.

Easa, S.M. and Hassan, Y.(2000) “Transitioned vertical curves: II sight distance." Easa, S.M. Geometric design. ln Civil Engineering Handbook, W.F. Chen and J,Y.Liew eds., CRC Press, Boca Raton, FL, Chapter 63, 2002, 1-39. Transp. Res., 34A(7),2000, PP. 565-584.

Essam Mohamed S. A. E. A. Dabbour. (2002). “Truck stability on different types of horizontal curves combined with vertical alignments”. MASc. thesis, Ryerson University, Toronto, Canada.

Easa, S.M, (2002). Geometric Design in Civil Engineering Handbook, W.F. Chen and J,Y.Liew eds., CRC Press, Boca Raton, FL, Chapter 63, 2002, pp. 1-39.

Easa, S. M.(2003). “Distributing Superelevation to Maximize Highway Design Consistency”. Journal of Transportation Engineering, ASCE. Vol.129, No.2. pp. 411-418.

Easa, S.M. and Dabbour, E. (2003). “Design Radius Requirements for Simple Horizontal Curves on 3D Alignments”. Canadian Journal of Civil Engineering [in press].

Easa, S.M., (2007). "New and Improved Unsymmetrical Vertical Curve for Highways". Transportation Research Record No. 1216-1221, TRB, National Research Council, Waehington, D.C.

Fuller, R. A. (1984). "Conceptualisation of driving behaviour as threat avoidance". Ergonomics, 27(11), 1139-1155.

Gibreel, G., Easa, S., Hassan, Y., and El-Dimeery, I. (1999). “State of the art of geometric design consistency”. Journal of Transportation Engineering, 125(4), 305–313.

Glauz, W.D. and Harwood, D.W. (1991). "Superelevation and Body Roll Effects on Offtracking of Large Trucks”. Transportation Research Record No. 1303, TRB, National Research Council, Washington, D.C., pp. 1-10.

Hickerson, T. F. (1964). Route location and design. McGraw-Hill, New York.

Harwood, D.W. and Mason, J.M. (1994). "Horizontal Curve Design For Passenger Cars And Trucks". Transportation Research Record 1445, TRB, National Research Council, Washington, D,C., pp. 22-33.

Kanellaidis, G. (1996). "Human factors in highway geometric design." Journal of Transportation Engineering, ASCE, 122(1), 59-66.

Krammes, R. A., et al. (1995). "Horizontal alignment design consistency for rural two-lane highways". Report No. FHWA-RD-94-034, Federal Highway Administration, Washington, D.C.

Lamm, R., Choueiri, E. M., and Mailaender, T. (1992). "Traffic safety on two continents—a ten-year analysis of human and vehicular involvements". Proc., Strategic Highway Research Program (SHRP) and Traffic Safety on Two Continents, Gothenburg, Sweden, 18–20.

Lamm, R., B. Psarianos, and T. Mailaender. (1999) "Highway Design and Traffic Safety Engineering Handbook". McGraw Hill, New York, pp. 10.1 - 10.69.

Lingo User Manual (2010). LINDO Systems Inc., 1415 North Dayton Street Chicago, Illinois 60642, USA

Lunenfeld, H., and Alexander, G. J. (1990). "A users' guide to positive guidance". 3rd Ed., Report No. FHWA-SA-90·017, Federal Highway Administration, Washington, D.C.

Mannering, F.L. and kilareski, W.P. (1998). "Principles Of Highway Engineering And Traffic Analysis". Wiley and Sons, New York, N.Y.,pp. 7-79

McLean, J. R. (1979). "An alternative to the design speed concept for low speed alignment design". Transp. Res. Rec. 702, Transp. Res. Bd., Washington, D.C., 55-63.

McLean, J. R. (1983). "Speeds on curves: Side friction considerations". Rep. No. ARR 126, Australian Rd. Res. Bd., Melbourne, Australia.

Naatanen, R., and Summala, H. (1976). Road user behaviour and traffic accidents. North-Holland and American Elsevier, Amsterdam, The Netherlands and New York, N.Y.

NCHRP (2001). "Synthesis 299: Recent Geometric Design research for Improved Safety and Operations". Transportation research Board" TRB, National Research Council, Washington, D.C.

Nicholson, A.J. (1998). "Superelevation, Side Friction and Roadway Consistency". American Society of Civil Engineers, Journal of Transportation Engineering, 124(5), 411-418.

NYSDOT.(2003). "Recommendation for AASHTO Superelevation Design". Design Quality Assurance Bureau.

Ottesen and Krames.(2000). "Speed Profile Model for Design in the United States". Transportation Research Transportation Research Record 1701, TRB National Research Council, Washington, D.C. pp. 85-185.

Rural road design. (1993). "Guide to the geometric design of rural roads". Austroads, Sydney, Australia.

Schrage, L. (1991a). User's manual for LINDO, Scientific Press, Palo Alto, Calif.

Schrage, L. (1991b). LINDO: An optimization modeling system, Scientific Press, Palo Alto, Calif.

Sonny D. Abia. (2010). “Application of Reliability Analysis to Highway Design Problems: Superelevation (e) Design, Left Turn Bay Design-Safety Evaluation and Effect of Variation of Peak Hour Volumes on Intersection Signal Delay Performance”. PhD thesis, University of Miami, Scholarly Repository, USA.

Summala, H. (1988). "Risk control is not risk adjustment: The zero-risk theory of driver behaviour and its implications". Ergonomics, 31(4), 491-506.

Taragin, A. (1954). "Driver performance on horizontal curves." Proc., Hwy. Res. Bd., Vol. 33, Washington, D.C., 446-466.

Transportation Association of Canada (1999). “Geometric Design Guide For Canadian Roads”. Transportation Association of Canada (TAC), Ottawa, ON, Canada.

Transportation Association of Canada (2007). “Geometric Design Guide For Canadian Roads”. Transportation Association of Canada (TAC), Ottawa, ON, Canada.

Winston, W. L. (1994). “Operations research: Applications and algorithms”. Duxbury Press, Belmont, Calif.

Wilde, G. J. S. (1982). "The theory of risk homeostasis: Implications for safety and health". Risk Analysis, 2(4), 209-225.

Wong, Y. D., and Nicholson, A. J. (1992). "Driver behaviour at curves: Risk compensation and the margin of safety". Accident Analysis and Prevention, 24(4),425-436.

Wong, Y. D., and Nicholson, A. J. (1993). "Speed and lateral placement on horizontal curves". Rd. and Transp. Res., 2(1), 74-87.

Appendix A

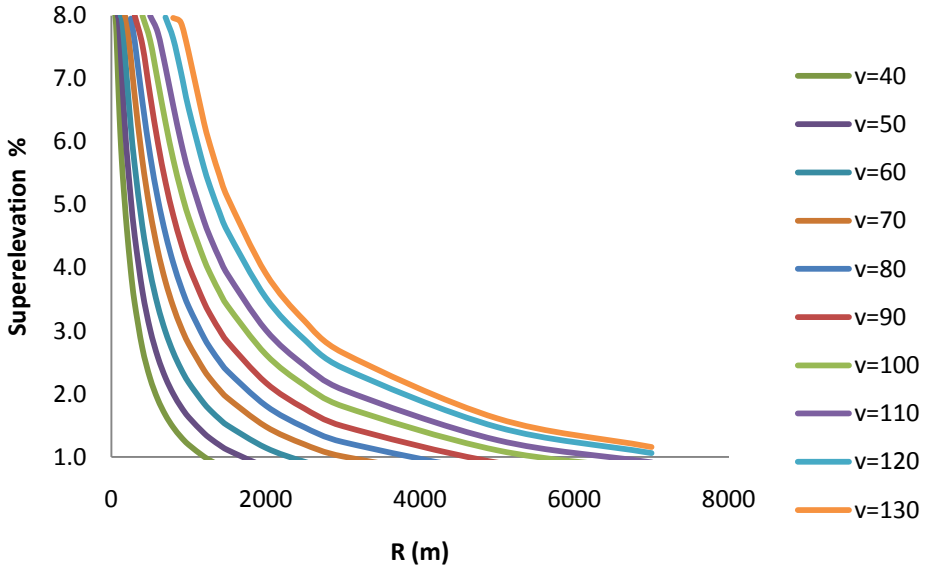

Figure A. 1 Method 5 Design Superelevation Rates for Maximum Superelevation Rate of 8

Percent

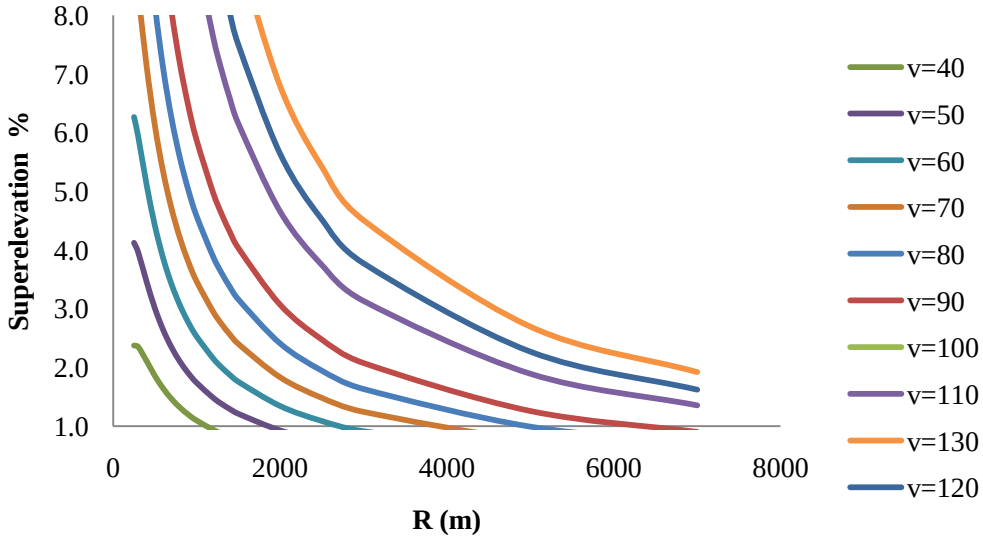

Figure A. 2 EAU Method Design Superelevation Rates for Maximum Superelevation Rate of 8

Percent

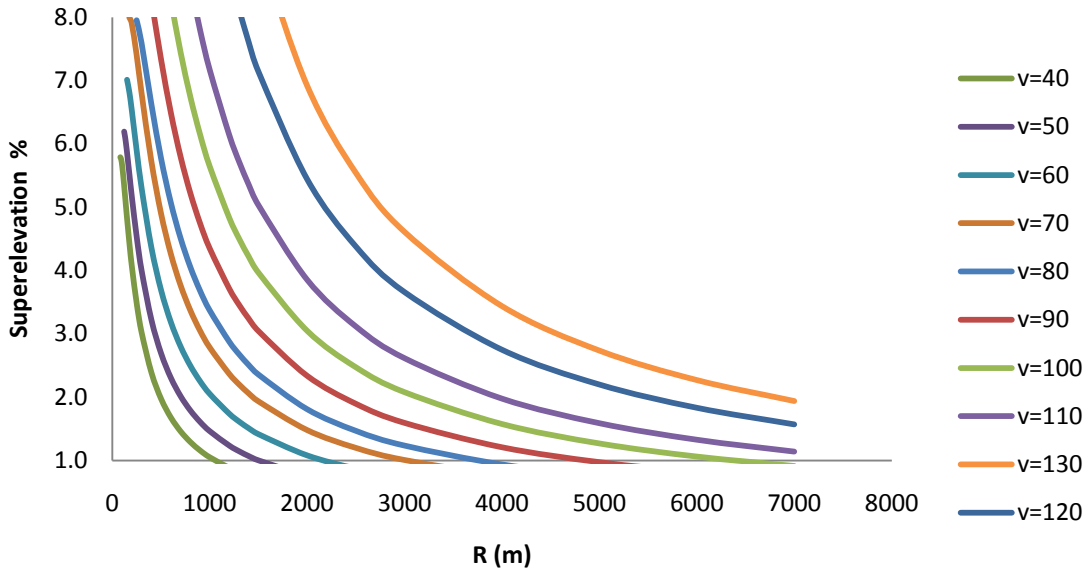

Figure A. 3 SAU Method Design Superelevation Rates for Maximum Superelevation Rate of 8 Percent

Appendix B

Parametric Cubic Model derivation (Cubic distribution of f)

Consider the general cubic curve designed for the f distribution, exposed by dash line within Figure 5.4. The Equation for the curve is

$$f = a + b\left(\frac{1}{R}\right) + c\left(\frac{1}{R}\right)^2 + d\left(\frac{1}{R}\right)^3 \quad (1)$$

At $R = \infty$, f=0, and consequently a=0. Furthermore, at R=R_{min} , f= f_{max}, and moreover

$$f_{max} = b\left(\frac{1}{R_{min}}\right) + c\left(\frac{1}{R_{min}}\right)^2 + d\left(\frac{1}{R_{min}}\right)^3 \quad (2)$$

Based on Equation (2)

$$b = f_{max}\, R_{min} - c\left(\frac{1}{R_{min}}\right) - d\left(\frac{1}{R_{min}}\right)^2 \quad (3)$$

Substitute of b from Equation (3) in Equation (1)

$$f = \left[f_{max}\, R_{min} - c\left(\frac{1}{R_{min}}\right) - d\left(\frac{1}{R_{min}}\right)^2\right]\left(\frac{1}{R}\right) + c\left(\frac{1}{R}\right)^2 + d\left(\frac{1}{R}\right)^3 \quad (4)$$

Equation (4) can be re-written as following:

$$f = \frac{f_{max}\, R_{min}}{R} - c\left(\frac{R - R_{min}}{R_{min}}\right)\left(\frac{1}{R}\right)^2 - d\left(\frac{R^2 - {R_{min}}^2}{{R_{min}}^2}\right)\left(\frac{1}{R}\right)^3 \quad (5)$$

By replacing the parameter (1/R) with (1000/R) in order to keep away from the scaling problem into get the optimum solution, subsequently for Curve Group i (noted that a=0)

$$f_i = f max_i\left(\frac{R\, min_i}{R_i}\right) - c\left(\frac{R_i - R\, min_i}{R\, min_i}\right)\left(\frac{1000}{R_i}\right)^2 - d\left(\frac{{R_i}^2 - {R\, min_i}^2}{{R\, min_i}^2}\right)\left(\frac{1000}{R_i}\right)^3, \forall i \quad (6)$$

where c and d = indefinite variables (decision variables). While the decision variables c and d might be negative or positive. For d=0 Equation (6) is returned to quadratic.

Appendix C

Example 8 (Comparison of Methods):

Table C. 1 Input Data for Example 8

VD	VR	e_{max}	f_{max}	e_{min}	R_{min}	R_{fo}	R_{eo}	R_{me}	R_{pi}
100	85	0.10	0.12	0.02	357.73	655.83	787	562.14	568.61

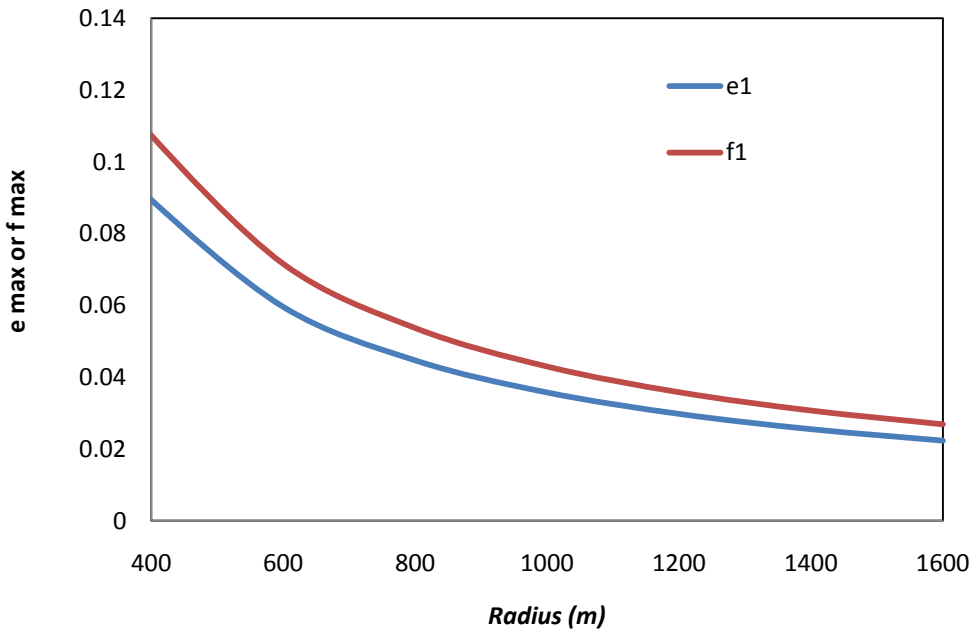

Figure C. 1 Superelevatlon and Sideways Friction versus Curve Radius (Method 1)

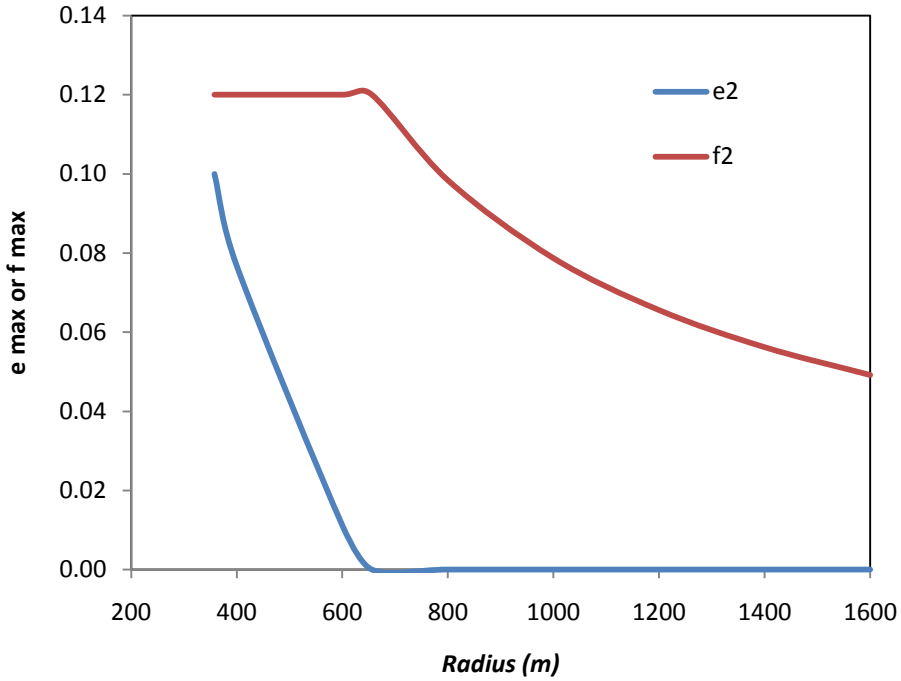

Figure C. 2 Superelevatlon and Sideways Friction versus Curve Radius (Method 2)

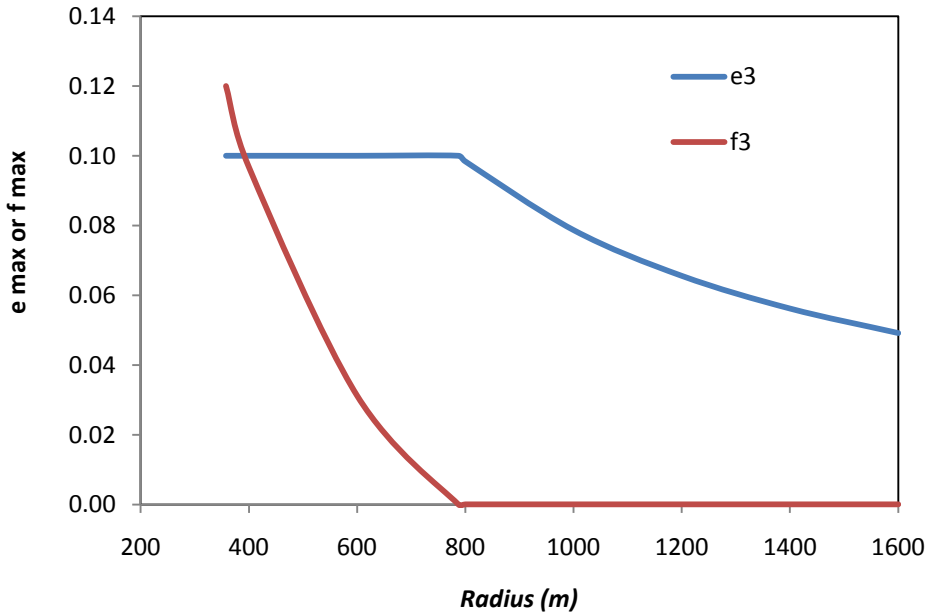

Figure C. 3 Superelevatlon and Sideways Friction versus Curve Radius (Method 3)

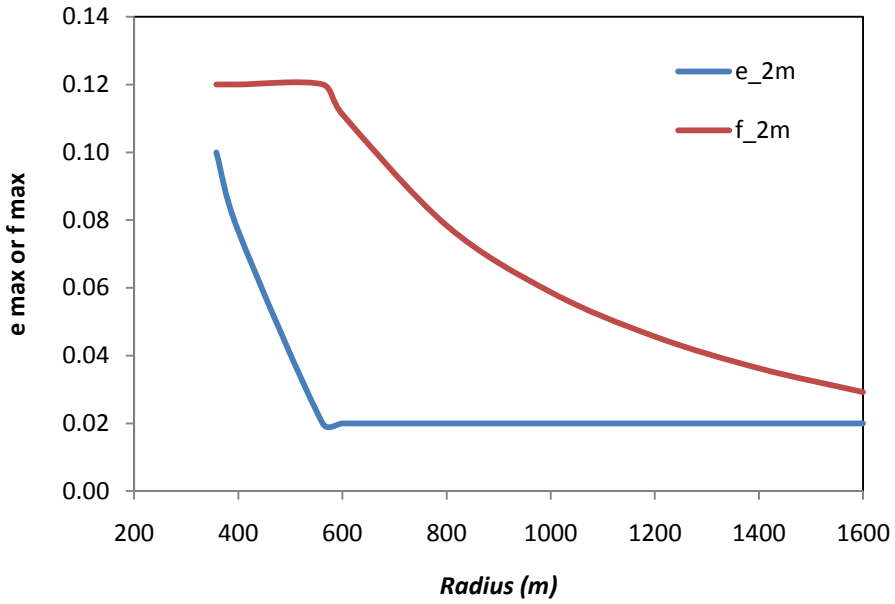

Figure C. 4 Superelevatlon and Sideways Friction versus Curve Radius (Method 2 Modiffed)

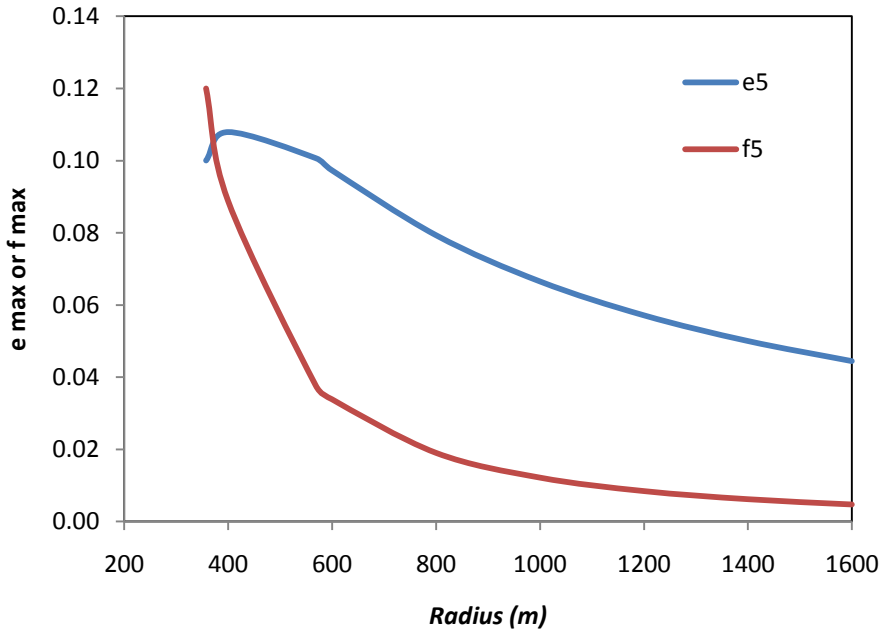

Figure C. 5 Superelevatlon and Sideways Friction versus Curve Radius (Method 5)

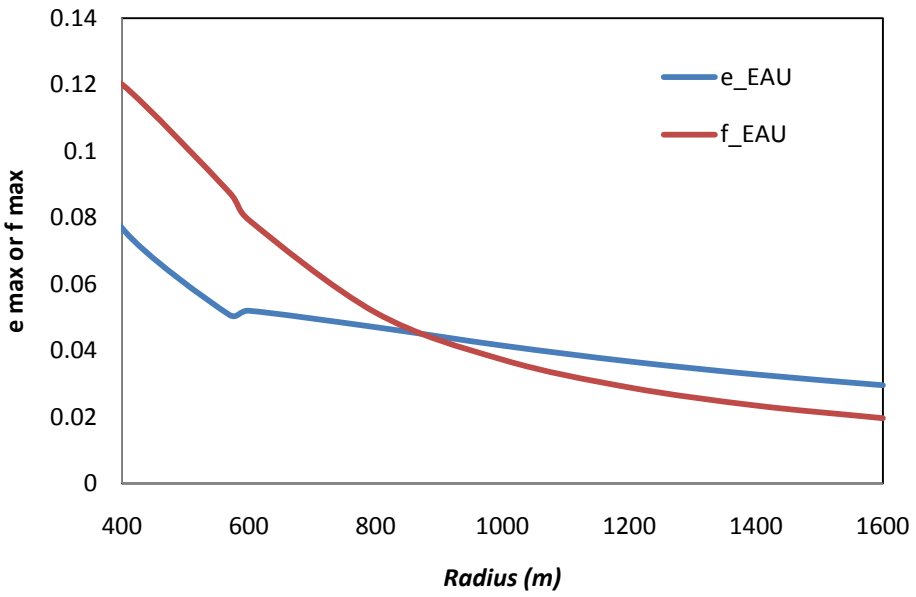

Figure C. 6 EAU Method for Superelevation and Side Friction versus Curve Radius

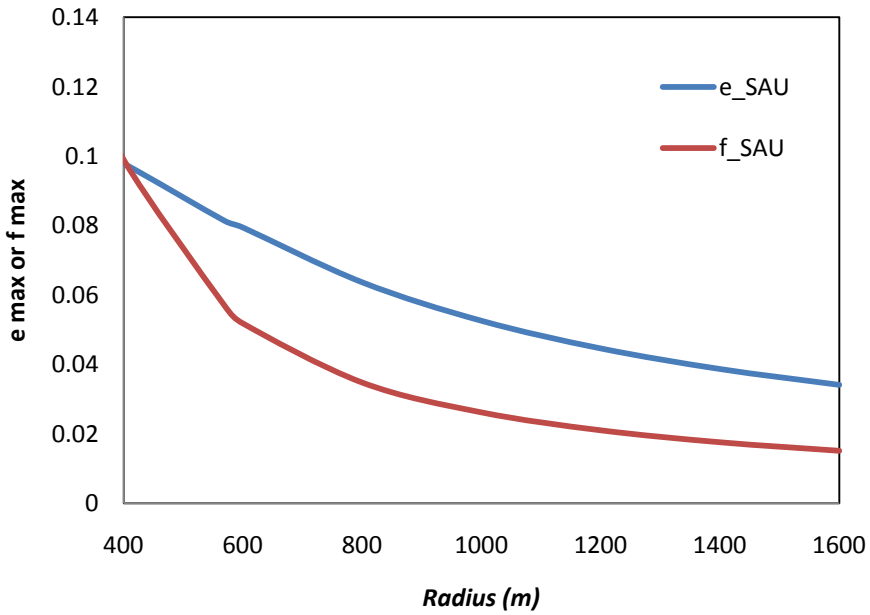

Figure C. 7 SAU Method for Superelevation and Side Friction versus Curve Radius

Appendix D

Table D. 1 EAU Method for Superelevation Distribution (Single Curve)

$$R_{min} = \frac{V_D^2}{127\,(0.01\,e_{max}+f_{max})} \quad (1)$$

$$R_{PI} = \frac{V_R^2}{1.27\,e_{max}} \quad (2)$$

$$h_{PI} = \left(\frac{(0.01\,e_{max})V_D^2}{V_R^2}\right) - 0.01\,e_{max} \quad (3)$$

$$g_1 = h_{PI} * R_{PI} \quad (4)$$

$$g_2 = \frac{f_{max}-h_{PI}}{\frac{1}{R_{min}}-\frac{1}{R_{PI}}} \quad (5)$$

$$A = g_2 - g_1 \quad (6)$$

$$L_1 = \frac{1}{R_{PI}} \quad (7)$$

$$L_2 = \frac{1}{R_{min}} - \frac{1}{R_{PI}} \quad (8)$$

$$L = L_1 + L_2 \quad (9)$$

$$X = \frac{1}{R} \quad (10)$$

$$R_{EAU} = \frac{L_1}{L} \quad (11)$$

$$r_1 = \frac{A(3-4R_{EAU})}{L};\ L_1 < L_2 \quad (12)$$

$$r_2 = \frac{A(-1+4R_{EAU})}{L};\ L_1 < L_2 \quad (13)$$

$$f_1 = g_1 x + \frac{r_1 x^2}{2};\ x \le L/2 \quad (14)$$

$$e_1 = \frac{V^2}{127\,R} - f_1;\ x \le L/2 \quad (15)$$

$$f_2 = f_{max} - g_2\,(L-x) + \frac{r_2\,(L-x)^2}{2};\ x > L/2 \quad (16)$$

$$e_2 = \frac{V^2}{127\,R} - f_2;\ x > L/2 \quad (17)$$

Table D. 2 SAU Method for Superelevation Distribution (Single Curve)

$R_{min} = \frac{V_D^2}{127\ (0.01\ e_{max}+f_{max})}$	(1)
$R_{PI} = \frac{V_R^2}{1.27\ e_{max}}$	(2)
$h_{PI} = \left(\frac{(0.01\ e_{max})V_D^2}{V_R^2}\right) - 0.01\ e_{max}$	(3)
$g_1 = h_{PI} * R_{PI}$	(4)
$g_2 = \frac{f_{max}-h_{PI}}{\frac{1}{R_{min}}-\frac{1}{R_{PI}}}$	(5)
$A = g_2 - g_1$	(6)
$L_1 = \frac{1}{R_{PI}}$	(7)
$L_2 = \frac{1}{R_{min}} - \frac{1}{R_{PI}}$	(8)
$L = L_1 + L_2$	(9)
$X = \frac{1}{R}$	(10)
$r_{PVC} = \left(\frac{-2A}{L^2}\right)(L_1 - 2\ L_2)$	(11)
$t = \left(\frac{6A}{L^3}\right)(L_1 - L_2)$	(12)
$f = g_1 x + \frac{r_{PVC}}{2} x^2 + \frac{t}{6} x^3$	(13)
$e = \frac{V^2}{127\ R} - f$	(14)

Table D. 3 EAU Method for Superelevation Distribution (System of Curves)

$$R_{min} = \frac{V_D^2}{127\,(0.01\,e_{max}+f_{max})}\,,\ \forall_i \quad (1)$$

$$R_{PI} = \frac{V_R^2}{1.27\,e_{max}}\,,\ \forall_i \quad (2)$$

$$h_{PI} = \left(\frac{(0.01\,e_{max})V_D^2}{V_R^2}\right) - 0.01\,e_{max}\,,\ \forall_i \quad (3)$$

$$g_1 = h_{PI} * R_{PI}\,,\ \forall_i \quad (4)$$

$$g_2 = \frac{f_{max}-h_{PI}}{\frac{1}{R_{min}}-\frac{1}{R_{PI}}}\,,\ \forall_i \quad (5)$$

$$A = g_2 - g_1\,,\ \forall_i \quad (6)$$

$$L_1 = \frac{1}{R_{PI}}\,,\ \forall_i \quad (7)$$

$$L_2 = \frac{1}{R_{min}} - \frac{1}{R_{PI}}\,,\ \forall_i \quad (8)$$

$$L = L_1 + L_2\,,\ \forall_i \quad (9)$$

$$X = \frac{1}{R}\,,\ \forall_i \quad (10)$$

$$R_{EAU} = \frac{L_1}{L}\,,\ \forall_i \quad (11)$$

$$r_1 = \frac{A(3-4R_{EAU})}{L};\ L_1 < L_2\,,\ \forall_i \quad (12)$$

$$r_2 = \frac{A(-1+4R_{EAU})}{L};\ L_1 < L_2\,,\ \forall_i \quad (13)$$

$$f_1 = g_1 x + \frac{r_1 x^2}{2};\ x \le L/2\,,\ \forall_i \quad (14)$$

$$e_1 = \frac{V^2}{127\,R} - f_1;\ x \le L/2\,,\ \forall_i \quad (15)$$

$$f_2 = f_{max} - g_2\,(L-x) + \frac{r_2\,(L-x)^2}{2};\ x > L/2\,,\ \forall_i \quad (16)$$

$$e_2 = \frac{V^2}{127\,R} - f_2;\ x > L/2\,,\ \forall_i \quad (17)$$

$$VL = \sqrt{\frac{R_i\,f\,max_i}{0.00787}}\left(1 + \frac{e_i}{2\,f\,max_i}\right),\ \forall_i \quad (18)$$

$$m_i = VL_i - VD_i,\ \forall_i \quad (19)$$

$$Mean = \frac{\sum_{i=1}^{k} q_i\,m_i}{\sum_{i=1}^{k} q_i} \quad (20)$$

$$Variance = \frac{\sum_{i=1}^{k} q_i\,(m_i - Mean)^2}{\sum_{i=1}^{k} q_i - 1} \quad (21)$$

$$SD = \sqrt{Variance} \quad (22)$$

$$CV = SD\ /\ Mean \quad (23)$$

Table D. 4 SAU Method for Superelevation Distribution (System of Curves)

$$R_{min} = \frac{V_D^2}{127\,(0.01\,e_{max}+f_{max})}\,,\ \forall_i \quad (1)$$

$$R_{PI} = \frac{V_R^2}{1.27\,e_{max}}\,,\ \forall_i \quad (2)$$

$$h_{PI} = \left(\frac{(0.01\,e_{max})V_D^2}{V_R^2}\right) - 0.01\,e_{max}\,,\ \forall_i \quad (3)$$

$$g_1 = h_{PI} * R_{PI}\,,\ \forall_i \quad (4)$$

$$g_2 = \frac{f_{max}-h_{PI}}{\frac{1}{R_{min}}-\frac{1}{R_{PI}}}\,,\ \forall_i \quad (5)$$

$$A = g_2 - g_1\,,\ \forall_i \quad (6)$$

$$L_1 = \frac{1}{R_{PI}}\,,\ \forall_i \quad (7)$$

$$L_2 = \frac{1}{R_{min}} - \frac{1}{R_{PI}}\,,\ \forall_i \quad (8)$$

$$L = L_1 + L_2\,,\ \forall_i \quad (9)$$

$$X = \frac{1}{R}\,,\ \forall_i \quad (10)$$

$$r_{PVC} = \left(\frac{-2A}{L^2}\right)(L_1 - 2\,L_2)\,,\ \forall_i \quad (11)$$

$$t = \left(\frac{6A}{L^3}\right)(L_1 - L_2)\,,\ \forall_i \quad (12)$$

$$f = g_1 x + \frac{r_{PVC}}{2}x^2 + \frac{t}{6}x^3,\ \forall_i \quad (13)$$

$$e = \frac{V^2}{127\,R} - f,\ \forall_i \quad (14)$$

$$VL = \sqrt{\frac{R_i\,f\,max_i}{0.00787402}}\left(1 + \frac{e_i}{2\,f\,max_i}\right),\ \forall_i \quad (15)$$

$$m_i = VL_i - VD_i,\ \forall_i \quad (16)$$

$$Mean = \frac{\sum_{i=1}^{k} q_i\,m_i}{\sum_{i=1}^{k} q_i} \quad (17)$$

$$Variance = \frac{\sum_{i=1}^{k} q_i\,(m_i - Mean)^2}{\sum_{i=1}^{k} q_i - 1} \quad (18)$$

$$SD = \sqrt{Variance} \quad (19)$$

$$CV = SD\ /\ Mean \quad (20)$$